Title
Regulation of lipogenic gene transcription during fasting and feeding/insulin: Role of USF, SREBP-1c, and BAF60c

Author
Wong, Roger Hoi Fung

Publication Date
2010

Peer reviewed|Thesis/dissertation

Regulation of Lipogenic Gene Transcription during Fasting and Feeding/insulin: Role of USF, SREBP-1c, and BAF60c

By

Roger Hoi Fung Wong

A dissertation submitted in partial satisfaction of the

requirements for the degree of

Doctor of Philosophy

in

Comparative Biochemistry

in the

Graduate Division

of the

University of California, Berkeley

Committee in Charge:

Professor Hei Sook Sul

Professor Mark S. Schlissel

Professor Jen-Chywan (Wally) Wang

Fall 2010

ABSTRACT

Regulation of Lipogenic Gene Transcription during Fasting and Feeding/insulin: Role of USF, SREBP-1c and BAF60c

by

Roger H. F. Wong

Doctor of Philosophy in Comparative Biochemistry

University of California, Berkeley

Professor Hei Sook Sul, Chair

Transcription of genes encoding enzymes involved in fatty acid and triacylglycerol synthesis, including fatty acid synthase and mitochondrial glycerol-3-phosphate acyltransferase, is coordinately induced in lipogenic tissues by feeding and insulin treatment. Dysregulation of lipognesis often contributes to metabolic diseases such as obesity, diabetes, and cardiovascular diseases. Transcription factors and signaling molecules involved in transcriptional activation of lipogenesis represent attractive targets for the prevention and treatment of metabolic diseases.

In transcriptional activation of fatty acid synthase by feeding/insulin, USF constitutively bound to the -65 E-box is required. In this study, USF was shown to function as a molecular switch by recruiting various interacting proteins during the fasting/feeding transition. First, USF was detected to directly interact with SREBP-1 that is induced by feeding and binds nearby -150 SRE. Cotransfection of USF and SREBP-1c with an FAS promoter-luciferase reporter construct resulted in high synergistic activation of the FAS promoter. Chromatin immunoprecipitation analysis of mouse liver demonstrated that USF binds constitutively to the fatty acid synthase promoter during fasting/feeding, whereas the binding of SREBP-1 was observed only during feeding, in a manner identical to that of the FAS promoter. These data show that USF recruits SREBP-1c to the lipogenic gene promoters upon feeding/insulin. Similar cooperative action of USF and SREBP-1c in the activation of the mitochondrial glycerol-3-phosphate acyltransferase promoter was also observed.

During feeding/insulin, USF-1 recruits three distinct families of proteins to the lipogenic promoters: 1) P/CAF which acetylates USF and functions as a coactivator, 2) DNA break/repair machinery including Ku70, Ku80, PARP-1, TopoIIB and DNA-PK, which causes a DNA break in the lipogenic gene promoter prior to the transcriptional

initiation in vivo, and 3) signaling molecules including PP1 and DNA-PK. PP1 dephosphorylates and activates DNA-PK upon feeding/insulin treatment. Thus in the fed state, activated DNA-PK phosphorylates USF-1 at S262, allowing the recruitment of and acetylation by P/CAF at K237, leading to promoter activation. P/CAF-mediated acetylation of USF is reversed by HDAC9 in the fasted state. Although total HDAC9 levels do not change during fasting/feeding, nuclear abundance of HDAC9 increases upon fasting, suggesting regulation of HDAC9 by nuclear translocation. DNA break/repair components associated with USF also bring about transient DNA breaks during feeding-induced FAS activation. In DNA-PK deficient SCID mice, feeding induced USF-1 phosphorylation/acetylation, DNA-breaks, and FAS activation leading to lipogenesis are impaired, resulting in decreased liver and circulating triglyceride levels. This study demonstrates that DNA-PK mediates the feeding/insulin-dependent lipogenic gene activation. BAF60c was also detected to be an USF interacting protein recruited to lipogenic gene promoters upon feeding. Among the three isoforms of BAF60s, BAF60c is the only BAF60 specific to lipogenesis and recruits other BAF subunits including BAF155 and BAF190 for the formation of lipoBAF. BAF60 proteins function as the bridge between transcription factors and the BAF complex. BAF60c was found to be phosphorylated at S247 by aPKC upon feeding/insulin. BAF60c was translocated from the cytosol to the nucleus in response to feeding/insulin and the nuclear localization was dependent on its S247 phosphorylation. Furthermore, this BAF60c phosphorylation together with USF acetylation were required for the interaction between the two proteins. Overexpression of BAF60c activated the lipogenic transcription program in mice even in the fasted state. This study provides a novel mechanism to fine-tune lipogenic transcription in response to feeding/insulin. Closely positioned E-boxes and sterol regulatory elements found in the promoters of several lipogenic genes suggest that USF functions as a master molecular switch as a common mechanism of induction by feeding/insulin. Taken together, identification of SREBP-1c, DNA-PK and BAF60c as USF interacting proteins has led to the discovery of novel players in insulin signaling cascade and has revealed an unexpected link between DNA break/repair and metabolism.

TABLE OF CONTENTS

Chapter I: Overview and Signifcance: Regulation of Regulation of Lipogenic Gene Transcription during Fasting and Feeding/insulin

A) Insulin Signaling in Fatty Acid and Fat Synthesis: a Transcriptional Perspective

ABSTRACT

Transcription of enzymes involved in FA and TAG synthesis is coordinately induced in lipogenic tissues by feeding and insulin treatment. The three major transcription factors involved are USF, SREBP-1c, and LXR□□□New insights into the insulin signaling pathway(s) that control lipogenic gene transcription via these factors have recently been revealed. Dephosphorylation/activation of DNA-PK by PP1 causes phosphorylation of USF that in turn recruits P/CAF to be acetylated for transcriptional activation. SREBP-1c can be induced by mTORC1, bifurcating lipogenesis from AKT-activated gluconeogenesis. LXR□ may serve as a glucose sensor and, along with ChREBP, may activate lipogenic genes in the fed state. Dysregulation of FA and TAG metabolism often contributes to metabolic diseases such as obesity, diabetes, and cardiovascular diseases. Transcription factors and signaling molecules involved in transcriptional activation of FA and TAG synthesis represent attractive targets for prevention and treatment of metabolic diseases.

INTRODUCTION

Triacylglycerol (TAG) is synthesized by esterification of glycerol-3-phosphate with fatty acids (FA) taken up from the diet as well as with FA synthesized de novo (de novo lipogenesis) from excess dietary carbohydrates (Figure 1). The two major tissues that synthesize FA and TAG at a high level in adults are the so-called lipogenic tissues, liver and adipose tissue. TAG synthesized in the liver is used for VLDL assembly to be secreted to the circulation so that various tissues take up FA from VLDL-TAG upon hydrolysis. TAG synthesized in adipose tissue, on the other hand, is stored as the main energy storage form in mammals, and is hydrolyzed in adipose tissue to release FA into the circulation to be used by other tissues during periods of energy demand.

Dysregulation of FA and TAG metabolism often contributes to metabolic diseases. Excess synthesis and storage of TAG in adipose tissue due to caloric intake above the expenditure, i.e., obesity, is a global health epidemic in modern times and is strongly associated with insulin resistance, liver steatosis, dyslipidemia, and cardiovascular diseases [1, 2]. Paradoxically, the metabolic abnormalities usually found in obesity are also associated with lipodystrophy which is characterized by selective loss of adipose tissue mass from particular regions of the body. Although the underlying molecular mechanisms are not clear, in lipodystrophic patients, metabolic complications may result from ectopic storage of TAG in tissues such as liver and muscle. Furthermore, in cancer cells, aerobic glycolysis, instead of oxidative phosphorylation, provides energy (so called Warburg effect) [3]. Increased glycolysis facilitates an increase in de novo lipogenesis, providing FA for membrane phospholipid biosynthesis in cancer cells. Thus, lipogenic enzymes are not only used as markers for certain types of human cancers, but also are being exploited as potential anti-cancer targets [4]. In light of the implications of this wide range of health problems, it is critical to understand the regulation of fatty acid and TAG synthesis. While this review provides a brief review of the transcriptional regulation of lipogenic genes during fasting/feeding, it focuses mainly on the recent development of the role of USF, SREBP-1c, and LXR□ on transcriptional activation of lipogenic genes by insulin.

REGULATION OF FATTY ACID AND TRIACLGLYCEROL SYNTHESIS

FA and TAG synthesis in lipogenic tissues is under nutritional and hormonal control. Many of the enzymes involved in FA and TAG synthesis are tightly and coordinately regulated during fasting/feeding. The coordinately regulated enzymes include: enzymes in the FA synthetic pathway, such as ATP-citrate lyase (ACL), acetyl-CoA carboxylase (ACC) and fatty acid synthase (FAS); enzymes involved in the production of NADPH required for FAS activity, such as malic enzyme and enzymes in hexose monophosphate shunt such as glucose-6-phosphate dehydrogenase; and enzymes for TAG esterification, such as mitochondrial glycerol-3-phosphate acyltransferase (mGPAT) and diacylglycerol acyltransferase (DGAT) (Figure 2). Some glycolytic enzymes such as liver pyruvate kinase (L-PK) and glucokinase (GK) are also regulated in a similar fashion to provide the carbon source for FA and TAG synthesis. Activities of these various enzymes are very low in the fasted condition, with the increase in circulating glucagon that raises intracellular cAMP levels. Conversely, in the fed condition, especially after a high carbohydrate meal, activities of these enzymes drastically increase with the rise in blood glucose and insulin levels. Some of these enzymes are under allosteric control by metabolites and/or are regulated by phosphorylation/dephosphorylation. For example, ACC, which catalyzes the key regulatory step in FA biosynthesis, is phosphorylated and inactivated by AMP-activated kinase, which senses the low energy state of cells. Malonyl-CoA produced in this way not only is a substrate for FAS, but inhibits CPT-1 activity preventing FA transport into mitochondria, and therefore coordinates synthesis and oxidation of FA. Furthermore, although the mechanism is not well understood, malonyl-CoA can affect transcription of neuropeptide genes in the hypothalamus to control food intake [5]. Nevertheless, the principal mode of long-term coordinate regulation of lipogenic enzymes in liver and adipose tissue is at the transcriptional level; fasting or insulin deficiency suppresses transcription, whereas a high carbohydrate meal or insulin administration activates these lipogenic genes. Studies on transcriptional activation of lipogenic enzymes during fasting/feeding not only provide fundamental information about lipogenic gene regulation, but also provide an excellent model system to study the cellular and metabolic response to insulin.

ROLE OF USF AND SREBP-1C IN THE LOPOGENIC GENE TRANSCRIPTION

In the earliest studies of insulin regulation of the FAS promoter, our laboratory showed that binding of the bHLH-LZ transcription factors, USF-1/USF-2 heterodimer, to the -65 E-box is required for transcriptional activation by insulin in 3T3-L1 adipocytes [6-8] (Figure 3A). Overexpression of dominant negative USF impaired FAS promoter activation. Furthermore, functional analysis and chromatin immunoprecipitation (ChIP) in mice transgenic for various 5' deletions and mutations of the FAS promoter-CAT reporter genes showed that USF binding to the -65 E-box is required for feeding/insulin-mediated FAS promoter activation in vivo [9]. The critical role of USF in lipogenic transcription was clearly shown in vivo in USF knockout mice that had significantly impaired lipogenic gene induction [10]. In this regard, quantitative trait mapping studies have identified USF-1 as a candidate gene for familial combined hyperlipidemia [11]. Others, however, reported that SREBP, another bHLH-LZ transcription factor, binds to the -65 E-box upon feeding/insulin treatment to activate FAS transcription. SREBP was originally identified as a transcription factor that binds to SRE for cholesterol regulation [12]. SREBP is present in the endoplasmic reticulum membrane as a transmembrane protein precursor. Nuclear entry of SREBP requires proteolytic cleavage of the

cytoplasmic N-terminal domain. Of the three members of the SREBP family, SREBP-1a, SREBP-1c and SREBP-2, SREBP-1c is highly expressed in lipogenic tissue, and is itself induced by feeding/insulin. A critical role of SREBP-1 in the transcriptional activation of lipogenic genes has been shown by hepatic overexpression of SREBP-1a in transgenic mice a well as in SREBP-1c knockout mice [13]. Interestingly, many of the lipogenic gene promoters have both the E-box and the SRE in close proximity (Figure 3B) [14]. However, due to an atypical tyrosine residue in place of arginine at its DNA-binding domain [15, 16], SREBP-1 can bind E-box in vitro and there has been a debate on the "true" binding site of SREBP-1c. We performed reporter activity and ChIP assays in transgenic mice harboring different deletions and mutations of the FAS promoter as well as double transgenic mice for various FAS promoter-reporters and for hepatic SREBP-1 overexpression. We found that that SREBP-1c failed to occupy the transgenic FAS promoter when the SRE was mutated in vivo even under high carbohydrate feeding, and the reporter activity was also blunted in these mice [9, 16], clearly showing that the SRE (Figure 3A), not the E-box, is the binding site for SREBP-1c on the FAS promoter in in vivo. The closely spaced arrangement of the E-box and SRE in many lipogenic promoters may allow USF and SREBP-1c to cooperatively activate lipogenic gene transcription [14]. We also found that SREBP-1c binding to the SRE is USF dependent, as SREBP-1c could not bind the SRE in the FAS promoter when the nearby E-box was mutated [9]. Furthermore, we found that the bHLH domain of USF directly interacts with the bHLH and an N-terminal region of SREBP-1c for their synergistic activation of the promoter [14]. Thus, USF bound to the -65 E-box recruits SREBP-1c to bind the nearby SRE during feeding/insulin [17]. This interaction might also explain how excess SREBP-1 was reported to bind to the E-box. SREBP-1 might associate with the E-box indirectly through its interaction with USF. To test the cooperative action between USF and SREBP-1, we employed the p53 promoter, which contains an E-box but does not respond to insulin. Upon insertion of an artificial SRE nearby, USF could recruit SREBP-1 to the SRE and the p53 promoter responded to insulin [17, 18], demonstrating their cooperative action.

INSULIN SIGNALING FOR TRANSCRIPTIONAL ACTIVATION OF LIPOGENESIS

Although USF plays a critical role in lipogenic induction by insulin, USF is bound to the E-box in both fasted and fed states [9]. This observation suggested that USF might recruit coactivators/corepressors in a fasting/feeding dependent manner. We recently performed tandem affinity purification coupled with mass spectrometry to identify USF interacting proteins [17]. We found that, in the fasted state, USF recruits HDAC9 which deacetylates USF and functions as a corepressor in lipogenic gene transcription. In this regard, USF is the first non-histone substrate for HDAC9 to be identified. In the fed state, USF recruits three distinct families of proteins to the lipogenic promoters: 1) P/CAF which acetylates USF and functions as a coactivator, 2) DNA break/repair machinery including Ku70, Ku80, PARP-1, TopoIIB and DNA-PK, which causes a DNA break in the lipogenic gene promoter prior to the transcriptional initiation in vivo, and 3) signaling molecules including PP1 and DNA-PK, which helped us to identify a novel insulin signaling pathway for lipogenic induction. In this regard, while many metabolic effects of insulin are mediated through protein phosphorylation via the well-characterized PI3K cascade that activates downstream PKB/AKT, insulin can also exert metabolic effects through dephosphorylation catalyzed mainly by PP1[19]. Although the underlying molecular mechanism is not well understood, PP1 is known to be

compartmentalized in cells by discrete targeting subunits [20]. We found that PP1 dephosphorylates and activates DNA-PK upon feeding/insulin treatment. Total DNA-PK levels remain the same during fasting/feeding, but phosphorylation of DNA-PK drastically decreases, increasing its kinase activity by 6-fold upon feeding. Thus, in the fed state, activated DNA-PK phosphorylates USF-1 at S262, allowing recruitment of and acetylation by P/CAF at K237, leading to promoter activation [17, 18]. As mentioned above, P/CAF-mediated acetylation of USF is reversed by HDAC9 in the fasted state. Although total HDAC9 levels do not change during fasting/feeding, nuclear abundance of HDAC9 increases upon fasting, suggesting regulation of HDAC9 by nuclear translocation. DNA-PK deficient SCID mice were used to demonstrate its requisite role of DNA-PK in the transcriptional activation of lipogenic genes during feeding/insulin treatment. In contrast, in the fasted state, USF-1 phosphorylation and acetylation is attenuated, blunting transcriptional activation of FAS and de novo lipogenesis. Identification of DNA-PK as a signaling molecule in activation of lipogenic genes by insulin has brought us a step closer to understanding how cells regulate metabolic processes in response to insulin. Besides lipogenesis, it is interesting to note that USF has been shown to activate the transcription of an inhibitor small heterodimer partner (SHP) to repress PEPCK and glucose-6-phosphatase transcription through the DNA-PK signaling pathway [21]. Last but not least, with DNA-PK's role as an insulin-signaling molecule to activate lipogenesis, DNA-PK could possibly serve as a pharmacological target for obesity and diabetes treatment.

As mentioned above, unlike USF whose levels remain constant, SREBP-1c itself is induced upon feeding or insulin treatment. The exact molecular details linking insulin and SREBP-1c transcription are still missing. The SREBP-1c promoter is regulated by SREBP-1c itself, potentially functioning together with USF, and by LXR□ [17, 22]. However, what coactivators are recruited by SREBP-1c is not clear. Although SREBP-1a and -2 have been shown to interact with various transcriptional coregulators, such as CBP/p300, PGC1□, ARC105 mediator, SIRT1, and SRC1, SREBP-1c interacts with these factors weakly, due to a missing activation domain. Therefore, identification of a "true" coactivator for SREBP-1c may help in understanding the mode of function for SREBP-1c in lipogenesis. Regardless, as SREBP-1c auto-regulates itself by binding to the SRE of its own promoter, USF binding to the E-box in the promoter may also be required to recruit SREBP-1c. In that case, SREBP-1c transcription might be via USF action and would be regulated through the DNA-PK signaling pathway in response to feeding/insulin [17]. So far, multiple insulin signaling pathways that can induce SREBP-1c expression have been reported. For example, insulin-mediated activation of atypical PKCλ, PKCζ and AKT via the PI3K pathway induces SREBP-1c expression and lipogenesis [23-26]. Recently, the Brown and Goldstein laboratory reported that the mammalian target of rapamycin complex 1 (mTORC1) mediates insulin-stimulated induction of SREBP-1c and that the induction was S6K-independent [27]. In this regard, due to inactive AKT, insulin suppression of glucose production is impaired in the insulin resistant state, but lipogenesis and TAG synthesis are still active for VLDL production, causing hyperlipidemia. It has been proposed that, independent of AKT, mTORC1 is activated due to high circulating amino acid levels in insulin resistance, and SREBP-1c induction through mTORC1 may be responsible for differing effects of impaired suppression of gluconeogenesis yet robust lipogenesis in insulin resistance [28]. Besides transcriptional regulation, insulin was reported to stimulate processing and nuclear translocation of SREBP-1c, which then initiates a feed-forward auto-regulatory loop [29]. In addition, MAPK was shown to phosphorylate SREBP-1a and 1c, and mutation of these sites abolished the transcriptional activation by SREBP [30]. In

addition, GSK-3, which is inhibited by AKT phosphorylation, was reported to phosphorylate SREBP-1a at a site conserved in SREBP-1c, enhancing degradation [31]. Interestingly, a recent report suggests that SREBP-1 is acetylated by SIRT1 orthologs in the fasted state to downregulate SREBP by ubiquitination and degradation, thus affecting lipid homeostasis in response to fasting cues [32].

Of the two LXR isoforms, LXR□ is abundantly expressed in lipogenic tissues and, by activating the SREBP-1c promoter, it plays an important role in the transcriptional activation of lipogenic genes. Thus, in LXR□□knockout as well as LXR□/□ double knockout mice, SREBP-1c and FAS levels were lower resulting in a decrease in hepatic and plasma TAG levels. Furthermore, LXR agonists such as T0901317 activated SREBP-1c and FAS transcription but had no effect in the LXR□□deficient animals [33]. In contrast, LXR□□transgenic mice showed higher expression of these genes [34]. LXR□□ but not LXR□□ binds to LXRE of the SREBP-1c promoter. LXRE is also found in other lipogenic genes, such as FAS and ACC. Although the canonical LXRE consists of two AGGTCA hexameric half sites, LXREs on LXR target genes vary considerably and LXR□ and LXR□ may have different affinities for various LXREs [35]. LXR may increase lipogenesis by activating SREBP-1c transcription, as well as by directly activating lipogenic genes by binding to their LXREs. Interestingly, recent studies showed that LXR□ interacts with RIP140 to upregulate SREBP-1c, but the same interaction negatively affected gluconeogenic gene transcription [36]. Furthermore, LXR□□itself is regulated by high carbohydrates/insulin at the transcriptional and post-translational levels. Insulin induces LXR□□expression in the liver in vivo [37], and the LXR□ promoter is regulated by an auto-regulatory mechanism since there are three LXREs in its promoter. In addition, as may be the case during fasting, PKA phosphorylates LXR□ to inhibit binding to LXRE by impairing dimerization of LXR□□with RXR, DNA binding and transactivation [38]. LXR□□has also been shown to be phosphorylated by MAPK, and this phosphorylation may have functional implications in insulin regulation of LXR□□[39]. It has been reported that LXR□□can activate the transcription of ChREBP, an E-box binding bHLH/LZ transcription factor that heterodimerizes with Mlx to bind carbohydrate response element (ChoRE) present in lipogenic genes to confer glucose-mediated activation in liver [40]. Furthermore, a report suggests a role for LXR□ as a glucose sensor since glucose or glucose-6-phosphate directly binds and activates LXR□ [41, 42]. A recent study showed that SREBP-1c induction upon high carbohydrate feeding in the liver was completely blunted in LXR□/□ double knockout mice. However, FAS induction was still present although blunted in some degree, whereas expression of ChREBP, L-PK, GK, or ACC was not affected in these mice [43]. This indicates complex and potentially varying mechanisms as well as synergistic action of multiple transcription factors for transcriptional activation of lipogenic genes by feeding/insulin.

CONCLUSION

FA and TAG synthesis is a highly regulated cellular process crucial to the metabolic homeostasis of organisms. Dysregulation of lipid metabolism can often lead to adverse consequences such as obesity, hepatic steatosis, diabetes and cardiovascular diseases. Therefore, it is crucial to dissect the process of FA and TAG synthesis. Transcription of lipogenic enzymes is highly regulated by insulin and glucose. For insulin-mediated regulation, the major transcription factors involved are USF, SREBP-1c, and LXR□□(Figure 4). The inter-

relationship among these transcriptional factors is complex as they regulate each other in a distinct manner. For example, SREBP-1c is crucial to lipogenic gene transcription, but its binding to SRE is USF dependent. LXR□ regulates the expression of SREBP-1c, FAS and, although still in debatable, ChREBP. FAS induction is still detected in LXR□deficient mice that have impaired SREBP-1c induction showing involvement of other transcription factors such as USF. Furthermore, FAS promoter-reporter transgenic mice studies showed that the FAS promoter that contains both an E-box and SRE, but lacks a LXRE, is sufficient for high level activation of the FAS promoter during fasting/feeding, suggesting that binding of USF and SREBP-1c is sufficient for the insulin response of FAS in vivo [9]. Furthermore, ChREBP, together with LXR□ that may function as a glucose sensor, may mediate glucose responsiveness to lipogenic induction upon feeding, in parallel with USF and SREBP-1c that mediate insulin signaling.

Many questions remain in our understanding of lipogenic promoter activation by these transcription factors. How are these transcription factors activated in response to glucose/insulin? Apart from HAT/HDAC, what other coactivators/corepressors, chromatin remodeling machinery, and mediators are required for lipogenic gene activation? Are there common mechanisms to explain the transcriptional regulation of coordinately regulated lipogenic genes? Is chromatin folding involved in sharing transcription machineries among lipogenic gene promoters? Further studies are necessary to understand the details of the transcriptional activation of lipogenic genes and will be critical for developing new drug targets for prevention and treatment of obesity, diabetes, and other associated diseases.

REFERENCES

1. Cheung O, Sanyal AJ: Recent advances in nonalcoholic fatty liver disease. Curr Opin Gastroenterol 2010, 26(3):202-208.
2. Postic C, Girard J: The role of the lipogenic pathway in the development of hepatic steatosis. Diabetes Metab 2008, 34(6 Pt 2):643-648.
• A review describes models that have provided evidence implicating lipogenesis in the development of non-alcoholic fatty liver disease.
3. Vander Heiden MG, Cantley LC, Thompson CB: Understanding the Warburg effect: the metabolic requirements of cell proliferation. Science 2009, 324(5930):1029-1033.
4. Liu H, Liu Y, Zhang JT: A new mechanism of drug resistance in breast cancer cells: fatty acid synthase overexpression-mediated palmitate overproduction. Mol Cancer Ther 2008, 7(2):263-270.
5. Lopez M, Vidal-Puig A: Brain lipogenesis and regulation of energy metabolism. Curr Opin Clin Nutr Metab Care 2008, 11(4):483-490.
6. Wang D, Sul HS: Upstream stimulatory factors bind to insulin response sequence of the fatty acid synthase promoter. USF1 is regulated. J Biol Chem 1995, 270(48):28716-28722.
7. Wang D, Sul HS: Upstream stimulatory factor binding to the E-box at -65 is required for insulin regulation of the fatty acid synthase promoter. J Biol Chem 1997, 272(42):26367-26374.
8. Sul HS, Latasa MJ, Moon Y, Kim KH: Regulation of the fatty acid synthase promoter by insulin. J Nutr 2000, 130(2S Suppl):315S-320S.
9. Latasa MJ, Griffin MJ, Moon YS, Kang C, Sul HS: Occupancy and function of the -150 sterol regulatory element and -65 E-box in nutritional regulation of the fatty acid synthase gene in living animals. Mol Cell Biol 2003, 23(16):5896-5907.
10. Casado M, Vallet VS, Kahn A, Vaulont S: Essential role in vivo of upstream stimulatory factors for a normal dietary response of the fatty acid synthase gene in the liver. J Biol Chem 1999, 274(4):2009-2013.
11. Pajukanta P, Lilja HE, Sinsheimer JS, Cantor RM, Lusis AJ, Gentile M, Duan XJ, Soro-Paavonen A, Naukkarinen J, Saarela J, Laakso M, Ehnholm C, Taskinen MR, Peltonen L: Familial combined hyperlipidemia is associated with upstream transcription factor 1 (USF1). Nat Genet 2004, 36(4):371-376.
12. Yokoyama C, Wang X, Briggs MR, Admon A, Wu J, Hua X, Goldstein JL, Brown MS: SREBP-1, a basic-helix-loop-helix-leucine zipper protein that controls transcription of the low density lipoprotein receptor gene. Cell 1993, 75(1):187-197.
13. Shimomura I, Shimano H, Korn BS, Bashmakov Y, Horton JD: Nuclear sterol regulatory element-binding proteins activate genes responsible for the entire program of unsaturated fatty acid biosynthesis in transgenic mouse liver. J Biol Chem 1998, 273(52):35299-35306.
14. Griffin MJ, Wong RH, Pandya N, Sul HS: Direct interaction between USF and SREBP-1c mediates synergistic activation of the fatty-acid synthase promoter. J Biol Chem 2007, 282(8):5453-5467.
•• Authors showed direct interaction between two lipogenic transcription factors USF and SREBP-1.
15. Kim JB, Sarraf P, Wright M, Yao KM, Mueller E, Solanes G, Lowell BB, Spiegelman BM: Nutritional and insulin regulation of fatty acid synthetase and leptin gene expression through

ADD1/SREBP1. J Clin Invest 1998, 101(1):1-9.
16. Latasa MJ, Moon YS, Kim KH, Sul HS: Nutritional regulation of the fatty acid synthase promoter in vivo: sterol regulatory element binding protein functions through an upstream region containing a sterol regulatory element. Proc Natl Acad Sci U S A 2000, 97(19):10619-10624.
17. Wong RH, Chang I, Hudak CS, Hyun S, Kwan HY, Sul HS: A role of DNA-PK for the metabolic gene regulation in response to insulin. Cell 2009, 136(6):1056-1072.
•• Authors provided evidence that USF functions as a master regulator for lipogenic gene transcription. They linked DNA break/repair to insulin signaling through identification of DNA-PK as an insulin signaling molecule.
18. Wong RH, Sul HS: DNA-PK: relaying the insulin signal to USF in lipogenesis. Cell Cycle 2009, 8(13):1977-1978.
19. Brady MJ, Saltiel AR: The role of protein phosphatase-1 in insulin action. Recent Prog Horm Res 2001, 56:157-173.
20. Printen JA, Brady MJ, Saltiel AR: PTG, a protein phosphatase 1-binding protein with a role in glycogen metabolism. Science 1997, 275(5305):1475-1478.
21. Chanda D, Li T, Song KH, Kim YH, Sim J, Lee CH, Chiang JY, Choi HS: Hepatocyte growth factor family negatively regulates hepatic gluconeogenesis via induction of orphan nuclear receptor small heterodimer partner in primary hepatocytes. J Biol Chem 2009, 284(42):28510-28521.
22. Horton JD, Goldstein JL, Brown MS: SREBPs: activators of the complete program of cholesterol and fatty acid synthesis in the liver. J Clin Invest 2002, 109(9):1125-1131.
23. Wang D, Sul HS: Insulin stimulation of the fatty acid synthase promoter is mediated by the phosphatidylinositol 3-kinase pathway. Involvement of protein kinase B/Akt. J Biol Chem 1998, 273(39):25420-25426.
24. Taniguchi CM, Emanuelli B, Kahn CR: Critical nodes in signalling pathways: insights into insulin action. Nat Rev Mol Cell Biol 2006, 7(2):85-96.
25. Taniguchi CM, Kondo T, Sajan M, Luo J, Bronson R, Asano T, Farese R, Cantley LC, Kahn CR: Divergent regulation of hepatic glucose and lipid metabolism by phosphoinositide 3-kinase via Akt and PKClambda/zeta. Cell Metab 2006, 3(5):343-353.
26. Farese RV, Sajan MP, Standaert ML: Insulin-sensitive protein kinases (atypical protein kinase C and protein kinase B/Akt): actions and defects in obesity and type II diabetes. Exp Biol Med (Maywood) 2005, 230(9):593-605.
27. Li S, Brown MS, Goldstein JL: Bifurcation of insulin signaling pathway in rat liver: mTORC1 required for stimulation of lipogenesis, but not inhibition of gluconeogenesis. Proc Natl Acad Sci U S A 2010, 107(8):3441-3446.
•• The study identified mTORC1 as the bifurcation point separating lipogenesis from gluconeogenesis in insulin resistance.
28. Laplante M, Sabatini DM: mTORC1 activates SREBP-1c and uncouples lipogenesis from gluconeogenesis. Proc Natl Acad Sci U S A 2010, 107(8):3281-3282.
29. Horton JD, Bashmakov Y, Shimomura I, Shimano H: Regulation of sterol regulatory element binding proteins in livers of fasted and refed mice. Proc Natl Acad Sci U S A 1998, 95(11):5987-5992.
30. Roth G, Kotzka J, Kremer L, Lehr S, Lohaus C, Meyer HE, Krone W, Muller-Wieland D: MAP kinases Erk1/2 phosphorylate sterol regulatory element-binding protein (SREBP)-1a at serine 117 in vitro. J Biol Chem 2000, 275(43):33302-33307.

31. Sundqvist A, Bengoechea-Alonso MT, Ye X, Lukiyanchuk V, Jin J, Harper JW, Ericsson J: Control of lipid metabolism by phosphorylation-dependent degradation of the SREBP family of transcription factors by SCF(Fbw7). Cell Metab 2005, 1(6):379-391.
32. Walker AK, Yang F, Jiang K, Ji JY, Watts JL, Purushotham A, Boss O, Hirsch ML, Ribich S, Smith JJ, Israelian K, Westphal CH, Rodgers JT, Shioda T, Elson SL, Mulligan P, Najafi-Shoushtari H, Black JC, Thakur JK, Kadyk LC, Whetstine JR, Mostoslavsky R, Puigserver P, Li X, Dyson NJ, Hart AC, Naar AM: Conserved role of SIRT1 orthologs in fasting-dependent inhibition of the lipid/cholesterol regulator SREBP. Genes Dev 2010, 24(13):1403-1417.
•• Authors described SIRT1 mediated deacetylation of SREBP-1 orthologs in metazoans results in degradation of SREBP-1, thus causing an inhibition on lipid synthesis and fat storage in response to fasting cues.
33. Baranowski M: Biological role of liver X receptors. J Physiol Pharmacol 2008, 59 Suppl 7:31-55.
34. Chawla A, Repa JJ, Evans RM, Mangelsdorf DJ: Nuclear receptors and lipid physiology: opening the X-files. Science 2001, 294(5548):1866-1870.
35. Oosterveer MH, Grefhorst A, Groen AK, Kuipers F: The liver X receptor: Control of cellular lipid homeostasis and beyond Implications for drug design. Prog Lipid Res 2010.
• A recent review on the function of LXR in lipid metabolism.
36. Herzog B, Hallberg M, Seth A, Woods A, White R, Parker MG: The nuclear receptor cofactor, receptor-interacting protein 140, is required for the regulation of hepatic lipid and glucose metabolism by liver X receptor. Mol Endocrinol 2007, 21(11):2687-2697.
37. Tobin KA, Ulven SM, Schuster GU, Steineger HH, Andresen SM, Gustafsson JA, Nebb HI: Liver X receptors as insulin-mediating factors in fatty acid and cholesterol biosynthesis. J Biol Chem 2002, 277(12):10691-10697.
38. Yamamoto T, Shimano H, Inoue N, Nakagawa Y, Matsuzaka T, Takahashi A, Yahagi N, Sone H, Suzuki H, Toyoshima H, Yamada N: Protein kinase A suppresses sterol regulatory element-binding protein-1C expression via phosphorylation of liver X receptor in the liver. J Biol Chem 2007, 282(16):11687-11695.
39. Chen M, Bradley MN, Beaven SW, Tontonoz P: Phosphorylation of the liver X receptors. FEBS Lett 2006, 580(20):4835-4841.
40. Postic C, Dentin R, Denechaud PD, Girard J: ChREBP, a transcriptional regulator of glucose and lipid metabolism. Annu Rev Nutr 2007, 27:179-192.
41. Mitro N, Mak PA, Vargas L, Godio C, Hampton E, Molteni V, Kreusch A, Saez E: The nuclear receptor LXR is a glucose sensor. Nature 2007, 445(7124):219-223. .
•• Authors reported glucose or glucose-6-phosphate can bind to LXR to regulates its activity implicating the role of LXR in glucose sensing.
42. Lazar MA, Willson TM: Sweet dreams for LXR. Cell Metab 2007, 5(3):159-161.
43. Denechaud PD, Bossard P, Lobaccaro JM, Millatt L, Staels B, Girard J, Postic C: ChREBP, but not LXRs, is required for the induction of glucose-regulated genes in mouse liver. J Clin Invest 2008, 118(3):956-964.

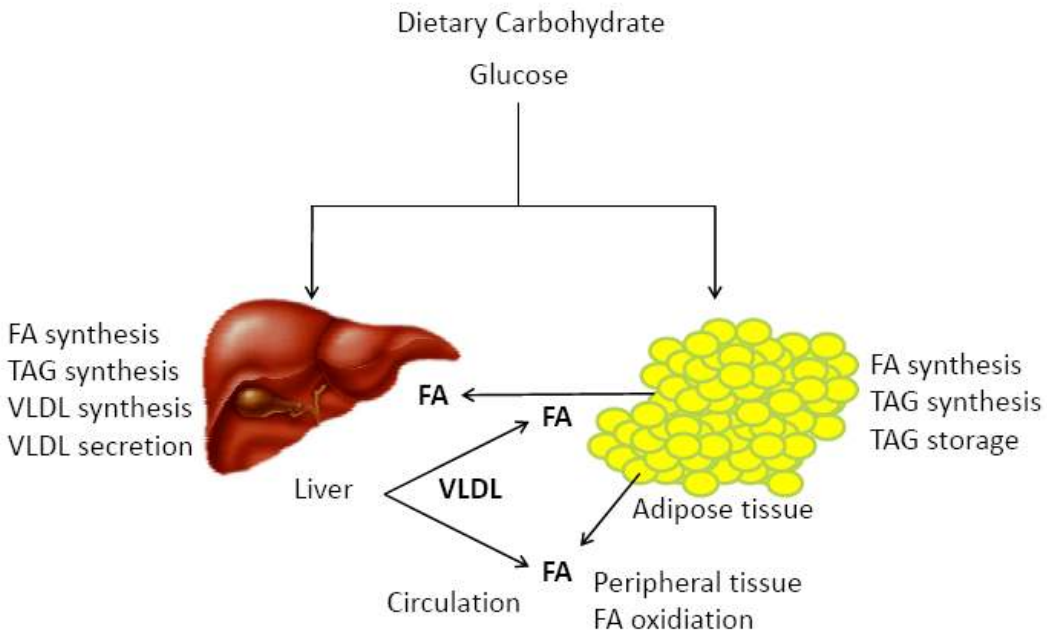

Figure I-1. Upon eating a high carbohydrate diet, de novo lipogenesis takes place in lipogenic tissues, liver and adipose tissue. In liver, de novo synthesized FA are incorporated into TAG to be packaged into VLDL and secreted into the circulation. Peripheral tissues take up FA from VLDL-TAG to use for oxidation. In adipose tissue, de novo synthesized FA, along with FA taken up from circulation, are esterified into TAG for storage. FA, fatty acids; TAG, triacylglycerol; VLDL, very low-density lipoprotein.

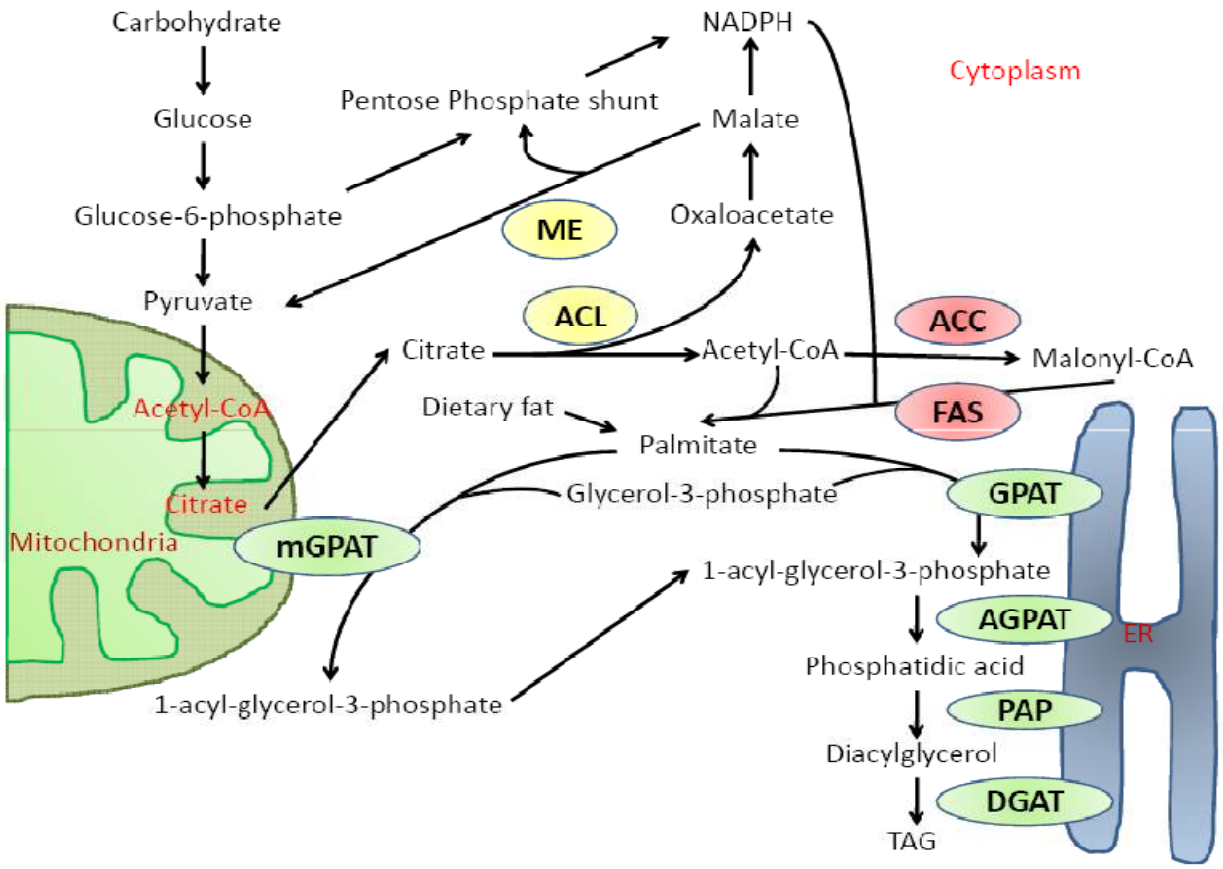

Figure I-2. Pathway of de novo lipogenesis and TAG synthesis. ACL, ATP-citrate lyase; ME, malic enzyme; ACC, acetyl-CoA carboxylase; FAS, fatty acid synthase; mGPAT, mitochondrial glycerol-3-phosphate acyltransferase; DGAT diacylglycerol acyltransferase; GPAT, glycerol-3-phosphate acyltransferase; AGPAT, 1-acylglycerol-3-phosphate acyltransferase; PAP, phosphatidate phosphatase.

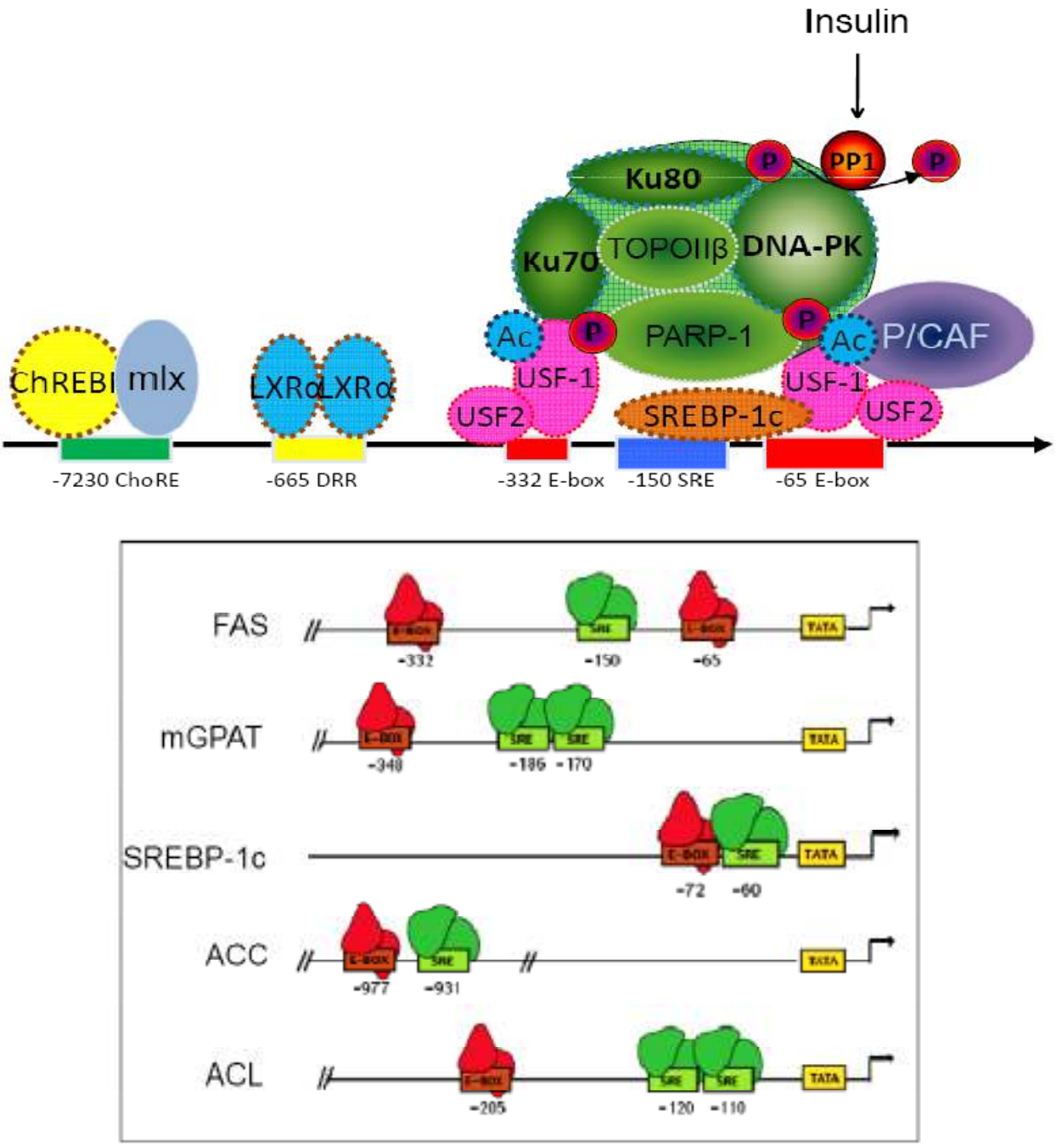

Figure I-3. The *cis*-acting elements and *trans*-acting factors involved in the regulation of transcription of the FAS gene by insulin. Numbers indicate the positions of each element relative to the transcription start site. SRE, sterol-regulatory element; SREBP, SRE-binding protein; TATA, TATA-box; USF, upstream-stimulatory factor. LXR, liver X receptor; ChoRE, carbohydrate-response element; ChREBP, ChoRE-binding protein. Upon feeding, DNA-PK, which is dephosphorylated/activated by PP1, phosphorylates USF-1, which then recruits SREBP-1 and other USF-1-interacting proteins. Thus, DNA-PK-catalyzed phosphorylation of USF-1 allows P/CAF recruitment and subsequent acetylation of USF-1. B. Schematic of E-box and SRE present in the proximal promoter regions of various genes encoding enzymes in FA and TAG synthesis.

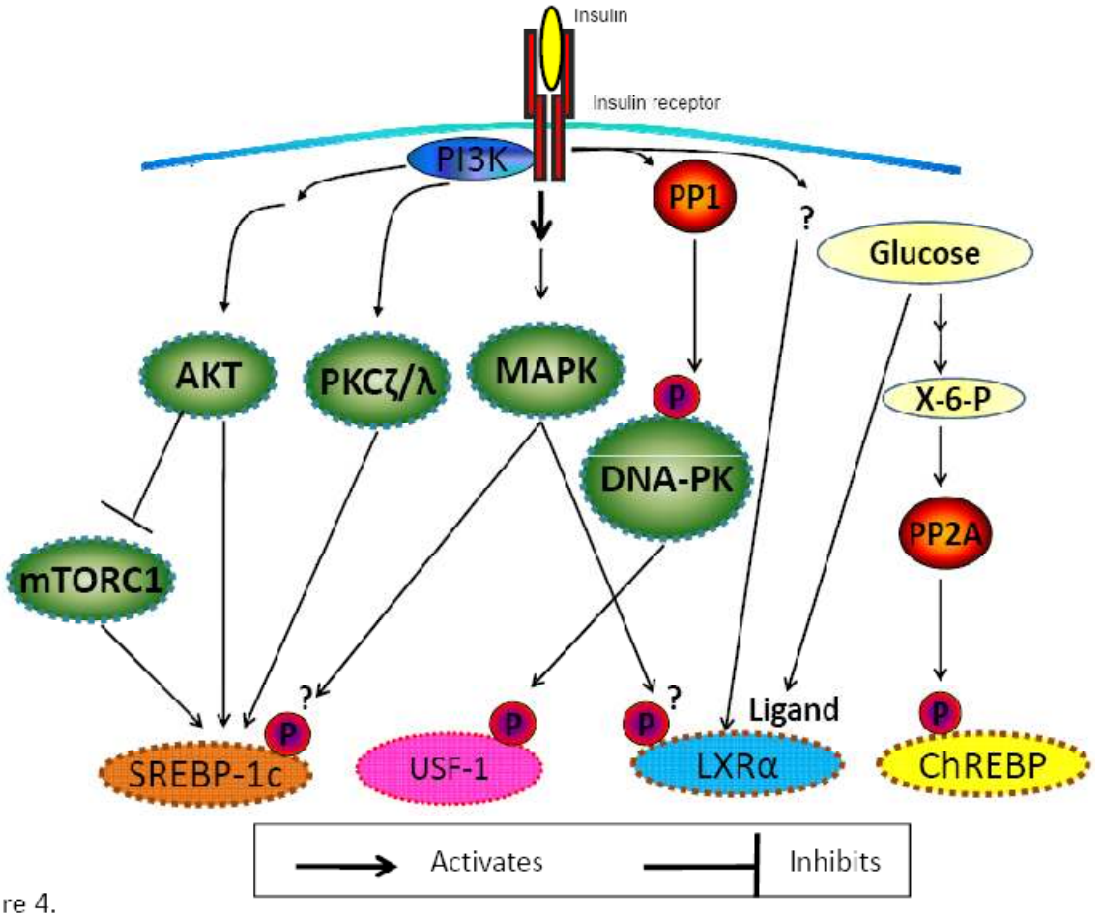

Figure 4.

Figure I-4. Activation of the lipogenic transcription factors, SREBP-1c, USF and LXRa, as well as ChREBP during feeding.

B) DNA-PK: Relaying the Insulin Signal to USF in Lipogenesis

To meet the constant energy requirement in the face of highly variable food supply, mammals employ intricate and precise mechanisms for energy storage. When total energy intake is in excess of energy expenditure such as after a meal, excess carbohydrates are converted to fatty acids (de novo lipogenesis). Excess fatty acids are then converted to triacylglycerol to be stored in adipose tissue and released as oxidative fuels for other tissues during times of energy need such as fasting and exercise. In sustaining the balance between energy excess and energy deficiency, the process of lipogenesis is tightly controlled by nutritional and hormonal conditions[1]. Thus, enzymes involved in fatty acid and fat synthesis are tightly and coordinately regulated during fasting/feeding: Activities of these enzymes are very low in fasting due to the increase in glucagon/cAMP levels. Conversely, in the fed condition, especially after a high carbohydrate meal, activities of these enzymes drastically increase as blood glucose and insulin levels rise[1]. Fatty acid synthase (FAS), a central lipogenic enzyme, plays a crucial role in de novo lipogenesis by catalyzing all of the seven reactions involved in fatty acid synthesis. While FAS is not known to be regulated by allosteric effectors or by covalent modification, its transcription is exquisitely regulated by fasting/feeding and by insulin[1]. The FAS promoter thus provides an excellent model system to dissect the transcriptional activation of lipogenesis by feeding/insulin.

In early studies of insulin regulation of the FAS promoter, we found that Upstream Stimulatory Factor (USF) binding to the -65 E-box is required for transcriptional activation by insulin[2,3,4]. The critical role of USF in the activation of the FAS promoter by insulin was further verified by overexpressing dominant negative or wild type forms of USF[2,3]. The induction of FAS by fasting/feeding was significantly impaired in USF knockout mice[5]. Functional analysis and chromatin immunoprecipitation (ChIP) in mice transgenic for various 5' deletions and mutations of the FAS promoter-CAT reporter gene showed that USF binding to the -65 E-box is required for feeding/insulin-mediated FAS promoter activation in vivo[6]. Notably, USF binding was detected in both fasted and fed states. On the FAS promoter, USF recruits another transcription factor SREBP-1, whose level increases upon insulin treatment via the PI3K pathway[7], to bind the -150 SRE and mediate insulin/feeding responsiveness[8]. Although early studies of ectopically expressed SREBP-1 in cultured cells has been shown to bind the -65 E-box[9], the functional analysis and chromatin immunoprecipitation (ChIP) in mice transgenic for various 5' deletions and mutations of the FAS promoter-CAT reporter gene clearly showed SREBP-1 binds the -150 SRE, but not -65 E-box to activate the FAS promoter during feeding/insulin treatment in vivo[6]. Although SRBEP-1c binding to the -150 SRE is critical for the feeding/insulin response, SREBP-1c itself cannot bind the SRE without being recruited by USF, which is constitutively bound to the -65 E-box[4, 6,10]. Many lipogenic promoters contain a closely spaced E-box and SRE in the proximal promoter region, and a similar mechanism for activation of several lipogenic genes has been documented previosuly[4]. Possibly, the SREBP-1c promoter is also regulated by USF and SREBP-1c in response to feeding/insulin. Thus, USF, along with SREBP-1c, plays a critical role in mediating the transcriptional activation of lipogenesis in response to feeding/insulin.

Studies have shown that LXR may play a role in the transcriptional regulation of lipogenesis by activating SREBP-1c transcription[11]. LXR has also been reported to directly regulate the FAS promoter in cultured cells[12]. A carbohydrate response element (ChoRE)

where ChREBP can bind has also been reported to be present far upstream of the FAS promoter region[13]. Nevertheless, FAS promoter-reporter transgenic mice studies showed that the FAS promoter that contains both an E-box and SRE, but lacks a LXRE or ChoRE, is sufficient for high level activation of the FAS promoter during fasting/feeding suggesting that binding of LXR or ChREBP may not be critical in vivo[6]. Regardless, questions remain in understanding the FAS promoter activation involving USF and SREBP. Apart from HAT/HDAC, are other coactivators required for activation? What chromatin remodeling machinery and mediators are recruited to the FAS promoter? Are there common mechanisms to explain the transcriptional regulation of other coordinately regulated lipogenic genes? Is chromatin folding involved in sharing transcription machineries among lipogenic gene promoters? Further studies are necessary to understand the details of the transcriptional activation of lipogenic genes.

While many metabolic effects of insulin are mediated through protein phosphorylation via the well characterized PI3K cascade which activates PKB/Akt, insulin can also exert metabolic effects through dephosphorylation catalyzed mainly by PP1[14]. Regardless, USF is bound to the E-box on the FAS promoter in both fasted and fed states and neither USF expression nor post-translational modification have been shown to be altered by insulin. Although it is suggested that USF mediates the insulin response of lipogenic gene promoters, the precise mechanism of how USF responds to insulin is not fully understood. We have recently demonstrated that feeding/insulin activates USF through DNA-PK, a kinase involved in DNA damage repair, and subsequently activates FAS transcription[10]. This insulin signaling pathway involving DNA-PK and USF is first initiated by PP1. Although the molecular mechanism is not well understood, the stimulation of PP1 by insulin has been well documented. For example, insulin inhibits breakdown and promotes synthesis of glycogen primarily by activating PP1. PP1 is known to be compartmentalized in cells by discrete targeting subunits[15]. The role of PP1 in transcriptional activation of FAS is to dephosphorylate/activate DNA-PK upon feeding or insulin treatment. USF-1 is then phosphorylated by DNA-PK, allowing recruitment of and acetylation by P/CAF, leading to promoter activation. We also demonstrated a requisite role of DNA-PK by employing DNA-PK deficient SCID mice; USF-1 phosphorylation and acetylation is attenuated, blunting transcriptional activation of FAS and de novo lipogenesis in fasting/feeding[10]. Thus we showed DNA-PK is a player in USF regulated transcriptional activation of the FAS gene.

USF regulated genes coding for other lipogenic and glycolytic enzymes, such as mitochondrial glycerol-3-phosphate acyltransferase, acetyl-CoA carboxylase and glucokinase, might be possible targets of DNA-PK mediated insulin signaling. Furthermore, in addition to USF, various transcription factors have been reported to regulate a battery of metabolic enzymes (those involved in glycolysis, gluconeogenesis and glycogen and triacylglycerol metabolism) that is regulated during fasting/feeding. What transcription factors aside from USF, if any, are phosphorylated by DNA-PK in response to feeding/insulin? In addition to phosphorylating transcription factor(s), DNA-PK might also play a role in regulating enzymes that are under control of feeding/insulin. In this regard, as an insulin signaling molecule, could DNA-PK potentially phosphorylate proteins including kinases that are activated by insulin? Last but not least, with DNA-PK's role as an insulin signaling molecule in activating lipogenesis, can DNA-PK serve as a pharmacological target for obesity and diabetes treatment? Identification

of DNA-PK as a signaling molecule in activating lipogenic genes by insulin has brought us a step closer to understanding how cells respond to insulin.

REFERENCES

1. Sul HS, Smith S. Fatty acid synthesis in eukaryotes. In: Vance DE, Vance JE, eds. *Biochemistry of Lipids, Lipoproteins and Membranes.* 5th ed. Hungary: Elsevier; 2008:156.
2. Wang D, Sul HS. Upstream stimulatory factors bind to insulin response sequence of the fatty acid synthase promoter. USF1 is regulated. J Biol Chem 1995; 270:28716-28722.
3. Wang D, Sul HS. Upstream stimulatory factor binding to the E-box at -65 is required for insulin regulation of the fatty acid synthase promoter. J Biol Chem 1997; 272:26367-26374.
4. Griffin MJ, Wong RH, Pandya N, Sul HS. Direct interaction between USF and SREBP-1c mediates synergistic activation of the fatty-acid synthase promoter. J Biol Chem 2007; 282:5453-5467.
5. Casado M, Vallet VS, Kahn A, Vaulont S. Essential role in vivo of upstream stimulatory factors for a normal dietary response of the fatty acid synthase gene in the liver. J Biol Chem 1999; 274:2009-2013.
6. Latasa MJ, Griffin MJ, Moon YS, Kang C, Sul HS. Occupancy and function of the -150 sterol regulatory element and -65 E-box in nutritional regulation of the fatty acid synthase gene in living animals. Mol Cell Biol 2003; 23:5896-5907.
7. Wang D, Sul HS. Insulin stimulation of the fatty acid synthase promoter is mediated by the phosphatidylinositol 3-kinase pathway. involvement of protein kinase B/Akt. J Biol Chem 1998; 273:25420-25426.
8. Latasa MJ, Moon YS, Kim KH, Sul HS. Nutritional regulation of the fatty acid synthase promoter in vivo: Sterol regulatory element binding protein functions through an upstream region containing a sterol regulatory element. Proc Natl Acad Sci U S A 2000; 97:10619-10624.
9. Kim JB, Sarraf P, Wright M, Yao KM, Mueller E, Solanes G, Lowell BB, Spiegelman BM. Nutritional and insulin regulation of fatty acid synthetase and leptin gene expression through ADD1/SREBP1. J Clin Invest 1998; 101:1-9.
10. Wong RH, Chang I, Hudak CS, Hyun S, Kwan HY, Sul HS. A role of DNA-PK for the metabolic gene regulation in response to insulin. Cell 2009; 136:1056-1072.
11. Repa JJ, Liang G, Ou J, Bashmakov Y, Lobaccaro JM, Shimomura I, Shan B, Brown MS, Goldstein JL, Mangelsdorf DJ. Regulation of mouse sterol regulatory element-binding protein-1c gene (SREBP-1c) by oxysterol receptors, LXRalpha and LXRbeta. Genes Dev 2000; 14:2819-2830.
12. Joseph SB, Laffitte BA, Patel PH, Watson MA, Matsukuma KE, Walczak R, Collins JL, Osborne TF, Tontonoz P. Direct and indirect mechanisms for regulation of fatty acid synthase gene expression by liver X receptors. J Biol Chem 2002; 277:11019-11025.
13. Ishii S, Iizuka K, Miller BC, Uyeda K. Carbohydrate response element binding protein directly promotes lipogenic enzyme gene transcription. Proc Natl Acad Sci U S A 2004; 101:15597-15602.
14. Brady MJ, Saltiel AR. The role of protein phosphatase-1 in insulin action. Recent Prog Horm Res 2001; 56:157-173.
15. Allen PB, Kwon YG, Nairn AC, Greengard P. Isolation and characterization of PNUTS, a putative protein phosphatase 1 nuclear targeting subunit. J Biol Chem 1998; 273:4089-4095.

Chapter II: Direct Interaction between USF and SREBP-1c Mediates Synergistic Activation of the Fatty-acid Synthase Promoter

ABSTRACT

To understand the molecular mechanisms underlying transcriptional activation of fatty-acid synthase (FAS), we examined the relationship between upstream stimulatory factor (USF) and SREBP-1c, two transcription factors that we have shown previously to be critical for FAS induction by feeding/insulin. Here, by using a combination of tandem affinity purification and coimmunoprecipitation, we demonstrate, for the first time, that USF and SREBP-1 interact ***in vitro*** and ***in vivo***. Glutathione ***S***-transferase pulldown experiments with various USF and sterol regulatory element-binding protein (SREBP) deletion constructs indicate that the basic helix-loop-helix domain of USF interacts directly with the basic helix-loop-helix and an N-terminal region of SREBP-1c. Furthermore, cotransfection of USF and SREBP-1c with an FAS promoter-luciferase reporter construct in ***Drosophila*** SL2 cells results in highly synergistic activation of the FAS promoter. We also show similar cooperative activation of the mitochondrial glycerol-3-phosphate acyltransferase promoter by USF and SREBP-1c. Chromatin immunoprecipitation analysis of mouse liver demonstrates that USF binds constitutively to the mitochondrial glycerol 3-phosphate acyltransferase promoter during fasting/refeeding ***in vivo***, whereas binding of SREBP-1 is observed only during refeeding, in a manner identical to that of the FAS promoter. In addition, we show that the synergy we have observed depends on the activation domains of both proteins and that mutated USF or SREBP lacking the N-terminal activation domain could inhibit the transactivation of the other. Closely positioned E-boxes and sterol regulatory elements found in the promoters of several lipogenic genes suggest a common mechanism of induction by feeding/insulin.

INTRODUCTION

Fatty-acid synthase (FAS),[2] a central enzyme in ***de novo*** lipogenesis in mammals, catalyzes all the reactions in the conversion of acetyl-CoA and malonyl-CoA to palmitate. FAS gene transcription is under tight nutritional and hormonal control in lipogenic tissues, namely liver and adipose tissue (1–5). FAS is not known to be regulated by allosteric effectors or covalent modification; rather, its regulation occurs mainly at the transcriptional level. In this regard, other enzymes in the lipid synthesis pathway, such as mitochondrial glycerol-3-phosphate acyltransferase (mGPAT), acetyl-CoA carboxylase (ACC), and ATP-citrate lyase, are also coordinately regulated during fasting/feeding (5–12). Transcription of the FAS and mGPAT genes is not detectable in the lipogenic tissues of fasted mice, whereas feeding a high carbohydrate, fat-free diet increases transcription dramatically, concomitant with a rise in circulating insulin/glucose and a decrease in glucagon levels (7, 8, 12).

By using 3T3-L1 adipocytes, we originally reported that the -65 E-box present in the FAS promoter, which binds the ubiquitous upstream stimulatory factors (USF-1 and USF-2), mediates insulin activation of the FAS promoter (13, 14). However, by generating mice transgenic for various 5′-deletion and mutant FAS promoter-chloramphenicol acetyltransferase constructs, we found that the -131 FAS promoter construct, containing the -65 E-box, is not sufficient for feeding/insulin-mediated activation of the FAS promoter ***in vivo***. Instead, a region from -278 to -131, containing the -150 sterol regulatory element (SRE), as well as a more upstream region from -444 to -278, containing an additional E-box at -332, are required

for high level activation of the FAS promoter by feeding/insulin (15, 16). Furthermore, both the E-box at -65 and the SRE at -150 are required for transcriptional activation of FAS ***in vivo***, as the induction of FAS transcription during fasting/refeeding was abolished in mice transgenic for mutations at these two sites (16).

USFs belong to the class C bHLH/LZ transcription factor family and stimulate transcription by binding to E-boxes (5′-CANNTG-3′) as USF-1/USF-2 heterodimers (17, 18). Sterol regulatory element-binding proteins (SREBPs) also belong to the bHLH/LZ family and stimulate transcription by binding to SREs present in the promoters of their target genes (19–23). However, because of an atypical tyrosine residue, which replaces a conserved arginine present in the basic regions of this family of transcription factors, SREBPs can also bind to E-boxes, at least ***in vitro*** (24, 25). Nevertheless, we have clearly shown by chromatin immunoprecipitation (ChIP) in transgenic mice that SREBP-1c functions through the -150 SRE and that USFs function through the -65 and -332 E-boxes ***in vivo*** (16). Gain-of-function studies using mice doubly transgenic for a truncated active form of SREBP-1a and various FAS-promoter reporter constructs indicate that SREBP-1a, even when overexpressed during fasting, cannot activate FAS transcription through the -65 E-box in a -131 FAS promoter construct (26). Regardless, loss-of-function studies in SREBP-1$^{-/-}$ and USF-1$^{-/-}$ knock-out mice clearly demonstrated that these transcription factors are critical in the regulation of FAS transcription (27–29).

So far, two coregulators for SREBP-1a binding and function have been described. These include Sp1 and NF-Y, both of which seem to be important for mediating a transcriptional response to cellular sterol depletion. For example, SREBP-1a was shown to cooperate with Sp1 on adjacent sites to regulate the FAS (30), low density lipoprotein receptor (31), and acetyl-CoA synthetase-1 genes (32), although a direct physical interaction between SREBP-1a and Sp1 in solution has not been reported. Given the apparent requirements for accessory factors in mediating a maximal response of target genes to SREBP-1a during sterol depletion, the identification of an analogous coregulator for SREBP-1c, the isoform specifically induced during feeding/insulin (15, 33), in mediating the lipogenic response would be an important finding, especially because SREBP-1c is an even weaker transcription factor than SREBP-1a on its own (34). The fact that SREBP-1c only modestly activates the FAS promoter ***in vitro*** (26), but dramatically activates FAS transcription ***in vivo*** (26, 34, 35), implicates the involvement of other factors that may be absent ***in vitro***.

In this study, by using a combination of tandem affinity purification (TAP) and coimmunoprecipitation, we demonstrate that USF and SREBP-1 directly interact ***in vivo***. We have mapped the interaction domains to the bHLH region of each protein as well as an N-terminal region of SREBP-1c. Furthermore, through cotransfection of USF-1 and SREBP-1c in ***Drosophila*** SL2 cells, we show that these two factors synergistically activate the FAS as well as the mGPAT promoters. Importantly, we also show that USF and SREBP bind to the proximal mGPAT promoter ***in vivo*** in a manner identical to that of FAS. Functional domain mapping using USF and SREBP deletion constructs indicates that the activation domains of both proteins are required for synergy. Furthermore, the presence of closely spaced E-boxes and SREs in several lipogenic genes suggests involvement of USF and SREBP in mediating the transcriptional response to fasting/refeeding ***in vivo***.

EXPERIMENTAL PROCEDURES

Plasmids and Constructs. USF-1 was cloned into pCTAP-A (encoding an in-frame streptavidin affinity tag followed by a calmodulin affinity tag) (Stratagene) by PCR amplification of human USF-1 in pCDNA 3.0 (14) using primers containing EcoRI and XhoI sites at the 5′- and 3′-ends, respectively, followed by digestion of amplified inserts and vector with the corresponding enzymes. A FLAG tag was also incorporated into the downstream primer. All PCR amplifications for subcloning USF and SREBP were conducted with *Pfu* Turbo DNA polymerase (Stratagene). Insertion of USF-1 into pCTAP-A was confirmed by sequencing. A Myc tag was added to the C terminus of human SREBP-1c by PCR amplification of SREBP-1a in pCDNA-3.1 (26) using the primers containing an EcoRI site at the 5′-end and an XhoI site and Myc tag at the 3′-end followed by digestion of inserts with EcoRI and XhoI. In all cases where a construct containing the extreme N terminus of SREBP-1c was amplified by PCR from pCDNA3.1-SREBP-1a, the SREBP-1a sequence was converted to SREBP-1c by incorporating nucleotides encoding the first 5 amino acids of SREBP-1c into the 5′-primer. Insertion of the coding region of SREBP-1c-Myc into the correct reading frame was confirmed by sequencing. To construct GST fusions of USF-1 and SREBP-1, primers were designed to amplify the appropriate region of each transcription factor from pCDNA 3.0-USF-1 and pCDNA3.1-SREBP-1a using EcoRI and XhoI sites at the 5′- and 3′-ends. Inserts were cloned into pGEX-4T-3 vector (Amersham Biosciences) followed by digestion with EcoRI and XhoI. Insertion of the USF and SREBP constructs into the correct reading frame was confirmed by sequencing. To construct *Drosophila* expression vectors for USF-1 and SREBP-1c, the coding regions of USF-1 and SREBP-1c were amplified from pCDNA 3.0-USF-1 and pCDNA3.1-SREBP-1a using primers containing BamHI and XhoI sites at the 5′- and 3′-ends, respectively. Inserts were ligated into the pPAC-Sp1 vector (36) after excision of the Sp1 coding sequence by digestion with BamHI and XhoI. Insertion into the correct reading frames was confirmed by sequencing. Reporter constructs for FAS (26) and GPAT (37) have been described previously.

Tandem Affinity Purification. 293FT cells were maintained in Dulbecco's modified Eagle's medium supplemented with 10% fetal bovine serum and 100 units/ml penicillin/streptomycin. The day before transfection, cells were seeded onto 150-mm dishes to achieve a confluency of ~30–40%. Ten 150-mm dishes were each transfected with 10 μg of SREBP-1c-Myc and 5 μg of pCTAP-A-FLAG-USF-1 or 5 μg of pCTAP-A using Lipofectamine (Invitrogen). Cells were maintained in serum free-media for ~16 h following transfection and then replaced with complete media. Approximately 48 h after transfection, cells were harvested by washing twice in PBS followed by scraping. Cells were centrifuged at 1000 × *g* at 4 °C and resuspended in lysis buffer (Stratagene). The TAP protocol was then performed according to the manufacturer's instructions, except that the streptavidin-binding reaction was incubated overnight. Eluted proteins were boiled in SDS loading buffer and resolved on 7.5% SDS-polyacrylamide gels. The presence of USF-1 and SREBP-1c-Myc was determined by immunoblotting with M2 anti-FLAG (Sigma) and anti-Myc antibodies (4A6, Upstate). For copurification of endogenous SREBP-1 protein with USF-FLAG-TAP, HEK 293F cells were transfected with USF-FLAG-TAP vector or empty TAP vector using 293-Fectin (Invitrogen). Nuclear extracts were prepared according to the method of Andrews and Faller (38) 72 h after

transfection and subjected to the TAP protocol. Immunoblotting was performed with anti-FLAG and anti-SREBP-1 antibodies (2A4, Santa Cruz Biotechnology).

Preparation of Mouse Liver Nuclear Extract. Mice were fasted for 48 h and then refed a high carbohydrate, fat-free diet for 18 h. Livers were excised and homogenized in cell lysis buffer (2 m sucrose, 10 mm Tris-Cl, pH 7.4, 25 mm KCl, 5 mm $MgCl_2$, 1 mm EDTA, 10% (v/v) glycerol, 1 mm DTT, protease inhibitor mixture). After centrifugation at 75,000 × *g* for 60 min, the supernatants were discarded, and nuclei were resuspended in high salt extraction buffer (400 mm NaCl, 10 mm Tris-Cl, pH 7.4, 100 mm KCl, 2 mm $MgCl_2$, 1 mm EDTA, 10% (v/v) glycerol, 1 mm DTT, protease inhibitors) and incubated on ice for 30 min. The extracts were centrifuged for 60 min at 250,000 × *g*, and supernatants were used as nuclear extracts for subsequent analysis.

Immunoprecipitation. To determine whether SREBP-1 could be coimmunoprecipitated with USF-1, COS-7 cells were cotransfected with 5 μg of pCDNA-FLAG-USF-1 and 10 μgof pCDNA 3.1-SREBP-1a and harvested 48 h after transfection. Cells were washed twice with PBS, scraped, collected by centrifugation at 1000 × *g* for 10 min, and then lysed by passing through a 21-guage needle 25 times in Triton X-100 lysis buffer (20 mm Tris-Cl, pH. 7.4, 150 mm NaCl, 10% glycerol, 1% Triton X-100, 1 mm EDTA, 1 mm DTT) supplemented with protease inhibitors (Sigma). Lysates were clarified by centrifuging at maximum speed in a tabletop refrigerated centrifuge for 10 min. Antibodies (10 μg/immunoprecipitation) against USF-1 (C-20, Santa Cruz Biotechnology), Sp1 (PEP-2, Santa Cruz Biotechnology), or control IgG were immobilized on protein A-agarose (100 μl) by incubating in 1 ml of Triton X-100 lysis buffer for 2–3 h followed by three washes in the same buffer to remove unbound antibodies. After the last wash, resins were resuspended in 800 μl of Triton X-100 lysis buffer + 200 μlof clarified lysates and incubated overnight with gentle rotation at 4 °C. The following day, immunoprecipitates were washed five times in Triton X-100 lysis buffer followed by two additional washes in the same buffer without Triton X-100. After the last wash, immunoprecipitates were boiled in 50 μlof1× SDS loading buffer, resolved by 7.5% SDS-PAGE, and transferred to nitrocellulose membranes. Immunoblotting was performed with anti-FLAG and anti-SREBP-1 (2A4, Santa Cruz Biotechnology) antibodies as described above. To determine whether USF-1 could be coimmunoprecipitated with SREBP-1c-Myc, cells were transfected with 5 μg of pCDNA 3.1 SREBP-1c-Myc and 10 μgof pCDNA-FLAG-USF-1. Immunoprecipitation was performed as described above except that 10 μg of anti-SREBP-1 antibodies (H160, Santa Cruz Biotechnology) were immobilized on protein A-agarose beads prior to immunoprecipitation.

GST-Pulldown Assay. *Escherichia coli* BL21 cells were transformed with various GST-USF-1 and GST-SREBP-1c fusion constructs. Ampicillin-resistant colonies were grown to an A_{600} of ~0.6 in 250 ml of LB media followed by induction of protein expression by addition of 1 mm isopropyl 1-thio-β-d-galactopyranoside for ~4 h. Cells were harvested by centrifugation at 3000 × *g* for 10 min and resuspended in 9 ml of PBS. Cells were lysed by five 1-min cycles of sonication on ice. Following sonication, glycerol and Triton X-100 were added to concentrations of 10 and 1%, respectively, and incubated with gentle rotation at room temperature for 1 h. Aliquots of the lysates were clarified by centrifugation at maximum speed in a tabletop refrigerated centrifuge. Approximately 500 μg of each lysate containing GST

fusion proteins were added to 100 µlof glutathione-agarose resin and brought to a final volume of 1 ml with PBS bead-binding buffer (1× PBS, 10% glycerol, 1% Triton X-100, 1 mm EDTA, 1 mm DTT). The lysates were incubated with glutathione-agarose resin for 2–3 h followed by three washes in binding buffer to remove unbound GST fusion proteins. FLAG-USF-1 or SREBP-1c in pCDNA 3.1 was used as DNA templates for *in vitro* transcription by T7 RNA polymerase, followed by *in vitro* translation with a rabbit reticulocyte lysate kit (Promega) supplemented with [^{35}S]methionine (2 µl of 10 mCi/ml) in the same reaction. Coupled *in vitro* transcription and translation reactions were incubated at 30 °C for 90 min. Immobilized GST fusion proteins were resuspended in 1 ml of binding buffer, and 5 µlof *in vitro* translated and transcribed ^{35}S-labeled USF-1 or SREBP-1c was added. Complexes were incubated overnight at 4 °C with gentle rocking and then washed seven times in 1 ml of binding buffer followed by boiling in 100 µl of SDS-loading buffer. Captured proteins were resolved by 7.5% SDS-PAGE, and the gels were dried and exposed to film to detect the presence of ^{35}S-USF-1 and ^{35}S-SREBP-1 by autoradiography. In parallel experiments to assess the correct size and integrity of GST fusion proteins, the same procedure was followed except that no *in vitro* transcribed and translated proteins were added to GST complexes, and SDS-polyacrylamide gels were analyzed by Coomassie staining of purified proteins. In experiments where ^{35}S-USF-1 was immunoprecipitated from the reticulocyte lysate reaction, 10% of the *in vitro* translation reaction was mixed with 1 µg of anti-USF-1 antibodies (C-20, Santa Cruz Biotechnology) in 1 ml of PBS bead-binding buffer and immunoprecipitated overnight. Immune complexes were collected with protein A-agarose, washed five times with PBS bead-binding buffer, and eluted with 100 mm glycine, pH 2.5, for 5 min. The eluates were neutralized with 1 m Tris, pH 7.4, and added to GST and GST-SREBP immobilized on glutathione-agarose beads and processed as described. For copurification of endogenous SREBP-1 with GST-USF-1-FLAG from mouse liver, nuclear extracts were added to immobilized GST or GST-USF-1-FLAG fusion protein and incubated overnight with gentle rotation. Following extensive washing, bound proteins were eluted with glutathione and then subjected to a second round of purification on anti-FLAG resin (Sigma). Eluted complexes were subjected to SDS-PAGE and Western blotting to detect the presence of GST-USF-1-FLAG and endogenous SREBP-1.

Transfection of SL2 Cells for Functional Studies. *Drosophila* SL2 cells were maintained as described (39). Approximately 16–20 h before transfection, cells were plated at a density of 0.25×10^6 cells/ml into 48-well plates. Cells were transfected using a standard calcium phosphate precipitation protocol. Each well received the indicated amount of pPAC-USF-1 and/or pPAC-SREBP-1c expression vector (generally 1–25 ng) and 500 ng of luciferase reporter construct along with 10 ng of the control plasmid pAC-5.1/V5-His/*lacZ* for normalization of transfection efficiency. The total amount of DNA transfected per well was brought to 1 µg with the empty expression vector pPAC-0 (470–500 ng/well). Cells were harvested ~48 h after transfection, and luciferase/β-galactosidase activities were assayed using the dual-light system (Applied Biosystems). Each transfection was carried out in triplicate.

*Chromatin Immunoprecipitation***.** Chromatin immunoprecipitation experiments on fasted/refed mice were performed as described previously (16). Primer sequences for amplification of the proximal region of the mouse mitochondrial GPAT promoter were 5′-ACAGCCACACTCACAGAGAATGGGGC-3′ and 5′-GAAGAGGCAGACTCGGCGTTCCGGAG-3′. This produces a predicted amplicon size of 182 bp.

RESULTS

Interaction of USF and SREBP-1c in Vivo

Our previous results in transgenic mice have indicated that binding sites in the FAS promoter for both USF and SREBP-1c are required for activation of FAS transcription by feeding/insulin. We also demonstrated that if binding of USF to the E-box at -65 is prevented by mutation, then SREBP does not bind to the -150 SRE ***in vivo*** (16, 40). In addition, functional studies in USF$^{-/-}$ and SREBP-1$^{-/-}$ mice showed that FAS transcription is significantly reduced when either factor is missing (27, 28). These highly suggestive data led us to investigate a possible mutual interaction of USF and SREBP-1c. To determine whether USF and SREBP-1c can physically interact ***in vivo***, we employed the tandem affinity purification (TAP) technique (41–44). A "bait" protein of interest is tagged with two affinity tags and transfected into cultured cells, then lysates containing putative protein complexes are purified over two successive affinity columns. We have made an in-frame fusion of FLAG-tagged human USF-1 with a streptavidin binding domain and a calmodulin binding domain (Fig. 1***A***). An expression vector containing full-length SREBP-1c with a Myc tag at the C terminus was cotransfected along with USF-FLAG-TAP vector into 293-FT cells, and the lysates were purified over a streptavidin-binding resin and a calmodulin-binding resin, and the eluates were subjected to Western blotting to detect the presence of USF and SREBP-1c. As expected, USF-FLAG-TAP was efficiently purified over the affinity resins (Fig. 1***B, left panel***). As shown by a very robust signal in the USF-FLAG-TAP lysates, SREBP-1c-Myc copurified with USF, but no signal was observed in eluates derived from cells transfected with an empty TAP vector. We next transfected 293F cells with USF-FLAG-TAP vector, and nuclear extracts were subjected to purification over the two affinity resins to determine whether endogenous SREBP-1 could be copurified with USF. As shown in Fig. 1***B*** (***right panel***), a strong signal was observed when the TAP eluates were immunoblotted with an anti-SREBP-1 antibody. These results indicate that USF and SREBP-1 can physically interact ***invivo***.

To confirm that USF interacts with SREBP-1c ***in vivo***, we also performed coimmunoprecipitation experiments. Cells were cotransfected with FLAG-tagged USF-1 (USF-1-FLAG) and SREBP-1a or Myc-tagged SREBP-1c (Fig. 1***A***), and then lysates were used for immunoprecipitation with polyclonal antibodies against USF-1 and SREBP-1. After extensive washing, the immunoprecipitates were resolved by 10% SDS-PAGE and analyzed for the presence of USF-1-FLAG and SREBP-1c-Myc by Western blotting. As shown in Fig. 1***C***, not only USF but also SREBP-1a was detected in anti-USF immunoprecipitates but not in lysates immunoprecipitated with control IgG antisera (***left panel***). Multiple bands were detected by the anti-SREBP-1 antibody, which is consistent with the results of others who have shown that SREBP-1 migrates on SDS-PAGE as a cluster of bands in the 55–70-kDa range (33, 45). In the inverse experiment, lysates were subjected to immunoprecipitation with an anti-SREBP-1 antibody, and as predicted, SREBP-1c-Myc was readily detectable. In addition, USF-1-FLAG was also clearly detected (Fig. 1***C, right panel***). These results further show that USF and SREBP-1c can physically interact ***in vivo***.

We also asked whether endogenous SREBP-1c could be "pulled out" of mouse liver by an affinity-tagged version of USF-1. Full-length USF-1 was cloned in-frame with glutathione ***S***-transferase at the N terminus and expressed in ***E. coli*** (Fig. 1***A, GST-USF-FLAG***). GST-USF-FLAG fusion protein was prepared from ***E. coli*** lysates and immobilized on glutathione-agarose beads followed by extensive washing. Nuclear extracts were prepared from mice that had been fasted for 24 h or fasted and then refed a fat-free, high carbohydrate diet. This manipulation has been shown to dramatically increase the expression of SREBP-1c in liver (15). Liver nuclear extracts were incubated with GST-bound resin or GST-USF-FLAG-bound resin; the resin was eluted with glutathione after washing, and the eluates were then re-incubated with an anti-FLAG affinity resin. The bound proteins were separated by SDS-PAGE and immunoblotted with anti-FLAG and anti-SREBP-1 antibodies. As shown in Fig. 1***D***, no signal was observed in either of the purifications with GST alone. However, immunoreactive bands were clearly detected by the SREBP antibody in the GST-USF-FLAG purifications from both fasted and fasted/refed mouse liver. Furthermore, the signal was higher from refed compared with fasted mice, consistent with the known induction of SREBP-1c. These results further confirm the USF-SREBP-1c interaction.

Identification of Domain(s) of USF that Interact with SREBP-1c

To determine whether the interaction between USF and SREBP is direct, we performed a GST pulldown using bacterially expressed USF and ***in vitro*** translated SREBP-1c. Full-length USF-1 was expressed as a fusion protein with GST in ***E. coli*** (Fig. 2, ***A*** and ***B***). Following immobilization of GST-USF-1 fusion protein on glutathione-agarose beads, ***in vitro*** transcribed and translated and ^{35}S-labeled SREBP-1c was added for overnight incubation. Following extensive washing, eluted complexes were subjected to SDS-PAGE and autoradiography to detect the presence of ^{35}S-SREBP-1c. As shown in Fig. 2***C***, ^{35}S-SREBP-1c was readily detectable in the purification with GST-USF-1 but not with GST alone. These results demonstrate that the interaction between USF and SREBP-1c is direct and specific.

We next asked which domains of USF are required for interaction with SREBP-1c. As shown in Fig. 2***A***, USF-1 consists of an N-terminal activation domain (residues 1–196), a bHLH region (residues 197–260), and the C-terminal leucine zipper (residues 261–310). We constructed a series of USF-1 truncations linked to GST and expressed them in ***E. coli*** (Fig. 2***B***). USF-1 fusion proteins were immobilized on glutathione-agarose beads and then incubated with ***in vitro***-translated ^{35}S-SREBP-1c. As shown in Fig. 2***C***, SREBP-1c efficiently interacted with USF-1-(197–310), even when the entire activation domain has been deleted (***lane 4***), signifying that the activation domain of USF is not required for interaction with SREBP-1c. However, when the bHLH region of USF was deleted, the interaction with SREBP-1c was abolished (Fig. 2***C, lane 6***), showing that the bHLH region of USF is required for interaction with SREBP-1c and that the leucine zipper may not be involved in the interaction. In support of this, SREBP-1c did not interact with the leucine zipper region of USF alone. The interaction of SREBP-1c was clearly detected when the bHLH region of USF alone was fused to GST (Fig. 2***C, lane 5***), indicating that the bHLH region of USF is sufficient for interaction with SREBP. No interaction of SREBP was observed with the activation domain (residues 1–196) of USF alone (Fig. 2***C, lane 7***), confirming that this region is not involved in the USF-SREBP interaction.

Identification of Domain(s) of SREBP-1c That Interact with USF

The domain structure of the mature form of SREBP-1c is shown in Fig. 3***A***. The extreme N terminus of SREBP-1c contains the putative activation domain (46, 47), followed by a Pro/Ser-rich region from amino acids 37 to 153 (23). Like USF, the bHLH/LZ region is located at the C terminus. To determine which region(s) in SREBP-1c interact with USF, we generated a series of 5′-deletion constructs linked to GST and expressed them in ***E. coli*** (Fig. 3, ***A*** and ***B***). Each of these fusion constructs were immobilized on glutathione-agarose beads and incubated with ***in vitro*** transcribed and translated ^{35}S-USF-1. As shown in Fig. 3***C***, USF efficiently copurified with full-length SREBP-1c-(1–436). USF also copurified with a truncated SREBP-1c-(37–436) that contains all regions except the putative activation domain, indicating that the activation domain of SREBP-1c is not required for interaction with USF. This is consistent with our observation that USF also interacts with SREBP-1a (Fig. 1***C, left panel***); the only difference between the SREBP-1a and -1c isoforms lies within the first exon that includes four unique amino acids for SREBP-1c. However, when the entire region from 1 to 299 of SREBP-1c was deleted, the interaction with USF was lost (Fig. 3***C, lane 5***), clearly indicating that the N-terminal region between 37 and 299 is required and that the bHLH region alone is not sufficient for interaction with USF.

To further define the region(s) of SREBP-1c that interact with USF, a second series of truncations was generated and fused to GST (Fig. 3, ***D*** and ***E***). Full-length GST-SREBP-1c-(1–436) was included as a positive control in this experiment. As shown in Fig. 3***F, in vitro*** translated ^{35}S-USF-1 efficiently interacted with GST-SREBP-1c-(1–436). None of the first three GST-SREBP fusion constructs depicted schematically in Fig. 3***D*** were capable of interacting with USF (Fig. 3***F, lanes 4–6***), indicating that these N-terminal regions alone are not sufficient for the interaction. Inclusion of the bHLH region of SREBP in the last two constructs shown in Fig. 3***D*** restored interaction with USF (Fig. 3***F, lanes 7*** and ***8***), although deletion of the Pro/Ser-rich region had no effect. This indicates that two regions of SREBP-1c are required for binding to USF as follows: an N-terminal uncharacterized region spanning amino acids 154–299, and the bHLH region spanning amino acids 300–370.

To confirm that the interaction between USF and SREBP is direct, we performed an additional experiment in which ***in vitro*** translated ^{35}S-USF-1 was first immunoprecipitated from the reticulocyte lysate reaction prior to incubation with full-length GST-SREBP. As shown in Fig. 3***G***, purified USF-1 still interacted with SREBP-1c, further confirming our results indicating that the two proteins interact directly.

Synergistic Activation of the FAS and GPAT Promoters by USF and SREBP-1c

Our previous studies have suggested that the effects of USF and SREBP-1c on FAS transcription are not independent and mutually exclusive (15, 16, 26). This is supported by the observation that FAS transcriptional activity ***in vivo*** is significantly reduced when either factor is missing (27–29) or when their respective binding sites are mutated (16). This is not the case in 3T3-L1 cells, where transfection of either factor alone results in a relatively potent activation of FAS transcription (15, 26). Regardless, because we found that USF and SREBP-1c directly interact ***in vitro*** and ***in vivo***, we hypothesized that introduction of both USF and SREBP-1c

would result in a synergistic activation of the FAS promoter. The "synergy index" can be defined here as the ratio of the fold activation of the FAS promoter when USF and SREBP-1c are cotransfected together to the ***sum*** of their ***individual*** fold activations when each factor is transfected separately. Although reports in the literature vary, a synergy index of 1.5–2.5 seems to be indicative of a high degree of functional cooperativity (48).

To determine whether USF and SREBP-1c can function synergistically in activation of the FAS promoter, we employed ***Drosophila*** SL2 cells. Although ***Drosophila*** has distantly related orthologs of USF (49) and SREBP (50), these cells lack many mammalian transcription factors and are commonly used as a null background for studying functional transcription factor interactions. Therefore, we reasoned that SL2 cells should provide an ideal minimal system for studying synergy between USF and SREBP-1. To that end, we generated ***Drosophila*** expression vectors for human USF-1 and SREBP-1c (pPAC-USF-1 and pPAC-SREBP-1c, respectively). We first asked whether cotransfection of USF and SREBP-1c would result in synergistic activation of the -248 FAS promoter, containing only the E-box at -65 and the SRE at -150 (26). Although introduction of SREBP-1c alone resulted in slight activation of this FAS promoter construct, no significant synergy with USF was observed (Fig. 4***A, left panel***). We next used the longer -444 FAS-Luc reporter construct that includes, in addition to the E-box at -65, a second E-box at -332 that we have shown previously to be a USF-binding site ***in vitro*** and ***in vivo*** (15, 26). A high degree of synergy between USF and SREBP-1c was observed with this construct (Fig. 4***A, right panel***), indicating that binding of USF to the E-box at -65 is not sufficient to mediate maximal synergy with SREBP at the -150 SRE and that the upstream E-box is required for cooperative activation. These results are consistent with our previous ***in vivo*** results, where we demonstrated that a -278-FAS promoter fragment has significantly reduced transcriptional activity in refed transgenic mice and that the region from -278 to -444, containing the -332 E-box, is required for high level activation (15). It is also worth noting that cotransfection of USF alone resulted in only a very modest activation of the FAS promoter (~2.5-fold), which is consistent with the lack of FAS transcriptional activation in livers of fasted mice when only USF is bound (16).

In our previous ***in vivo*** experiments using transgenic animals, we demonstrated that mutation of the -65 E-box abolishes induction of FAS transcription in response to fasting/refeeding (16). To determine whether the -65 E-box is required for synergistic activation by USF and SREBP, we used a -444 FAS promoter construct containing a mutation at the E-box that prevents binding of either protein (26). As shown in Fig. 4***B***, mutation of the E-box at -65 not only abolished synergy between USF and SREBP but also reduced the promoter activity to levels similar to that of the promoterless vector pGL2basic (***filled bars***). Thus, the -65 E-box is crucial for both basal and stimulated activity of the FAS promoter, and these ***in vitro*** results are in agreement with our results ***in vivo***.

To determine whether USF can augment FAS promoter activation by SREBP in a dose-dependent manner, and vice versa, we cotransfected increasing amounts of pPAC-SREBP-1c along with constant pPAC-USF-1 (10 ng/well) and the -444 FAS reporter construct. As shown in Fig. 4***C***, SREBP-1c alone activated the FAS promoter to a maximum of about 20-fold at 10 ng of expression plasmid/well. However, inclusion of 10 ng/well pPAC-USF-1 boosted the activation by SREBP-1c at all concentrations and reached a maximum of ~80-fold at 10 ng of

pPAC-SREBP-1c (Fig. 4***C***). At the highest concentration of SREBP-1c (20 ng/well), we observed a reduction in promoter activity, probably as a result of "squelching." Importantly, no activation of the promoterless pGL2-basic vector by USF or SREBP was observed in these experiments (Fig. 4***C, open squares*** and ***circles***). Overall, these results indicate that SREBP-1c-mediated activation of the FAS promoter is highly synergistic with USF.

In the inverse experiment, we transfected increasing amounts of pPAC-USF-1 in the presence of 10 ng/well pPAC-SREBP-1c. As shown in Fig. 4***D***, the cotransfection of SREBP-1c significantly boosted activation by USF-1 to a maximum of about 60-fold. The highest synergy was observed at 10 ng of each transcription factor/well, similar to the results shown in Fig. 4***C***. At this concentration of each factor in both experiments, the fold activation of the FAS promoter obtained when both USF and SREBP were added together was about three times higher than the sum of their individual fold activations, indicating that USF and SREBP are not acting in an additive and independent manner.

To determine whether the functional collaboration between USF and SREBP-1c might constitute a common mechanism for lipogenic gene induction during feeding/insulin, we next asked whether cotransfection of USF and SREBP-1c would result in synergistic activation of the mGPAT promoter as well. Mitochondrial GPAT catalyzes the condensation of fatty acids with the ***sn***-1 position of glycerol 3-phosphate and, like FAS, is strongly induced by feeding/insulin at the transcriptional level (8, 11). For this purpose we used the -1447 mGPAT promoter, which we previously demonstrated to have high activity in 3T3-L1 adipocytes (37) and which has already been shown to be activated by SREBP-1a through an SRE-like element at -64 (51). There are also several E-boxes in this construct, including one at position -321 which is identical in sequence to that of the E-box in the FAS promoter at -65. Despite this observation, USF alone was unable to activate the -1447 mGPAT promoter in SL2 cells (Fig. 5***A, circles***). However, in the presence of 10 ng/well pPAC-SREBP-1c, USF-1 activated the mGPAT promoter in a dose-dependent manner up to a maximum of ~50-fold at a concentration of 10 ng/well (Fig. 5***A, squares***). Likewise, SREBP-1c alone only weakly activated the mGPAT promoter (Fig. 5***B, circles***) to a maximum of ~9-fold at a concentration of 10 ng/well. However, in the presence of 10 ng/well USF-1, the activation of mGPAT by SREBP was significantly higher at 5 or 10 ng/well (Fig. 5***B, squares***). No squelching was observed in the experiment shown in Fig. 5***B***, probably because we used a lower concentration of SREBP-1c plasmid than in the experiments with the FAS promoter. The fold activation of both transcription factors added together was nearly six times higher than the sum of their individual fold activations (Fig. 5***C, left panel***), indicating a high degree of synergy between USF and SREBP-1c in activation of the -1447 mGPAT promoter.

The proximal mGPAT promoter contains three potential SREBP-binding sites at -64, -170, and -186 (Fig. 5***C***). However, only the SRE-like element at -64 was shown to be important for promoter regulation in 3T3-L1 cells (51). Our results are in agreement with this, as removal of the two distal SREs by deletion did not reduce activation by SREBP-1c alone (Fig. 5***C, right panel***). As shown above, the USF-binding site at -65 in the FAS promoter is not sufficient to mediate synergy with SREBP-1c. Therefore, we next tested whether the single putative USF-binding site present at -321 is sufficient for cooperative activation of the mGPAT promoter with SREBP-1c. For this purpose, we used the shorter -322 mGPAT promoter

construct. As shown in Fig. 5***C*** (***middle panel***), full synergy was still observed with this construct, suggesting that only one E-box for USF is required for synergy with SREBP-1c in activation of the mGPAT promoter. In addition, cooperative activation was completely abolished in the -86 mGPAT construct that includes the SRE at -64 but lacks the upstream E-box (Fig. 5***C***). In fact, SREBP-1c-mediated activation of this construct was actually inhibited by coexpression of USF-1 (Fig. 5***C, right panel, filled bar***). Thus, it is possible that in the absence of a USF-binding site, the interaction of SREBP with USF in solution precludes the binding of SREBP to its target sequence or prevents productive interaction of SREBP with other proteins such as coactivators or general transcription factors.

Occupancy of the FAS and mGPAT Promoters by USF and SREBP in Vivo

We next asked whether USF-1 and SREBP-1 occupy the mGPAT promoter in mouse liver during fasting/refeeding, as we have shown in earlier studies for the FAS promoter. Indeed, by using ChIP analysis, we readily detected ***in vivo*** binding of both USF and SREBP-1c to the proximal region of the mGPAT promoter in a manner indistinguishable from what we observed previously for the FAS promoter (16). Specifically, binding of USF-1 to the FAS and mGPAT promoters was detected in both the fasted and refed states, whereas SREBP-1 binding was detectable only during refeeding (Fig. 6). These results suggest a direct role for both USF and SREBP in regulation of the mGPAT promoter during fasting/refeeding ***in vivo***.

The Activation Domains of USF and SREBP Are Required for Synergistic Activation of the FAS Promoter

We hypothesized that synergy between USF and SREBP-1c could potentially arise through two distinct mechanisms. First, because the bHLH regions of both proteins are involved in the physical interaction, synergy between USF and SREBP-1c could arise from recruitment or enhanced binding of SREBP to the promoter through interaction with USF, as suggested by our previous results ***in vivo***. Second, the synergy could also involve recruitment of one or more coactivators by either or both activation domains of USF and SREBP. First, to determine whether the activation domain of USF is required for synergistic activation of the FAS promoter, we made a single deletion construct of USF-1 that has the entire activation domain deleted (amino acids 1–196) but preserves the bHLH/LZ region (amino acids 197–310). We reasoned that if the mechanism of synergy between USF and SREBP-1c results entirely from recruitment of SREBP by USF, removing the activation domain of USF-1 but preserving its bHLH/LZ region would not attenuate the synergy because the 113-amino acid bHLH/LZ domain of USF still both interacts with SREBP-1c (Fig. 2***C***) and binds E-boxes (52). As shown in Fig. 7***A***, this truncated USF-1 displayed little transactivation (***dotted bar***), consistent with others who have reported that the activation domain of USF is indispensable for transcriptional activation (53). We next cotransfected pPAC-USF-1-(197–310) along with full-length SREBP-1c into SL2 cells at the same concentration of each, which gave maximum synergy observed with full-length USF in this experiment. As shown in Fig. 7***A***, synergy with SREBP-1c was not only abolished with this construct, but cotransfection of the truncated version of USF-1 actually inhibited SREBP-1c-mediated promoter activity by ~70% (Fig. 7***A, checkered bar***). This suggests that the synergy we have observed cannot be attributed

solely to cooperative DNA binding and that recruitment of coactivators may be required for maximal activation.

To determine which domain(s) of SREBP-1c are functionally required for synergy with USF, we next generated a series of N-terminal SREBP-1c deletion constructs (Fig. 7***B***) and cotransfected them along with full-length USF-1 in SL2 cells. The three deletion constructs employed were pPAC-SREBP-1c-(37–436), pPAC-SREBP-1c-(154–436), and pPAC-SREBP-1c-(300–436), which are deleted for the first 36, 153, and 299 amino acids of SREBP-1c, respectively. As shown in Fig. 7***B*** (***middle panel***), deletion of the N-terminal region of SREBP-1c abolishes its transcriptional activity, despite the fact that these constructs contain the bHLH/LZ region and should therefore retain the ability to bind DNA. This functionally confirms the results of others who have shown that the putative activation domain of SREBP-1c maps to the N-terminal region (46, 47, 54). When cotransfected along with 10 ng/well pPAC-USF-1, which itself resulted in only a very modest ~5-fold induction (Fig. 7***B, middle panel***), synergy of the first two SREBP-1c deletion mutants with USF was abolished under conditions in which full-length SREBP-1c was highly synergistic with USF (***filled bar***). Notably, these two SREBP-1c mutants, SREBP-1c-(37–436) and SREBP-(154–436), appeared to actually inhibit the modest 5-fold activation by USF. To determine whether these deletion mutants can inhibit activation by USF when USF is transfected at a higher concentration, we cotransfected 20 ng/well pPAC-USF-1 along with 10 ng/well of each SREBP-1c deletion construct (Fig. 7***B, right panel***). Transfection of 20 ng/well pPAC-USF-1 alone resulted in a more robust ~25-fold activation (Fig. 7***B, dotted bar***), and the first two SREBP-1c deletion constructs displayed a strong inhibition of USF-mediated activation (~74 and ~81%, respectively). However, the shortest construct, containing only the 136-amino acid bHLH/LZ region of SREBP-1c, had no effect on activation by USF (Fig. 7***B, checkered bar***). Importantly, the first two constructs can clearly interact physically with USF (as indicated by GST pulldown assay), whereas SREBP-1c-(300–436) was completely unable to interact with USF (Fig. 3***C***) but still retains the ability to bind DNA (52). These data suggest that the potent inhibition of USF transcriptional activity observed with SREBP-1c-(37–436) and SREBP-1c-(154–436) is not simply because of occupancy of the E-boxes in the FAS promoter by these truncated inactive proteins, but rather that these constructs may interact with USF and function in a dominant negative manner. In addition, these functional deletion studies corroborate the results of our interaction domain mapping and strongly imply that physical interactions between USF and SREBP-1c are required for synergistic activation of the FAS and mGPAT promoters.

DISCUSSION

Tissue-specific and hormonal/nutritional regulation of genes depends critically on the activities and protein-protein interactions within and between transcription factors that bind to the ***cis***-acting elements located in their respective promoters. The molecular mechanism for activation of the FAS promoter by feeding/insulin is likely to be complex and probably involves a multitude of ***cis***-acting elements and protein-protein interactions between several different classes of transcriptional regulators. Our previous results and data from this study support a model in which two principal players, USF and SREBP-1c, directly collaborate to regulate FAS transcription. We show, for the first time, that USF and SREBP-1c not only physically interact, but also synergistically activate the FAS promoter as well as the mGPAT promoter. The role of

USF in activation of FAS transcription by SREBP-1c in response to feeding/insulin appears to be analogous to the roles of Sp1 and NF-Y in mediating transcriptional activation of several genes, including FAS, by SREBP-1a during cellular sterol depletion. SREBPs may generally require auxiliary factors for maximal transactivation (22, 30–32, 55–59). It is worth noting that we observed a strong activation of the FAS and GPAT promoters by USF and SREBP-1c in ***Drosophila*** SL2 cells, which lack Sp1 and NF-Y (31, 36), suggesting that these latter factors are dispensable for high level activation of the FAS promoter, at least ***in vitro***.In contrast, induction of FAS transcription by fasting/refeeding is significantly reduced in USF-$1^{-/-}$ and USF-$2^{-/-}$ knock-out mice (27). Taken together, our results indicate that USF, rather than Sp1 or NF-Y, may be the principal coregulator of SREBP-1c in transcriptional activation of the fatty-acid synthase gene in response to feeding/insulin.

The synergistic activation of the mitochondrial mGPAT promoter by USF and SREBP-1c was an intriguing result, because a role for USF in activation of the mGPAT promoter, to our knowledge, has never been investigated. Previous attempts to show activation of the mGPAT promoter by USF might have failed, as USF alone was unable to activate the mGPAT promoter, as shown in our study. This occurred despite the presence of multiple E-boxes, including one at -321 which is identical in sequence to the -65 E-box in the FAS promoter. In this regard, the ability of USF to activate transcription of target genes independently of other transcription factors may be related to the proximity of the E-box to the TATA-box, as has been shown for activation of the adenovirus major late promoter, where USF and TFIID bind cooperatively (60–62). In fact, the -65 E-box in the FAS promoter is approximately the same distance from the TATA-box as in the adenovirus major late promoter. Thus, the lack of activation of the mGPAT promoter by USF alone may be explained by the absence of any E-box motif in close proximity to the TATA-box. Nevertheless, in the presence of SREBP-1c, USF activates the mGPAT promoter in a dose-dependent manner up to 50-fold (Fig. 5***A***). Because mGPAT is strongly induced by feeding/insulin in a coordinate manner with FAS (8, 11), it is quite possible that interaction between USF and SREBP-1c mediates activation of mGPAT ***in vivo***. In support of this, the pattern of USF and SREBP-1c binding to the mGPAT promoter during fasting/refeeding by ChIP (Fig. 6) was indistinguishable from what we observed previously for the FAS promoter (16).

In this study we provide clear evidence for cooperative activation of both the FAS and mGPAT promoters by USF and SREBP. In addition to FAS and GPAT, there is suggestive evidence for a role of both proteins in activation of another lipogenic enzyme gene, acetyl-CoA carboxylase-α (ACC-α). Barber ***et al.*** (63) used ChIP analysis to show binding of both USF and SREBP-1 to the ovine ACC-α promoter. In this study, USF binding did not change significantly between the nonlactating and lactating states, whereas recruitment of SREBP to the promoter during lactation was associated with a strong induction of ACC-α transcription. In addition, USF was reported to activate the cardiac ACC-β gene through an E-box located in the proximal promoter region (64), and ACC-β has been shown by ChIP to be occupied by SREBP-1 at a nearby site, at least in liver (65). Thus, it is possible that the interactions we have observed here might also be involved in synergistic activation of the ACC promoter. Furthermore, the presence of closely spaced E-boxes and SRE-like elements in the promoters of several lipogenic genes (Fig. 8) implicates a possible role for USF and SREBP-1c in

mediating the overall transcriptional response to fasting/refeeding in a manner similar to FAS and mGPAT (13–16, 26, 51, 65–74).

The fact that USFs and SREBPs are both highly related bHLH/LZ proteins suggests the obvious possibility that USFs and SREBPs could form a heterodimer on E-boxes, as has already been proposed (63). However, several lines of evidence indicate that this is not the case. First, we did not detect heterocomplex formation between USF and SREBP-1c on the -65 E-box in our earlier gel-shift experiments with either nuclear extracts or recombinant proteins (14). Second, in our ChIP assays, we detected binding of USF, but not SREBP-1, to a truncated -131 FAS promoter containing only the -65 E-box, but lacking the -150 SRE, in transgenic mice (16). Furthermore, in our present domain mapping experiments, we have clearly demonstrated that the isolated bHLH/LZ region of SREBP does not by itself interact with USF (Fig. 3***C, lane 5***), which would be highly suggestive of heterodimer formation. In addition, others have shown that a truncated SREBP-1 containing only the bHLH/LZ domain efficiently forms homodimers but does not form heterodimers with other Myc family members, including USF and Max (52). It therefore seems likely that if USF and SREBP formed a heterodimer, then the bHLH/LZs of both proteins alone would be sufficient to mediate a stable interaction. Overall, these observations clearly rule out that the mode of interaction between USF and SREBP involves simultaneous binding of each factor to E-boxes.

Together with our previous ***in vivo*** data, the present results indicate that the mechanism of synergy may involve both recruitment of SREBP by USF to the FAS promoter followed by interaction of the activation domains of both proteins with yet-to-be identified coactivators. This is supported by our observations that deletion of the N-terminal activation domain of either protein potently inhibits the transactivation ability of its partner. A similar observation has been described for the cooperative interaction between USF and Ets-1 on the human immunodeficiency virus, type 1, enhancer in T cells, where deletion of the activation domain of the latter transcription factor inhibits activation by USF ***in vitro*** (75). These authors proposed that recruitment of Ets-1 by USF enables Ets-1 to interact with the basal transcription apparatus. Although the mechanistic details may differ, an analogous situation for the relation between USF and SREBP may explain the results we observe here. Identification of those factors recruited by USF and SREBP-1c would aid in understanding at the molecular level how physical interactions between USF and SREBP lead to synergistic activation of the FAS and mGPAT genes.

In conclusion, we have clearly shown that USF interacts with SREBP-1, and this requires the bHLH domains of both proteins, as well as an additional N-terminal region in SREBP. Cotransfection of USF and SREBP-1c into ***Drosophila*** SL2 cells results in a synergistic activation of the FAS as well as the mGPAT promoters, and the activation domains of both proteins are required for synergy. These studies provide a better understanding of the molecular mechanism leading to increased lipogenic gene transcription and lipid storage in feeding/insulin.

References

1. Gibson, D. M., Lyons, R. T., Scott, D. F., and Muto, Y. (1972) Adv. Enzyme Regul. 10, 187-204
2. Lakshmanan, M. R., Nepokroeff, C. M., and Porter, J. W. (1972) Proc. Natl. Acad. Sci. U. S. A. 69, 3516-3519
3. Nepokroeff, C. M., Lakshmanan, M. R., Ness, G. C., Muesing, R. A., Kleinsek, D. A., and Porter, J. W. (1974) Arch. Biochem. Biophys. 162, 340-344
4. Volpe, J. J., and Vagelos, P. R. (1974) Proc. Natl. Acad. Sci. U. S. A. 71, 889-893
5. Hillgartner, F. B., Salati, L. M., and Goodridge, A. G. (1995) Physiol. Rev. 75, 47-76
6. Sul, H. S., and Wang, D. (1998) Annu. Rev. Nutr. 18, 331-351
7. Soncini, M., Yet, S. F., Moon, Y., Chun, J. Y., and Sul, H. S. (1995) J. Biol. Chem. 270, 30339-30343
8. Paulauskis, J. D., and Sul, H. S. (1988) J. Biol. Chem. 263, 7049-7054
9. Sul, H. S., Wise, L. S., Brown, M. L., and Rubin, C. S. (1984) J. Biol. Chem. 259, 555-559
10. Sul, H. S., Wise, L. S., Brown, M. L., and Rubin, C. S. (1984) J. Biol. Chem. 259, 1201-1205
11. Shin, D. H., Paulauskis, J. D., Moustaid, N., and Sul, H. S. (1991) J. Biol. Chem. 266, 23834-23839
12. Paulauskis, J. D., and Sul, H. S. (1989) J. Biol. Chem. 264, 574-577
13. Wang, D., and Sul, H. S. (1995) J. Biol. Chem. 270, 28716-28722
14. Wang, D., and Sul, H. S. (1997) J. Biol. Chem. 272, 26367-26374
15. Moon, Y. S., Latasa, M. J., Kim, K. H., Wang, D., and Sul, H. S. (2000) J. Biol. Chem. 275, 10121-10127
16. Latasa, M. J., Griffin, M. J., Moon, Y. S., Kang, C., and Sul, H. S. (2003) Mol. Cell. Biol. 23, 5896-5907
17. Sirito, M., Lin, Q., Maity, T., and Sawadogo, M. (1994) Nucleic Acids Res. 22, 427-433
18. Sirito, M., Walker, S., Lin, Q., Kozlowski, M. T., Klein, W. H., and Sawadogo, M. (1992) Gene Expr. 2, 231-240
19. Guan, G., Dai, P., and Shechter, I. (1998) J. Biol. Chem. 273, 12526-12535
20. Guan, G., Dai, P. H., Osborne, T. F., Kim, J. B., and Shechter, I. (1997) J. Biol. Chem. 272, 10295-10302
21. Lopez, J. M., Bennett, M. K., Sanchez, H. B., Rosenfeld, J. M., and Osborne, T. E. (1996) Proc. Natl. Acad. Sci. U. S. A. 93, 1049-1053
22. Ericsson, J., Jackson, S. M., and Edwards, P. A. (1996) J. Biol. Chem. 271, 24359-24364
23. Yokoyama, C., Wang, X., Briggs, M. R., Admon, A., Wu, J., Hua, X., Goldstein, J. L., and Brown, M. S. (1993) Cell 75, 187-197
24. Kim, J. B., Sarraf, P., Wright, M., Yao, K. M., Mueller, E., Solanes, G., Lowell, B. B., and Spiegelman, B. M. (1998) J. Clin. Invest. 101, 1-9
25. Kim, J. B., Spotts, G. D., Halvorsen, Y. D., Shih, H. M., Ellenberger, T., Towle, H. C., and Spiegelman, B. M. (1995) Mol. Cell. Biol. 15, 2582-2588
26. Latasa, M. J., Moon, Y. S., Kim, K. H., and Sul, H. S. (2000) Proc. Natl. Acad. Sci. U. S. A. 97, 10619-10624

27. Casado, M., Vallet, V. S., Kahn, A., and Vaulont, S. (1999) J. Biol. Chem. 274, 2009-2013
28. Shimano, H., Yahagi, N., Amemiya-Kudo, M., Hasty, A. H., Osuga, J., Tamura, Y., Shionoiri, F., Iizuka, Y., Ohashi, K., Harada, K., Gotoda, T., Ishibashi, S., and Yamada, N. (1999) J. Biol. Chem. 274, 35832-35839
29. Liang, G., Yang, J., Horton, J. D., Hammer, R. E., Goldstein, J. L., and Brown, M. S. (2002) J. Biol. Chem. 277, 9520-9528
30. Magana, M. M., Koo, S. H., Towle, H. C., and Osborne, T. F. (2000) J. Biol. Chem. 275, 4726-4733
31. Sanchez, H. B., Yieh, L., and Osborne, T. F. (1995) J. Biol. Chem. 270, 1161-1169
32. Ikeda, Y., Yamamoto, J., Okamura, M., Fujino, T., Takahashi, S., Takeuchi, K., Osborne, T. F., Yamamoto, T. T., Ito, S., and Sakai, J. (2001) J. Biol. Chem. 276, 34259-34269
33. Horton, J. D., Bashmakov, Y., Shimomura, I., and Shimano, H. (1998) Proc. Natl. Acad. Sci. U. S. A. 95, 5987-5992
34. Shimano, H., Horton, J. D., Shimomura, I., Hammer, R. E., Brown, M. S., and Goldstein, J. L. (1997) J. Clin. Invest. 99, 846-854
35. Shimano, H., Horton, J. D., Hammer, R. E., Shimomura, I., Brown, M. S., and Goldstein, J. L. (1996) J. Clin. Invest. 98, 1575-1584
36. Courey, A. J., and Tjian, R. (1988) Cell 55, 887-898
37. Jerkins, A. A., Liu, W. R., Lee, S., and Sul, H. S. (1995) J. Biol. Chem. 270, 1416-1421
38. Andrews, N. C., and Faller, D. V. (1991) Nucleic Acids Res. 19, 2499
39. Roder, K., Latasa, M. J., and Sul, H. S. (2002) J. Biol. Chem. 277, 30543-30550
40. Griffin, M. J., and Sul, H. S. (2004) IUBMB Life 56, 595-600
41. Drakas, R., Prisco, M., and Baserga, R. (2005) Proteomics 5, 132-137
42. Gould, K. L., Ren, L., Feoktistova, A. S., Jennings, J. L., and Link, A. J. (2004) Methods (Amst.) 33, 239-244
43. Puig, O., Caspary, F., Rigaut, G., Rutz, B., Bouveret, E., Bragado-Nilsson, E., Wilm, M., and Seraphin, B. (2001) Methods (Amst.) 24, 218-229
44. Knuesel, M., Wan, Y., Xiao, Z., Holinger, E., Lowe, N., Wang, W., and Liu, X. (2003) Mol. Cell. Proteomics 2, 1225-1233
45. Wang, X., Sato, R., Brown, M. S., Hua, X., and Goldstein, J. L. (1994) Cell 77, 53-62
46. Yang, F., Vought, B. W., Satterlee, J. S., Walker, A. K., Jim Sun, Z. Y., Watts, J. L., DeBeaumont, R., Saito, R. M., Hyberts, S. G., Yang, S., Macol, C., Iyer, L., Tjian, R., van den Heuvel, S., Hart, A. C., Wagner, G., and Naar, A. M. (2006) Nature 442, 700-704
47. Toth, J. I., Datta, S., Athanikar, J. N., Freedman, L. P., and Osborne, T. F. (2004) Mol. Cell. Biol. 24, 8288-8300
48. Kardassis, D., Falvey, E., Tsantili, P., Hadzopoulou-Cladaras, M., and Zannis, V. (2002) Biochemistry 41, 1217-1228
49. Moore, A. W., Barbel, S., Jan, L. Y., and Jan, Y. N. (2000) Proc. Natl. Acad. Sci. U. S. A. 97, 10436-10441
50. Rosenfeld, J. M., and Osborne, T. F. (1998) J. Biol. Chem. 273, 16112-16121
51. Ericsson, J., Jackson, S. M., Kim, J. B., Spiegelman, B. M., and Edwards, P. A. (1997) J. Biol. Chem. 272, 7298-7305
52. Rishi, V., Gal, J., Krylov, D., Fridriksson, J., Boysen, M. S., Mandrup, S., and Vinson, C. (2004) J. Biol. Chem. 279, 11863-11874

53. Kirschbaum, B. J., Pognonec, P., and Roeder, R. G. (1992) Mol. Cell. Biol. 12, 5094-5101
54. Oliner, J. D., Andresen, J. M., Hansen, S. K., Zhou, S., and Tjian, R. (1996) Genes Dev. 10, 2903-2911
55. Xiong, S., Chirala, S. S., and Wakil, S. J. (2000) Proc. Natl. Acad. Sci. U. S. A. 97, 3948-3953
56. Bennett, M. K., and Osborne, T. F. (2000) Proc. Natl. Acad. Sci. U. S. A. 97, 6340-6344
57. Dooley, K. A., Millinder, S., and Osborne, T. F. (1998) J. Biol. Chem. 273, 1349-1356
58. Athanikar, J. N., Sanchez, H. B., and Osborne, T. F. (1997) Mol. Cell. Biol. 17, 5193-5200
59. Yieh, L., Sanchez, H. B., and Osborne, T. F. (1995) Proc. Natl. Acad. Sci. U. S. A. 92, 6102-6106
60. Roy, A. L., Meisterernst, M., Pognonec, P., and Roeder, R. G. (1991) Nature 354, 245-248
61. Sawadogo, M., and Roeder, R. G. (1985) Cell 43, 165-175
62. Meisterernst, M., Horikoshi, M., and Roeder, R. G. (1990) Proc. Natl. Acad. Sci. U. S. A. 87, 9153-9157
63. Barber, M. C., Vallance, A. J., Kennedy, H. T., and Travers, M. T. (2003) Biochem. J. 375, 489-501
64. Makaula, S., Adam, T., and Essop, M. F. (2006) Arch. Biochem. Biophys. 446, 91-100
65. Oh, S. Y., Park, S. K., Kim, J. W., Ahn, Y. H., Park, S. W., and Kim, K. S. (2003) J. Biol. Chem. 278, 28410-28417
66. Sul, H. S., Latasa, M. J., Moon, Y., and Kim, K. H. (2000) J. Nutr. 130, Suppl. 2S, 315S-320S
67. Sato, R., Okamoto, A., Inoue, J., Miyamoto, W., Sakai, Y., Emoto, N., Shimano, H., and Maeda, M. (2000) J. Biol. Chem. 275, 12497-12502
68. Moon, Y. A., Lee, J. J., Park, S. W., Ahn, Y. H., and Kim, K. S. (2000) J. Biol. Chem. 275, 30280-30286
69. Amemiya-Kudo, M., Shimano, H., Yoshikawa, T., Yahagi, N., Hasty, A. H., Okazaki, H., Tamura, Y., Shionoiri, F., Iizuka, Y., Ohashi, K., Osuga, J., Harada, K., Gotoda, T., Sato, R., Kimura, S., Ishibashi, S., and Yamada, N. (2000) J. Biol. Chem. 275, 31078-31085
70. Moustaid, N., Beyer, R. S., and Sul, H. S. (1994) J. Biol. Chem. 269, 5629-5634
71. Misra, S., Sakamoto, K., Moustaid, N., and Sul, H. S. (1994) Biochem. J. 298, 575-578
72. Kim, K. S., Park, S. W., Moon, Y. A., and Kim, Y. S. (1994) Biochem. J. 302, 759-764
73. Moustaid, N., Sakamoto, K., Clarke, S., Beyer, R. S., and Sul, H. S. (1993) Biochem. J. 292, 767-772
74. Hoffer, M. J., van Eck, M. M., Petrij, F., van der Zee, A., de Wit, E., Meijer, D., Grosveld, G., Havekes, L. M., Hofker, M. H., and Frants, R. R. (1993) Biochem. Biophys. Res. Commun. 191, 880-886
75. Sieweke, M. H., Tekotte, H., Jarosch, U., and Graf, T. (1998) EMBO J. 17, 1728-1739

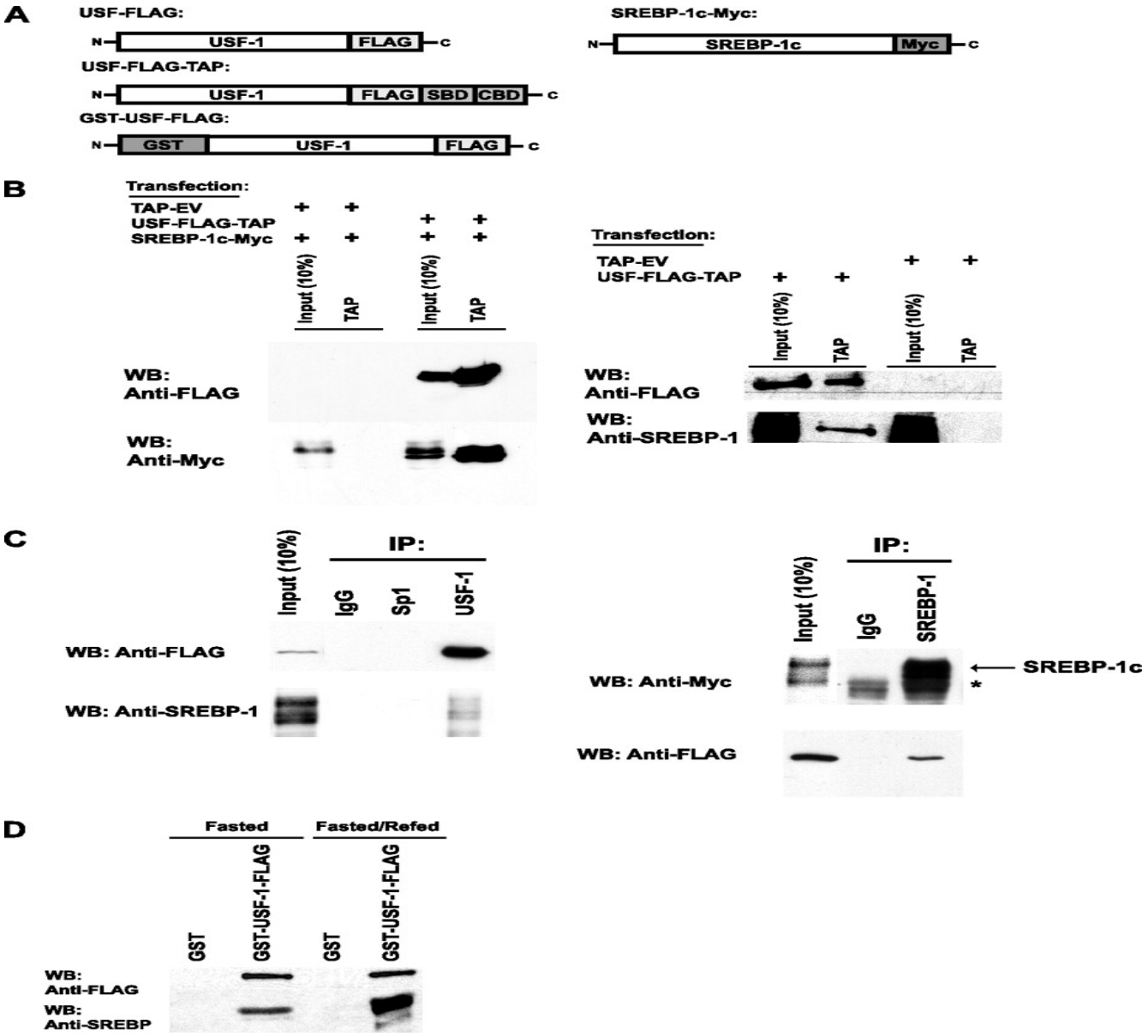

FIGURE II-1. Physical interaction of USF and SREBP-1c *in vivo*. *A,* schematic of constructs. USF-FLAG-TAP consists of a C-terminal FLAG tag and two affinity tags as follows: a streptavidin-binding domain (*SBD*) and a calmodulin-binding domain (*CBD*). GST-USF-FLAG contains a GST tag at the N terminus and a FLAG tag at the C terminus. Human SREBP-1c was tagged with a Myc epitope at the C terminus for detection by Western blotting (*WB*). *B,* 293FT cells were cotransfected with 5 µg of an expression vector for USF-FLAG-TAP or empty TAP vector (*TAP-EV*) and 10 µgof SREBP-1c-Myc (*left panel*). For the experiment shown in the *right panel*, 293F cells were transfected with USF-FLAG-TAP or TAP-EV. TAP complexes were purified using the interplay mammalian TAP system (Stratagene). After purification and elution, samples were boiled in SDS-loading buffer and subjected to 7.5% SDS-PAGE. Transferred proteins were detected by immunoblotting with antibodies against FLAG, Myc, and SREBP-1. *C*, coimmunoprecipitation of SREBP-1a with USF-1 in COS-7 cells (*left panel*) and coimmunoprecipitation of USF-1-FLAG with SREBP-1c-Myc (*right panel*). Cells were transfected with expression vectors for FLAG-USF-1, SREBP-1c-Myc, or SREBP-1a (5–10 µg/dish) and subjected to immunoprecipitation (*IP*) with control IgG, anti-Sp1, anti-USF-1, or anti-SREBP-1 antibodies. Complexes were boiled in SDS sample buffer, resolved on 7.5% SDS-PAGE, transferred to nitrocellulose membranes, and immunoblotted with anti-FLAG, anti-SREBP, or anti-Myc antibodies. * denotes the IgG heavy chain band detected by the secondary antibody used for Western blotting. *D*, two-round purification of SREBP-1 with USF-1 from mouse liver. GST or GST-USF-FLAG fusion protein was prepared in *E. coli* and immobilized on glutathione-agarose beads. Nuclear extracts were prepared from livers of mice that had been fasted or fasted/refed and incubated with purified GST fusion protein. After several rounds of washing, complexes were eluted with reduced glutathione and subjected to a second round of purification with an anti-FLAG resin. Eluted complexes were separated on 7.5% SDS-PAGE, transferred to nitrocellulose membranes, and immunoblotted with anti-FLAG and anti-SREBP-1 antibodies.

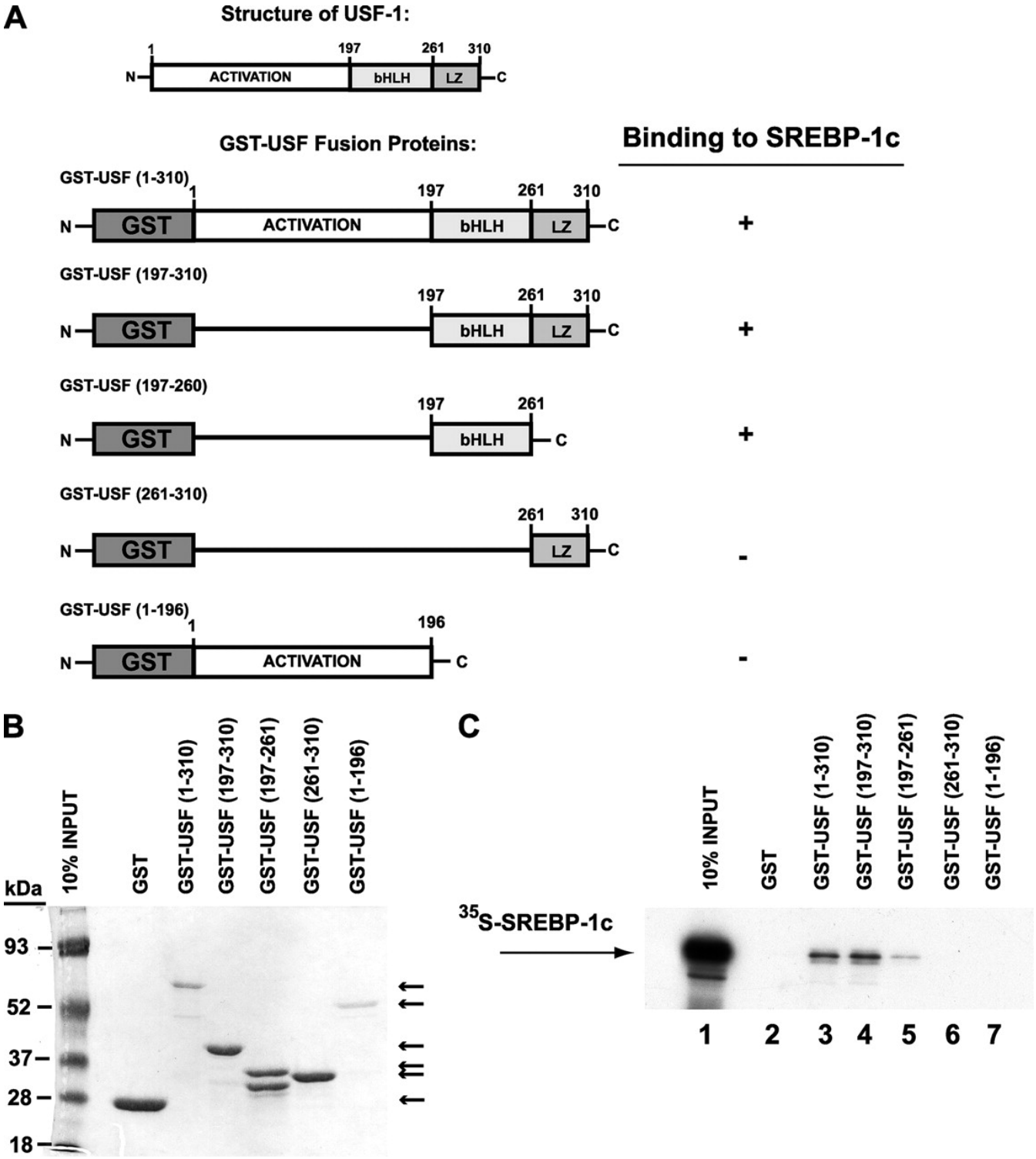

FIGURE II-2. SREBP-1c interacts directly with the bHLH region of USF. *A,* schematic of constructs. USF-1 consists of an N-terminal activation domain (residues 1–196), the bHLH region (residues 197–260), and the leucine zipper (residues 261–310). Various GST-USF-1 fusion constructs are shown. *B,* assessment of correct size and integrity of GST-USF-1 fusion protein by Coomassie staining. *Arrows to the right* of the figure denote the positions of fusion proteins. *C,* autoradiogram showing interaction of *in vitro*-transcribed and -translated ^{35}S-SREBP-1c with various GST-USF-1 fusion proteins. GST-USF fusion proteins were expressed in *E. coli* and bound to glutathione-agarose beads. ^{35}S-SREBP-1c was added to immobilized complexes overnight. Unbound ^{35}S-SREBP-1c was removed by extensive washing, and the complexes were resolved by SDS-PAGE, and captured ^{35}S-SREBP-1c was visualized by autoradiography.

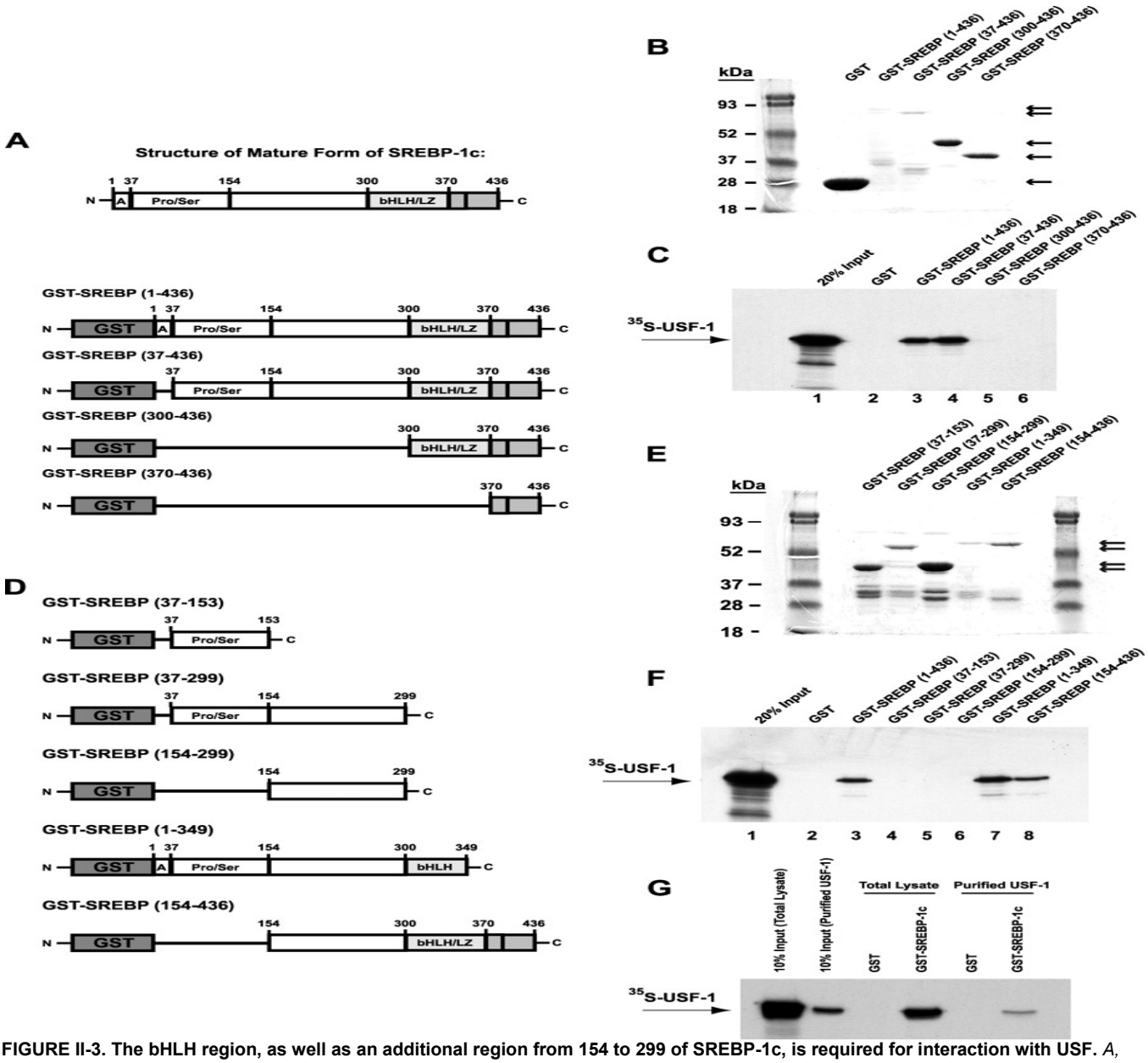

FIGURE II-3. The bHLH region, as well as an additional region from 154 to 299 of SREBP-1c, is required for interaction with USF. *A,* schematic of constructs used. Four 5′-deletions of SREBP-1c were constructed to test requirements for interaction with USF-1. "*A*" denotes the region containing the putative activation domain of SREBP-1c at the N terminus. *B,* assessment of correct size and integrity of GST-SREBP-1c fusion proteins by Coomassie staining. *Arrows to the right* of the figure denote the positions of fusion proteins. *C*, GST-SREBP-1c fusion proteins were expressed in *E. coli* and bound to glutathione-agarose beads. *In vitro*-translated and -transcribed ^{35}S-USF-1 was added to immobilized complexes overnight. Unbound ^{35}S-USF-1 was removed by extensive washing, and the complexes were resolved by SDS-PAGE and captured ^{35}S-USF-1 visualized by autoradiography. *D,* schematic of additional GST-SREBP-1c deletion constructs. Five more deletions of SREBP-1c were constructed to test domain requirements for specific interaction with USF-1. *E,* assessment of correct size and integrity of GST-SREBP-1c fusion proteins by Coomassie staining. *Arrows to the right* of the figure denote the positions of fusion proteins. *F,* GST-SREBP-1c fusion proteins were expressed in *E. coli* and bound to glutathione-agarose beads. *In vitro* translated and transcribed ^{35}S-USF-1 was added to immobilized complexes overnight. Unbound ^{35}S-USF-1 was removed by extensive washing, and the complexes were resolved by SDS-PAGE, and captured ^{35}S-USF-1 was visualized by autoradiography. *G,* immunopurified USF-1 interacts with SREBP-1c. ^{35}S-USF-1 was immunoprecipitated from the *in vitro* transcription/translation reaction in rabbit reticulocyte lysates, and then eluates were added to immobilized GST or GST-SREBP. Complexes were washed extensively followed by SDS-PAGE and autoradiography. *In vitro* translated ^{35}S-USF-1 without immunoprecipitation (*Total Lysate*) was used as a control.

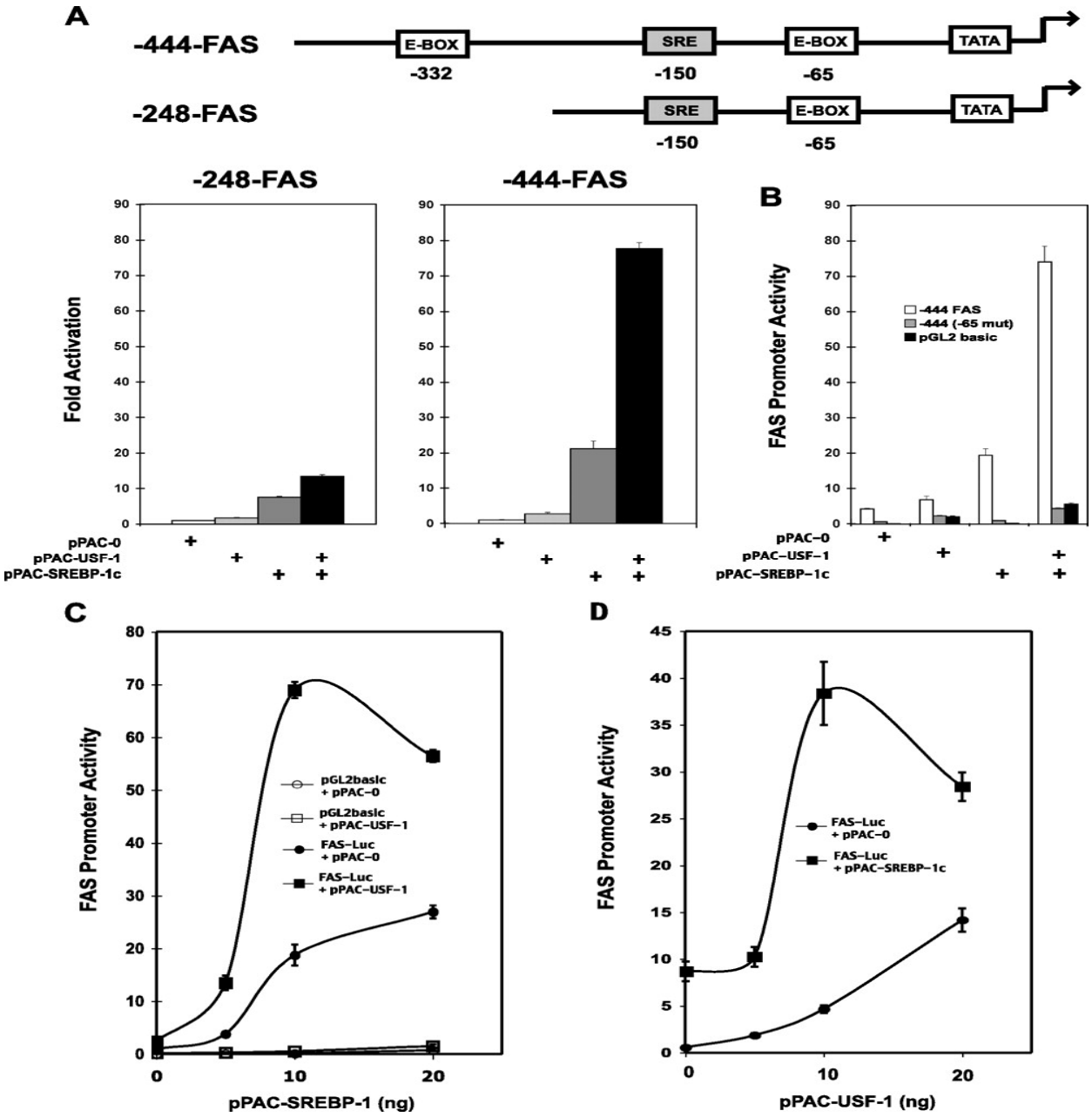

FIGURE II-4. USF and SREBP-1c synergistically activate the FAS promoter in *Drosophila* SL2 cells. *A,* SL2 cells were cotransfected with 10 ng of pPAC-USF-1 and/or 10 ng of pPAC-SREBP-1c with the -248 or -444 FAS promoter construct as indicated, and luciferase activity was measured as described under "Experimental Procedures." Values are expressed as fold activation, where fold activation is calculated as the ratio of normalized luciferase activity observed in the presence of the indicated transcription factor *versus* in the absence of any expression vector encoding USF or SREBP. All transfections were performed in triplicate, and the total amount of expression vector in each transfection was brought to 500 ng with the empty vector pPAC-O. Results are representative of at least two independent experiments. *B,* mutation of the E-box at -65 abolishes induction of FAS promoter activity by USF and SREBP. Results are expressed as normalized promoter activity (luciferase/β-galactosidase, ± S.E.) and are representative of at least two independent experiments. *C,* USF promotes activation of the -444 FAS promoter by SREBP-1c. SL2 cells were cotransfected with increasing pPAC-SREBP-1c and the empty vector pPAC-0 or constant pPAC-USF-1 plasmid (10 ng/well) along with the -444 FAS-Luc reporter construct. Normalized FAS promoter activities are plotted as the ratio of luciferase/β-galactosidase (±S.E.). Transfections were performed in triplicate. Activation of the pGL2 basic vector by USF and SREBP-1c is shown as a control. Results are representative of at least two independent experiments. *D,* SREBP-1c promotes activation of the FAS promoter by USF. SL2 cells were cotransfected with increasing pPAC-USF-1 along with the empty vector pPAC-0 (*circles*) or constant pPAC-SREBP-1c plasmid (10 ng/well; *squares*) along with the -444 FAS-Luc reporter construct. Normalized luciferase activities and fold activation are calculated as in *C*. Results are representative of at least two independent experiments.

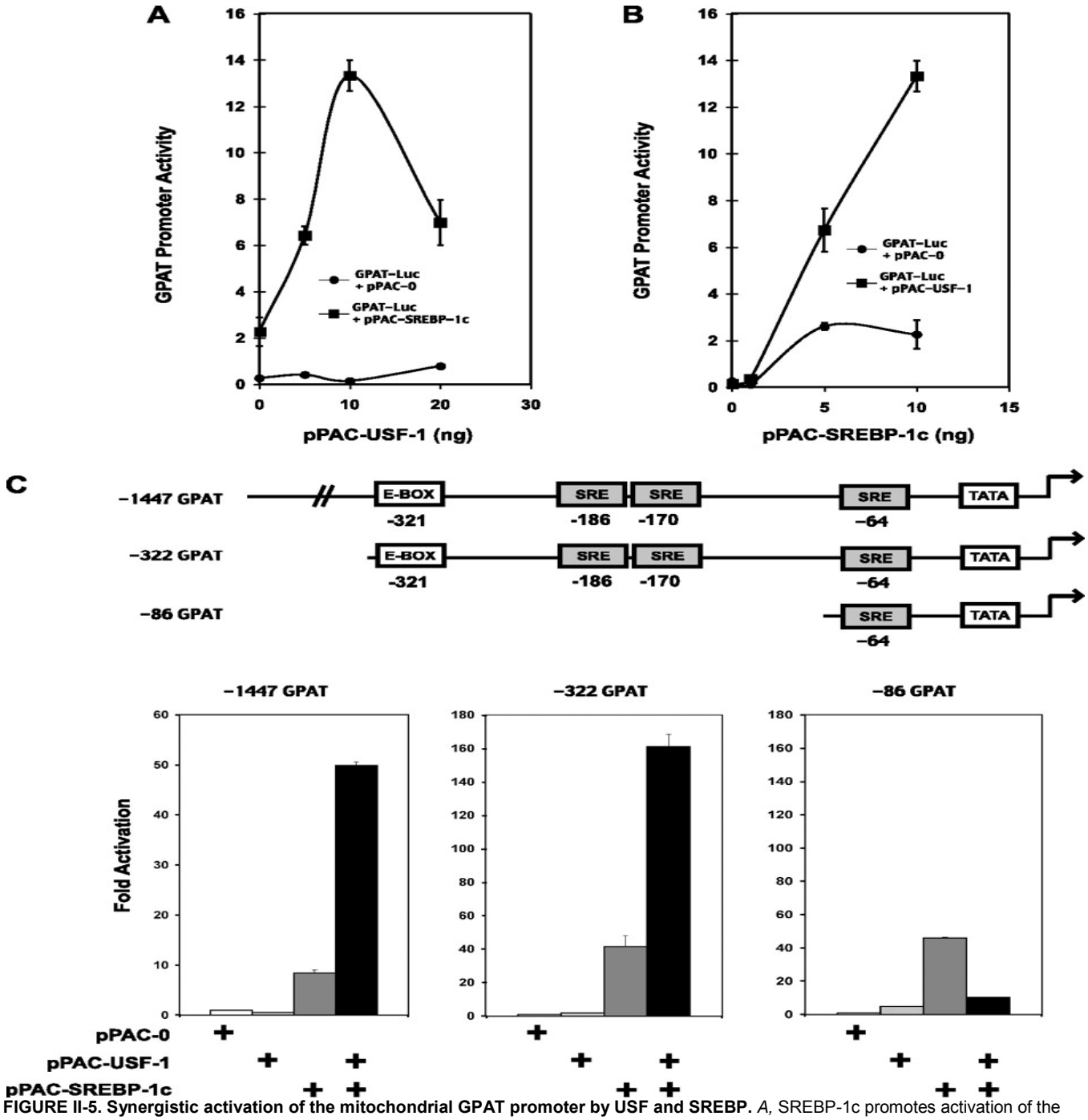

FIGURE II-5. Synergistic activation of the mitochondrial GPAT promoter by USF and SREBP. *A,* SREBP-1c promotes activation of the mGPAT promoter by USF. *Drosophila* SL2 cells were cotransfected with increasing pPAC-USF-1 and the empty vector pPAC-0 (*circles*) or constant pPAC-SREBP-1c (10 ng/well; *squares*) along with the -1447 GPAT-Luc reporter construct. Forty eight hours after transfection, cells were harvested, and luciferase activity was measured as described under "Experimental Procedures." Normalized GPAT promoter activities are plotted as the ratio of luciferase/β-galactosidase (±S.E.). Transfections were performed in triplicate. Results are representative of at least two independent experiments. *B,* USF promotes activation of the mGPAT promoter by SREBP-1c. *Drosophila* SL2 cells were cotransfected with increasing pPAC-SREBP-1c along with the empty vector pPAC-0 (*circles*) or constant pPAC-USF-1 plasmid (10 ng/well; *squares*) and the -1447-GPAT-Luc reporter construct. Normalized luciferase activities are calculated as in *A*. *C,* the -322 GPAT promoter confers synergistic activation by USF and SREBP. Values are expressed as fold activation. In all transfections, the total amount of expression vector in each transfection was brought to 500 ng with the empty vector pPAC-0. Results are representative of at least two independent experiments.

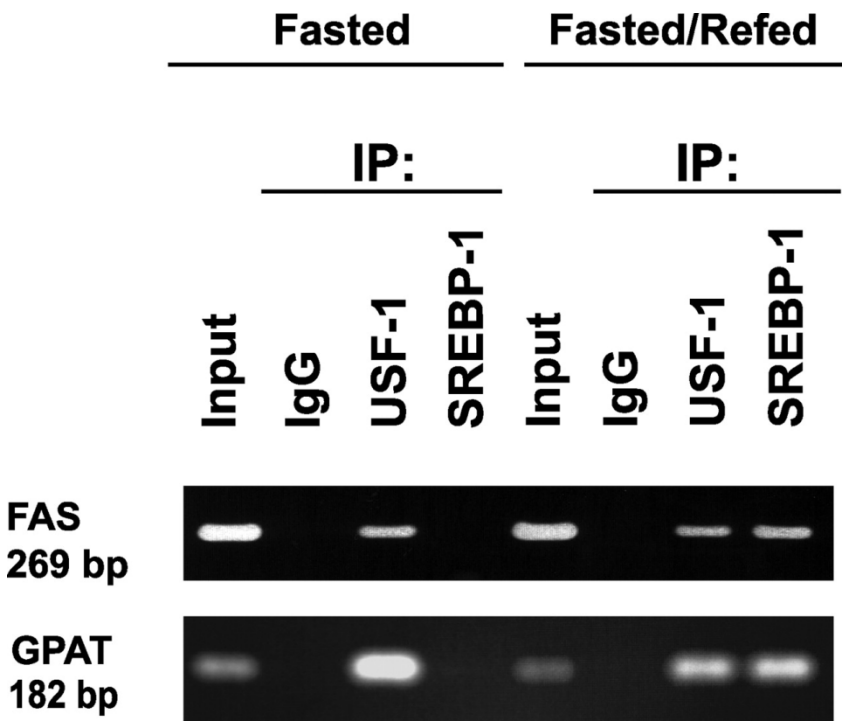

FIGURE II-6. Chromatin immunoprecipitation analyses of USF-1 and SREBP-1 binding to the FAS and mGPAT promoters in mouse liver. Mice were fasted for 24 h or fasted for 24 h followed by refeeding a high carbohydrate, fat-free diet for 18 h. Livers were excised and cross-linked with formaldehyde. Following sonication of chromatin, supernatants were immunoprecipitated (*IP*) with antibodies against USF-1 and SREBP-1. After reversing the cross-links, immunoprecipitated DNA was purified, and the presence of mGPAT promoter fragments was analyzed by PCR. The amplicon size is 269 bp for FAS and 182 bp for mGPAT.

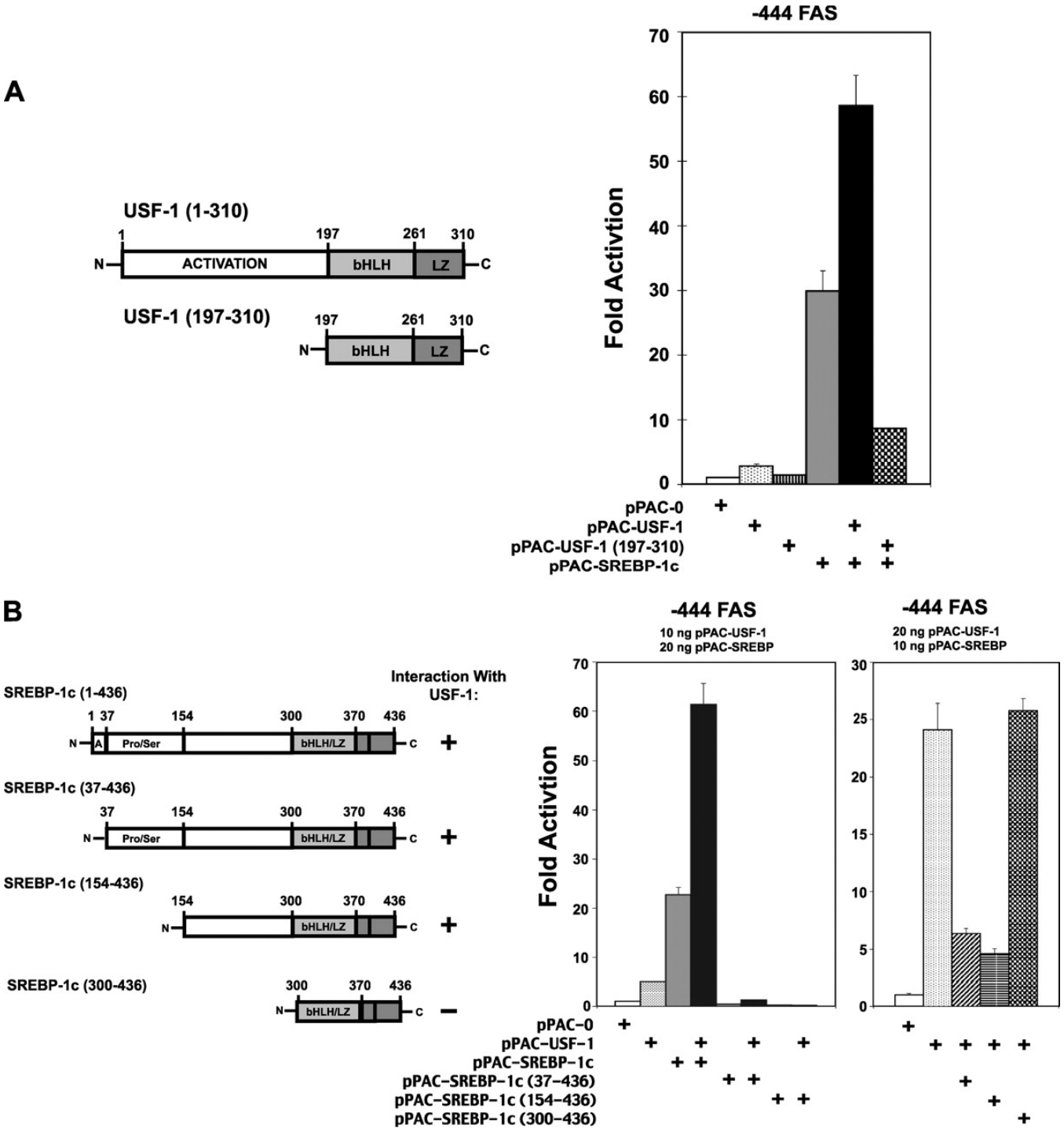

FIGURE II-7. The activation domains of USF and SREBP are required for synergistic activation of the FAS promoter. *A,* N-terminal deletion mutant of USF-1 inhibits activation of the FAS promoter by SREBP-1c. In the *left panel*, a schematic of full-length USF and USF deleted of the first 196 amino acids is shown. SL2 cells were cotransfected with the indicated construct (10 ng/well for each USF construct and 10 ng/well for pPAC-SREBP-1c) along with the -444 FAS-Luc reporter construct. Forty-eight hours after transfection, cells were harvested, and luciferase activity was measured as described under "Experimental Procedures." Results are expressed as fold activation. Each transfection was carried out in triplicate, and essentially identical results were obtained in two independent experiments. *B,* N-terminal SREBP-1c deletion mutants inhibit activation of the FAS promoter by USF. In the *left panel*, a schematic of full-length SREBP-1c and N-terminal deletion constructs in the pPAC-vector used is shown. SL2 cells were cotransfected with 10 or 20 ng/well pPAC-USF-1 in the absence or presence of 10 or 20 ng/well of the indicated SREBP-1 constructs, along with the -444 FAS-Luc reporter. In all transfections, the total amount of expression vector was brought to 500 ng with the empty vector pPAC-0. Results are representative of at least two independent experiments.

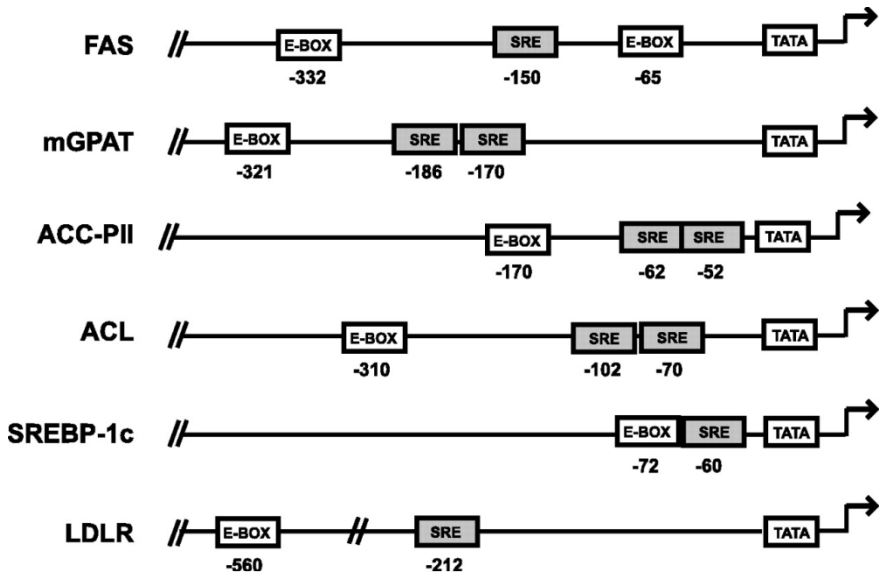

FIGURE II-8. Schematic of E-box and SRE elements present in the proximal promoter regions of various mouse or rat lipid metabolic genes. For simplicity, only the E-boxes in closest upstream proximity to putative SREs are shown, except in the case of the FAS promoter, which contains an additional E-box at -65. In the mouse LDLR promoter, a putative SRE at -212 and an E-box at -560 were identified by sequence analysis. The putative SRE in the mouse LDLR promoter differs by 1 bp from the well characterized SRE in the human LDLR promoter. In the mouse mGPAT and rat ATP-citrate lyase (*ACL*) promoters, the E-boxes shown were also identified by sequence analysis.

CHAPTER III: USF functions as a molecular switch during fasting/feeding to regulate lipogenesis. The role of DNA-PK.

ABSTRACT
Lipogenesis is exquisitely regulated by nutritional/hormonal states. Transcription of fatty acid synthase (FAS), a central enzyme in lipogenesis, is low in fasting but increases drastically with feeding. In transcriptional activation of FAS by feeding/insulin, USF constitutively bound to the -65 E-box is required. Here, we show that USF functions as a molecular switch by recruiting various interacting proteins during the fasting/feeding transition. During feeding/insulin, USF-1 recruits and is phosphorylated by DNA-PK, which is dephosphorylated/activated by PP1. Phosphorylation of USF-1 allows recruitment of and acetylation by P/CAF, resulting in the FAS promoter activation. In fasting, USF-1 is deacetylated by HDAC9 causing promoter inactivation. DNA break/repair components associated with USF also bring about transient DNA breaks during feeding-induced FAS activation. In DNA-PK deficient SCID mice, feeding induced USF-1 phosphorylation/acetylation, DNA-breaks, and FAS activation leading to lipogenesis are impaired, resulting in decreased liver and circulating triglyceride levels. Our study demonstrates that DNA-PK mediates the feeding/insulin-dependent lipogenic gene activation.

INTRODUCTION
To meet the constant energy requirement in the face of highly variable food supply, mammals employ intricate and precise mechanisms for energy storage. During feeding, excess carbohydrates are converted to fatty acids (*de novo* lipogenesis) for synthesis/storage of triacylglyerol, which can then be utilized during energy shortage, i.e., fasting. Lipogenesis is under tight nutritional and hormonal control (Sul and Wang, 1998). Enzymes involved in fatty acid and triglyceride synthesis, such as Fatty Acid Synthase (FAS) (Paulauskis and Sul, 1988; Paulauskis and Sul, 1989) and mitochondrial glycerol-3-phosphate acyltransferase (mGPAT) (Dircks and Sul, 1997; Jerkins et al., 1995; Shin et al., 1991; Yet et al., 1993; Yet etal., 1995), are coordinately regulated during fasting/feeding. The expression of the lipogenic enzymes is very low in fasting, and is drastically upregulated during feeding accompanied by an increase in insulin secretion (Sul et al., 2000; Wang et al., 1998). Thus, precise temporal changes in patterns of gene repression and activation are required for lipogenic gene regulation during fasting and feeding/insulin treatment.

By catalyzing 7 reactions in fatty acid synthesis, FAS is a central enzyme in lipogenesis. Regulation of FAS is mainly at the transcriptional level. We have been studying the FAS promoter as a model system to dissect the transcriptional activation by feeding/insulin. We mapped the insulin response sequence (IRS) of the FAS promoter in cultured cells at the -65 E-box (Moustaid et al., 1993; Moustaid et al., 1994) where Upstream Stimulatory Factor (USF) -1/2 heterodimer binds (Moustaid and Sul, 1991; Sawadogo and Roeder, 1985; Wang and Sul, 1995; Wang and Sul, 1997). Functional analysis and Chromatin Immunoprecipitation (ChIP) in mice transgenic for various 5'-deletions and mutations of the FAS promoter-CAT reporter gene (Latasa et al., 2000; Moon et al., 2000; Soncini et al., 1995), however, showed that both USF binding to the E-box and sterol regulatory element-binding protein-1c (SREBP-1c) binding to the nearby sterol response element (SRE) are required for feeding/insulin mediated FAS promoter activation *in vivo*. Furthermore, although increased expression of SREBP-1c (Shimomura et al., 1999) mainly through insulin activation of the PI3K pathway(Engelman et al., 2006; Taniguchi et al., 2006) to bind the FAS promoter is critical for feeding/insulin response, SREBP-1c itself cannot bind its SRE without being recruited by USF which is constitutively bound to the -65 E-box (Griffin, Wong, et al, 2007; Latasa, Griffin, et al, 2003). Many of the

lipogenic promoters contain closely spaced E-box and SRE at the proximal promoter region and we documented a similar mechanism for activation of FAS and mGPAT promoters (Griffin et al., 2007). Thus, USF, along with SREBP-1c, play a critical role in mediating the transcriptional activation of lipogenesis in response to feeding/insulin.

The requirement of USF (Sirito et al., 1994) in induction of lipogenic genes, such as FAS, has been demonstrated in USF deficient mice (Casado et al., 1999). In humans, SNP studies have implicated USF-1 as a prime candidate of familial combined hyperlipidemia (FCHL) (Pajukanta et al., 2004). How does USF regulate lipogenic gene transcription? USF levels do not change during fasting/feeding and it is constitutively bound to the FAS promoter in both conditions (Wang and Sul, 1995). It is possible that posttranslational modifications of USF underlie its function during fasting/feeding. Insulin regulates metabolism primarily through protein phosphorylation by the well characterized PI3K cascades (Engelman et al., 2006). Many of the metabolic effects of insulin are also mediated by protein dephosphorylation catalyzed mainly by protein phosphatase-1 (PPl) (Brady and Saltiel, 2001). In this regard, USF has been previously reported to be phosphorylated by various kinases (Corre and Galibert, 2005). However, the significance of USF phosphorylation in lipogenic gene transcription during feeding/insulin is not known. Moreover, USF may not independently function to regulate transcription but recruit coactivators/corepressors. Such recruited factors may also include signaling molecules that transduce extracellular signals to bring about covalent modifications of USF. Thus, it can be postulated that USF and/or its potentially recruited cofactors need to be regulated by dynamic modifications such as phosphorylation/dephosphorylation in response to feeding/insulin.

Here, we report a novel mechanism for the sensing of nutritional/hormonal status by USF to regulate lipogenic gene transcription. We demonstrate that USF-1 phosphorylation by DNA-dependent protein kinase (DNA-PK), which is first dephosphorylated/activated by PP1, is an immediate response to feeding/insulin treatment. Phosphorylation of USF-1 also allows recruitment and acetylation by p300 associated factor (P/CAF). In contrast, during fasting, USF-1 association with histone deacetylase 9 (HDAC9) leads to USF-1 deacetylation. Thus, upon feeding, DNA-PK deficient SCID mice show impaired USF-1 phosphorylation/acetylation, DNA-break, transcriptional activation of the FAS gene and lipogenesis. Our present study, for the first time, shows that DNA-PK is critical for the feeding-dependent activation of lipogenic genes, linking DNA-PK to the insulin signaling pathway.

RESULTS

Identification of USF interacting proteins and their occupancy on lipogenic gene promoters during fasting/feeding

We have previously shown that USF is required for regulation of FAS promoter activity in fasting/feeding (Wang and Sul, 1995; Wang and Sul, 1997). However, USF is constitutively bound to the FAS promoter (Griffin et al., 2007; Latasa et al., 2003). We postulated that USF may repress or activate the FAS promoter by recruiting distinct cofactors in fasted and fed conditions. We performed tandem affinity purification (TAP) and mass spectrometry (MS) analysis. The USF interacting proteins were purified from nuclear extracts prepared from 293 cells overexpressing USF-1 tagged with streptavidin and calmodulin binding peptides (TAP-tagged) as well as a FLAG epitope at its carboxyl terminus. In addition to USF-1 and USF-2,

we identified 7 polypeptides in the eluates by MS analysis (Fig. 1A, left panel and S. Table 2). These proteins fall into 3 categories, a) DNA break/repair components DNA-PK and its regulatory subunits, Ku70, Ku80, as well as poly(ADP-ribose) polymerase-1 (PARP-1), and Topoisomerase IIß (TopoIIβ), b) protein phosphatase PP1, and c) P/CAF which belongs to the histone acetyltransferases (HAT) family. Interestingly, we detected some of the USF interacting proteins to be poly(ADP-ribosyl)ated (S. 5E). TAP using cells that were first cross-linked by DSP showed identical USF-1 interacting proteins (data not shown).

We detected at least five of the polypeptides having molecular weights corresponding to the above identified proteins by silver staining of the TAP-eluates separated by SDS-PAGE (Fig. 1A, 2nd left panel). Blue native (BN) gel electrophoresis of the TAP-eluates revealed the presence of a large USF-1 containing complex (S. 1B). Immunoblotting of the eluates using antibodies against each of the 7 polypeptides further confirmed the presence of all 7 polypeptides that were co-purified with TAP-tagged USF-1 (Fig. 1A, 3rd left panel). These identified proteins were specific to USF-1, because none of them were found with the control TAP-tag. Confirming USF-1 interaction, coimmunoprecipitation followed by immunoblotting revealed the presence of all interacting proteins in endogenous USF-1 immunoprecipitates (Fig. 1A 2nd right panel). Furthermore, GST-pull down assay showed that DNA-PK and PARP-1, but not TopoII□, Ku70/Ku80 and PP1, can directly interact with USF-1 (S. 1A).

We also attempted to purify and identify USF interacting proteins by incubating liver nuclear extracts with bacterially expressed TAP-tagged USF immobilized on agarose beads. MS analysis identified an additional USF interacting protein HDAC9, a transcriptional corepressor that belongs to the class II HDAC family, which was co-purified with USF-1 when the nuclear extracts from fasted mice were used (data not shown). The interaction between HDAC9 and USF-1 was confirmed by detection of HDAC9 co-purified with USF-1 by TAP in cells overexpressing HDAC9 and USF-1 (Fig. 1A, right panel). Overall, except for P/CAF which has been implicated to function with USF for histone modification in chromosomal silencing (West et al., 2004), none of the above proteins have previously been shown to interact with USF.

All of the USF interacting proteins were expressed in lipogenic tissues, liver and white adipose tissue (WAT) (Fig. 1B). We next performed ChIP in livers of fasted and fed transgenic mice expressing a CAT reporter gene driven by the -444 FAS promoter, a minimal FAS promoter sufficient for full response to fasting/feeding and diabetes/insulin treatments (Latasa et al., 2000; Latasa et al., 2003; Moon et al., 2000). As shown before, we detected binding of USF in both fasted and fed conditions (Fig. 1C, left panel). In the fasted state, however, we detected the corepressor HDAC9 bound to the FAS promoter, but not other interacting proteins that we identified by TAP-MS. Upon feeding, HDAC9 was no longer bound to the promoter, but the FAS promoter was now occupied by the coactivator P/CAF, DNA break/repair components that include DNA-PK, Ku70/80, PARP-1, TopoIIβ, as well as PP1 (Fig. 1C, left panel). We also performed ChIP analysis of the mGPAT promoter using antibodies against proteins that represent each of the 3 categories of the USF interacting proteins. Similar to what we observed with the FAS promoter, USF-1 was bound to the mGPAT promoter in both fasted and fed conditions (Fig. 1C, right panel). Furthermore, as seen with the FAS promoter, HDAC9 was bound to the mGPAT promoter only in fasting, whereas DNA-PK, PPI and P/CAF were bound only in the fed state. We also verified the regulated expression of FAS and mGPAT in these mice. As predicted, FAS and mGPAT mRNA levels were very low in livers of

fasted mice, but upon feeding, they were induced drastically to approximately 50 and 25- fold, respectively (Fig. 1D). The similar binding pattern of USF interacting proteins suggests a common mechanism for lipogenic induction involving USF and its interacting proteins in response to feeding. Overall, USF-1 is constitutively bound to the FAS and other lipogenic promoters in both metabolic states, while USF interacting proteins are bound in a fasting/feeding dependent manner. We next investigated whether this is due to the differential interaction of USF with these proteins by employing insulin responsive HepG2 cells overexpressing USF-1. The levels of various USF interacting proteins in HepG2 cells were similar when cells were cultured in the presence or absence of insulin (S. 1D). As shown in Figure 1E, in insulin treated cells, USF-1 preferentially coimmunoprecipitated with those proteins that were found to be bound to the lipogenic promoters in the fed condition, whereas in the absence of insulin, USF-1 preferentially interacted with HDAC9.

To further address whether the binding of the various interacting proteins to the FAS promoter is USF dependent, we performed ChIP in transgenic mice containing CAT driven by the -444 FAS promoter with a specific mutation at the USF binding site of -65 E-box (-444(-65m)). We have previously shown that, due to the loss of the critical -65 E-box where USF binds, the -444(-65m) FAS promoter does not have any activity although the promoter contains an additional USF binding site at -332 (Latasa et al., 2003). We did not detect binding of any of the USF-1 interacting proteins to this FAS promoter containing the -65 E-box mutation, even though USF-1 was bound to the -332 E-box in both fasted and fed states (Fig. 1F, left panel). Furthermore, siRNA-mediated knock-down of USF-1 prevented recruitment of the USF-1 interacting proteins to the wild type FAS promoter (Fig. 1F, right panel). Taken together, these data clearly demonstrate the requirement of USF-1 binding to the -65 E-box for recruitment of various proteins to the FAS promoter.

Since USF binding to the E-box is necessary for SREBP binding to the nearby SRE in lipogenic promoters and USF and SREBP-1 directly interact for promoter activation (Latasa et al., 2003; Griffin et al., 2007), we examined whether the binding of the USF-1 interacting proteins to the FAS promoter is dependent on the SREBP-1 binding to SRE. We performed ChIP in transgenic mice containing CAT driven by the -444 FAS promoter with a specific mutation at the -150SRE (-444(-150m)). As shown in Figure 1G, we could not detect recruitment of the various interacting proteins to the FAS promoter containing the -150 SRE mutation during feeding. Similar results were observed in HepG2 cells when transfected with -444(-150m) FAS-Luc or SREBP-1 siRNA (S. 2A & 2B), correlating with the diminished FAS promoter activation (S. 2E). As a control, we examined the p53 promoter which has a proximal E-box but does not respond to feeding/insulin (S. 1C and S. 2D). Upon insertion of an artificial SRE, the p53 promoter was activated by USF-1 recruiting various interacting proteins in response to insulin (S. 2D & 2E), demonstrating that nearby SRE is critical for USF-1 to recruit various interacting proteins.

As shown, the components of DNA break/repair machinery were recruited to the FAS promoter in fed state. In this regard, it has recently been reported that a transient DNA break is required for estrogen receptor regulated transcription (Ju et al., 2006). By end-labeling using biotin-UTP and subsequent ChIP, we clearly detected DNA breaks in the -444 FAS-CAT as well as the endogenous FAS promoters after 3 hrs of feeding, a time point when binding of DNA-PK and TopoIIβ was detected (Fig. 1H). The observed DNA breaks in the FAS promoter region

preceded the maximal FAS transcription that occurs 6 hrs after the start of feeding (Paulauskis and Sul, 1989).

Feeding induced phosphorylation of USF-1

Constitutive binding of USF-1, despite its differential recruitments during fasting/feeding, prompted us to investigate whether USF-1 is posttranslationally modified. We immunoprecipitated USF-1 from liver nuclear extracts of fasted or fed mice and performed MS analysis. Notably, we detected a phosphoserine residue at the S262 of USF-1 only in nuclear extracts from fed mice. We detected higher S262 phosphorylation of USF-1 in the fed state than in the fasted state (Fig. 2A, panel 2) using antibodies against a USF-1 peptide containing phosphorylated S262 (referred as anti-P-USF-1) that we generated. ChIP analysis of the FAS-CAT promoter using anti-P-USF-1 showed that this specific phosphoUSF-1 occupied the FAS promoter only in the fed state, even though USF-1 occupancy was detected in both fasted and fed conditions (Fig. 2B). Similarly, USF-1 bound to the mGPAT promoter was phosphorylated at S262 in fed state (S. 5D). To test the functional significance of this S262 phosphorylation, we expressed FLAG-tagged-USF-1 containing a mutation at the S262 (S262D or S262A). We detected similar protein levels of transfected S262 mutants and wild type (WT) USF-1 (Fig. 2C, bottom panel). ChIP analysis of the FAS promoter using anti-FLAG antibodies showed no differences in promoter occupancy between WT and FLAG-tagged USF-1 proteins harboring S262 mutation (Fig. 2C, top panel). However, the S262D mutant that mimics hyperphosphorylation activated the FAS promoter at a much higher level than WT USF-1, whereas the nonphosphorylatable S262A mutant could no longer activate the FAS promoter (Fig. 2C, bottom panel). By immunoblotting lysates from these cells, we also detected changes in FAS protein levels corresponding to the FAS promoter activity (Fig. 2C, bottom panel). Taken together, these data suggest that the feeding dependent phosphorylation of USF-1 at S262 is linked to FAS promoter activation.

Feeding induced acetylation of USF-1

As shown in Fig. 1, USF-1 interacting proteins, HDAC9 and P/CAF, occupied the lipogenic gene promoters in fasted and fed states, respectively. During the MS analysis of USF-1 for posttranslational modification(s), we identified two acetylated lysine residues at K237 and K246 of USF-1. However, when we performed MS analysis of immunoprecipitates from cells cotransfected with USF-1 and P/CAF that interacts with USF in the fed state, we detected acetylation of only K237, but not K246. We therefore raised antibodies against USF-1 peptide containing acetylated K237 (anti-Ac-USF-1) and used them to compare acetylation of USF-1 at K237 in fasted and fed states. Indeed, we detected higher K237 acetylation of USF-1 in the fed state (Fig. 2D, panel 2) compared to the fasted state. ChIP analysis of the FAS-CAT promoter using anti-Ac-USF-1 showed that the USF-1 bound to the FAS promoter was acetylated at K237 only in the fed state, even though USF-1 was bound to the FAS promoter in both fasted and fed states (Fig. 2E). These data indicate that K237 is likely to be a regulatory site of USF-1 during fasting/feeding and its acetylation might be catalyzed by P/CAF in the fed state.

To test the functional effects of this putative acetylation site, we expressed FLAG-tagged USF-1 with a mutation at the K237 (K237A or K237R) in 293 cells. ChIP analysis of the FAS promoter using anti-FLAG antibodies showed no difference in recruitment among WT USF-1, FLAG tagged USF-1 with the K237A mutation that mimics hyperacetylation, and the FLAG tagged USF-1 with nonacetylatable K237R mutation (Fig. 2F, top panel). However, in the FAS

promoter-reporter assay, cotransfection of the K237A mutant activated the FAS promoter at a much higher level than WT USF-1, whereas 237R mutant could no longer activate the FAS promoter (Fig. 2F, bottom panel). These differences in promoter activation were reflected in FAS protein levels upon immunoblotting of cell lysates (Fig. 2F, bottom panel). These data suggest that the feeding dependent acetylation of USF-1 is responsible for FAS promoter activation in the fed condition.

DNA-PK mediates feeding-dependent phosphorylation of USF-1

The first step in understanding how the feeding dependent phosphorylation of USF-1 activates the FAS promoter would be to identify the kinase that catalyzes this S262 phosphorylation. Search of numerous phosphoprotein databases predicted that a member of the PIKK family of kinases likely phosphorylates the S262 site. DNA-PK is a multimeric nuclear serine/threonine protein kinase, composed of the DNA-PK catalytic subunit and the Ku70/Ku80 regulatory subunits (Collis et al., 2005). We found all of the DNA-PK subunits to be the USF-1 interacting proteins and bound to the FAS promoter in the fed state. Therefore, to examine if S262 of USF-1 is a target of DNA-PK, we performed *in vitro* phosphorylation of bacterially expressed USF-1 by DNA-PK. Indeed, we could easily detect S262 phosphorylation of USF-1 by DNA-PK (Fig. 3A, lane 1) *in vitro*, which is DNA-PK concentration-dependent (S. 3A). S262 phosphorylation was abolished when wortmannin was added at a concentration (Hashimoto et al., 2003) effective to inhibit DNA-PK activity (Fig. 3A, lane 2). However, we could not detect S262 phosphorylation by PKA or PKC *in vitro*, nor did we detect changes in phosphorylation upon cotransfection with PKB (S. 3B). Based on these results and the fact that DNA-PK is associated with USF-1 in the fed state, we conclude that the S262 of USF-1 is a specific target of DNA-PK.

We next tested S262 phosphorylation of USF-1 by DNA-PK in cultured cells. We overexpressed USF-1 along with WT DNA-PK or kinase dead DNA-PK containing a T3950D mutation (this hyperphosphorylation mimicking mutation causes a reduction in its kinase activity (Douglas et al., 2007)) or constitutive active DNA-PK containing a T3950A mutation that mimics dephosphorylation. We detected higher S262 phosphorylation of USF-1 immunoprecipitated from cells overexpressing WT DNA-PK (Fig. 3B, left panel, lane 2) but not from cells expressing DNA-PK with T3950D mutation (lane 3) or control cells (lane 1). Furthermore, we detected even higher S262 phosphorylation of USF-1 from cells expressing DNA-PK with T3950A mutation compared to WT DNA-PK expressing cells (Fig. 3B, middle panel, lane 3). Next, to investigate whether DNA-PK mediated phosphorylation of USF-1 is S262 specific, we overexpressed WT USF-1 or the S262A mutant along with DNA-PK. WT USF-1 but not USF-1 containing S262A mutation was detected to have higher phosphorylation upon cotransfection with DNA-PK (Fig. 3B, right panel, lane 2 and 3). To further verify the role of DNA-PK in S262 phosphorylation, we performed siRNA-mediated knockdown of DNA-PK. We observed low but detectable S262 phosphorylation of USF-1 (Fig. 3C, left panel, lane 5). S262 phosphorylation was significantly reduced in the DNA-PK siRNA transfected cells that had more than an 80% decrease in DNA-PK levels (lane 6). FAS promoter activity in DNA-PK siRNA transfected cells was reduced by 65% compared to control siRNA transfected cells (Fig. 3C, right panel), which was similar to that observed upon transfection of nonphosphorylatable S262A USF-1 mutant (Fig. 2C). These results demonstrate that S262 phosphorylation of USF-1 is mediated by DNA-PK.

PP1 mediated dephosphorylation/activation of DNA-PK causes USF-1 phosphorylation upon feeding

We found that DNA-PK phosphorylates USF-1 at S262 and that S262 phosphorylation is lower in the fasted state but increases upon feeding. This prompted us to ask whether the changes in DNA-PK activity account for the differences in S262 phosphorylation during fasting/feeding. Using the specific DNA-PK substrate, a biotinylated p53 peptide, we compared DNA-PK activity in liver nuclear extracts of fasted or fed mice (Fig. 3D). While total DNA-PK protein levels remained the same (data now shown), DNA-PK activity in the fed state was 6-fold higher than in the fasted state. Wortmannin treatment drastically reduced DNA-PK activity when measured with the DNA-PK specific peptide as a substrate (Fig. 3D). This demonstrates that the kinase activity we detected can be attributed to DNA-PK.

DNA-PK activity is known to be regulated by phosphorylation/dephosphorylation, independent of its activation by DNA. Thus, autophosphorylation of DNA-PK results in a decrease in its kinase activity, whereas dephosphorylation by PP1 activates DNA-PK (Douglas et al., 2001; Douglas et al., 2007). Among the PIKK family members, DNA-PK is the only kinase that is activated by dephosphorylation. To examine the involvement of DNA-PK in USF phosphorylation, we first examined the phosphorylation status of DNA-PK in fasted and fed states. DNA-PK phosphorylation was detected using phosphoserine/threonine antibodies that detect autophosphorylation at the S/TQ motifs of DNA-PK. As shown in Figure 3E, top panel, phosphorylation of DNA-PK was higher in the fasted state than in the fed state while DNA-PK protein levels did not change. We also found DNA-PK phosphorylation was not detectable in insulin treated HepG2 cells, whereas phosphorylation was easily detected in non-insulin treated cells (Fig. 3E, bottom panel).

During the examination of the occupancy of USF interacting proteins, we found that PP1 along with DNA-PK was bound to lipogenic gene promoters in the fed state (Fig. 1C) when lipogenesis is induced. It is possible that PP1 which we found to be a USF interacting protein mediates the feeding/insulin signal by dephosphorylating DNA-PK. We therefore tested the S262 phosphorylation status of USF-1 upon treatment with okadaic acid (OA) which is known to prevent dephosphorylation of DNA-PK (Douglas et al., 2001). As expected, phosphorylation of DNA-PK greatly increased in OA treated cells (Fig. 3F, left panel, lane 4), whereas DNA-PK autophosphorylation was reduced in cells overexpressing PP1□ (S. 3C). We next examined S262 phosphorylation in OA treated cells by Western blotting of immunoprecipitated USF-1 with anti-FLAG or anti-P-USF-1 antibodies. Compared to a single USF-1 band detected in control DMSO treated cells, several USF-1 bands were detected in OA treated cells, suggesting a multi-site phosphorylation of USF-1 (Fig. 3F, lane 6). However, S262 phosphorylation of USF-1 that was easily detected in control cells was hardly detectable in OA treated cells (Fig. 3F, lane 9). To further test the specificity of PP1 on S262 phosphorylation status, we also used tautomycin (Taut) which is known to more selectively inhibit PP1. As expected, we easily detected phosphorylated DNA-PK in cells treated with Taut at 1uM but not in control cells (Fig. 3F, right panel). On the other hand, S262 phosphorylation of USF-1 was detected in control cells as expected but was decreased in cells treated with Taut at 10 nM and was hardly detectable at 1 uM (Fig. 3F, right panel). We also tested the role of PP1 by using a siRNA approach. S262 phosphorylation of USF-1 did not increase, but rather, greatly decreased in PP1 knockdown cells (Fig. 3G, lane 2), indicating that PP1 does not directly dephosphorylate S262 phosphorylation. Furthermore, S262 phosphorylation could be restored

upon cotransfection of constitutively active DNA-PK (S. 3D). This indicates that S262 phosphorylation is through DNA-PK that is first dephosphorylated/activated by PP1. When we compared the abundance of PP1 in liver nuclear extracts, we detected higher levels of PP1 in the nucleus in the fed state than in the fasted state, while PP1 protein levels in total cell lysates as well as PP1 gene expression levels did not change (Fig. 3H, left panel and S. 3E). Similarly, PP1 was not detected in nuclear extracts from control HepG2 cells but was increased upon insulin treatment (Fig. 3H, right panel). Overall, we conclude that the feeding-dependent S262 phosphorylation of USF-1 is mediated by DNA-PK. But, first, DNA-PK is dephosphorylated/activated by PP1 whose level in nucleus increases in response to feeding/insulin.

P/CAF mediated acetylation of USF-1 activates the FAS promoter, whereas HDAC9 mediated deacetylation causes promoter inactivation.

HDAC9 and P/CAF are recruited by, and interact with, USF-1in a fasting/feeding dependent manner. Therefore, we next, examined if acetylation and deacetylation of USF-1 is through P/CAF and HDAC9, respectively. When we cotransfected USF-1 and P/CAF, by using pan-acetyl lysine antibodies, we detected higher acetylation of USF-1 (Fig. 4A, top panel, lane 6). As shown in Figure 4A bottom panel, USF-1 was acetylated ***in vitro*** by P/CAF (lane 3), while acetylation was not detected in the absence of P/CAF or acetyl CoA (lane 1 and 2). MS analysis of USF-1 in cells overexpressing P/CAF revealed a regulatory site at K237, the residue that was acetylated upon feeding (Figure 2). To examine if this site was a target of P/CAF, we overexpressed FLAG-tagged WT USF-1 or USF-1 mutated at K237 along with P/CAF. As detected by pan-acetyl lysine antibodies, only WT USF-1 was efficiently acetylated by P/CAF (Fig. 4B, top left panel, lane 1) but the K237A USF-1 mutant was not (lane 2). We next employed anti-Ac-USF-1 antibodies specific for USF-1 acetylated at K237 and detected higher K237 acetylation in cells overexpressing P/CAF (Fig. 4B, top right, lane 1). To further investigate whether P/CAF mediated acetylation of USF-1 is K237 specific, we overexpressed WT USF-1 and various (K237 and K246) USF-1 mutants along with P/CAF. WT and K246R (Fig. 4B, bottom panel, lane 1, 4 and 5) but not K237R or K237R/K246R (lane 2 and 3) of USF-1 were found to be acetylated upon cotransfection with P/CAF, demonstrating that acetylation of K237 but not K246, is mediated by P/CAF.

With the binding of HDAC9 to the lipogenic promoters only in the fasted state, we speculated that HDAC9 would be an ideal candidate to remove the P/CAF mediated acetylation of USF-1 in the fed state. We transfected USF-1 and P/CAF along with HDAC9 or a control empty vector into 293 cells. We detected a decrease in P/CAF catalyzed acetylation of USF-1 in cells cotransfected with HDAC9 (Fig. 4C, lane 2). Furthermore, we detected significant HDAC9 protein levels in liver nuclear extracts from fasted, but not fed, mice or in nuclear extracts of HepG2 cells cultured in the absence, but not in the presence, of insulin (S. 4A) while its expression did not change in various conditions (S. 4B). These experiments indicate that, in the fasted state, nuclear HDAC9 is in higher abundance and is recruited to the FAS promoter to deacetylate USF-1.

We found by GST-pull down that USF-1 can directly interact with HDAC9 and P/CAF (but not p300) (S. 4C). We therefore dissected the domains of USF-1 required for interaction with P/CAF and HDAC9. As shown in Figure 4D, the bHLH domain of USF-1, the domain containing K237 that is acetylated by P/CAF, was sufficient for the interaction with P/CAF

although the leucine-zipper (LZ) domain could weakly interact with P/CAF. On the other hand, for the USF-1 interaction with HDAC9, the LZ domain of USF-1 was sufficient for its interaction with HDAC9. Thus, the domains of USF-1 required for interaction are in proximity to K237, the residue modified by these HAT/HDAC.

Cotransfection of USF-1 together with HDAC9 resulted in a 50% decrease in FAS promoter activity in a fashion similar to that we detected upon cotransfection of USF-1 containing a K237R mutation (Fig. 4E and Fig. 2F). In contrast, the expression of USF-1 with P/CAF resulted in a 2-fold higher promoter activity in a manner similar to that observed upon cotransfection of USF-1 containing the K237A mutation (Fig. 4E and Fig. 2F). Furthermore, cotransfection of P/CAF enhanced, while cotransfection of HDAC9 suppressed, USF-1 activation of the FAS promoter in a dose-dependent manner (Fig. 4F). We detected changes in FAS protein levels parallel to the FAS promoter activity. In addition, cotransfecting P/CAF or HDAC9 with USF-1 containing K237A or K237R mutation did not change the FAS promoter activity or FAS protein levels (S. 4E). These data indicate that acetylation and deacetylation of USF-1 catalyzed by P/CAF and HDAC9, respectively, functions as a dynamic switch for the transition between fasting/feeding in FAS promoter regulation.

Phosphorylation dependent acetylation of USF-1

Since USF-1 is both phosphorylated and acetylated at nearby sites and these posttranslational modifications are critical for USF-1 function in FAS promoter activation, we tested whether an increase in S262 phosphorylation of USF-1 could affect K237 acetylation. We cotransfected USF-1 and DNA-PK and examined S262 phosphorylation and K237 acetylation of USF-1. If S262 phosphorylation affects acetylation, cotransfection of DNA-PK would cause not only S262 phosphorylation of USF-1, but also K237 acetylation. Indeed, S262 phosphorylation of USF-1 upon DNA-PK transfection strongly enhanced USF-1 acetylation at K237 (Fig. 5A, lane 2). Conversely, we detected a significant level of K237 acetylation of USF-1 in control cells, which was reduced in OA treated cells (Fig. 5B, left panel, lane 2). Likewise, K237 acetylation of USF was high in control cells but was reduced to an undetectable level in PP1 siRNA transfected cells (right panel, lane 1). Inactivation of PP1 by OA treatment or siRNA mediated knockdown of PP1 caused phosphorylation/inactivation of DNA-PK resulting in reduced S262 phosphorylation of USF-1. This suggests that S262 phosphorylation brings about K237 acetylation. We then asked whether phosphorylation of USF-1 at S262 could affect USF-1 acetylation status by transfecting FLAG-tagged WT USF-1 or S262 mutants and examining the K237 acetylation status of the various USF-1 forms. We found that the S262A mutant had the lowest K237 acetylation among the three USF-1 forms (Fig. 5C, lane 6), whereas the S262D mutant displayed the highest acetylation, to a level significantly higher than WT USF-1 (Fig. 5C, lane 7). Overall these results demonstrate phosphorylation dependent acetylation of USF-1.

The simplest hypothesis underlying S262 phosphorylation-dependent acetylation of USF-1would be that S262 phosphorylation/dephosphorylation affects recruitment of P/CAF and HDAC9 causing acetylation and deacetylation of K237 of USF-1, respectively. Coimmunoprecipitation assay showed that the S262D mutant preferentially interacted with P/CAF in comparison to the S262A mutant (Fig. 5D). On the other hand, compared to the S262D mutant, the S262A mutant preferentially interacted with HDAC9, although the signal was low probably due to the low HDAC9 levels in the nucleus. We next examined whether S262 mutation of the USF-1 affects interaction of USF with SREBP-1 that we previously

reported. We found that the S262D USF mutant, as compared to S262A mutant, preferentially interacted with SREBP-1. Taken together, these results show that the phosphorylation dependent acetylation of USF-1 functions as a sensitive molecular switch, detecting nutritional status during the transition between fasting/feeding.

Feeding/insulin-dependent phosphorylation/acetylation of USF-1 are diminished in DNA-PK deficiency

To further demonstrate the requirement of DNA-PK in mediating the feeding/insulin dependent phosphorylation/acetylation of USF-1, we transfected DNA-PK siRNA into HepG2 cells. Insulin treatment of these cells markedly increased S262 phosphorylation as well as K237 acetylation in control siRNA-transfected cells, while USF-1 levels remained the same (Fig. 5E, lane 1 and 2). In contrast, insulin mediated S262 phosphorylation/K237 acetylation of USF-1 in cells transfected with DNA-PK siRNA was markedly reduced and undetectable (Fig. 5E, lane 3 and 4). We next compared the human glioblastoma cell line, M059J, that lacks DNA-PKcs and DNA-PK activity, and the related M059K cells containing WT DNA-PK (Feng et al., 2004) as a control. Treatment of M059K cells with insulin increased S262 phosphorylation and K237 acetylation of USF-1 (Fig. 5F, lane 3 and 4), whereas insulin treatment of M059J cells did not result in any significant increase in USF modifications (lane 1 and 2). These data demonstrate that DNA-PK is required not only for S262 phosphorylation but also for K237 acetylation of USF-1 upon insulin treatment.

By ChIP, we also tested whether recruitment of various proteins to FAS promoter by USF is dependent on DNA-PK (Fig. 5G). Those proteins that were found to be bound to the lipogenic gene promoters in the fed condition were recruited by USF in insulin treated M059K cells, but not in the DNA-PK deficient M059J cells. In the absence of insulin, HDAC9 was recruited by USF in both M059J and M059K cells, mostly likely because cytoplasmic export of HDAC9 was not affected by DNA-PK. Similarly, coimmunoprecipitation showed that USF-1 can interact better with various partners in insulin treated M059K but not in M059J cells (S. 5A). Furthermore, USF-1 interaction and recruitment of various proteins were abolished in 293 cells upon treatment with Taut that inhibits DNA-PK activity (S. 5B & 5C). Overall these results show that the recruitment of various proteins by USF-1 in feeding/insulin treatment is dependent on DNA-PK and DNA-PK mediated S262 USF-1 phosphorylation.

We next examined *in vivo* the DNA-PK mediated and feeding dependent S262 phosphorylation/K237 acetylation of USF-1*,* by employing DNA-PK deficient SCID (Severe Combined Immune Deficiency) mice. A spontaneous mutation in the DNA-PK gene causes a 90% reduction of the protein in SCID mice (Danska et al., 1996), producing a phenotype highly reminiscent of DNA-PK null mice. Indeed, feeding-induced phosphorylation of USF-1 at S262 was greatly reduced in SCID mice compared to that observed in WT mice (Fig. 5H, lane 4 and 3). ChIP analysis showed that the USF-1 detected on the FAS promoter in SCID mice in the fed state was not phosphorylated at S262 compared to the phosphoUSF-1 detected on the promoter in WT mice (Fig. 5I). Similarly, USF-1 bound to the mGPAT promoter was not phosphorylated at S262 in SCID mice in the fed state (S.5D). Furthermore, we could not detect occupancy by DNA-PK, Ku80, TopoIIβ and PP1 on the FAS promoter in SCID mice upon feeding (Fig. 5I). Since K237 acetylation of USF-1 is dependent on S262 phosphorylation as shown above, we investigated whether K237 acetylation was also reduced in SCID mice. We found that K237 acetylation upon feeding was greatly reduced in SCID mice compared to

that detected in WT mice (Fig. 5J, lane 4 and 2). The acetylated USF-1 bound to the FAS promoter in the fed state also was greatly reduced in SCID mice in ChIP analysis (Fig. 5K). This decrease in acetylated USF-1 bound to the FAS promoter could be explained by the decreased recruitment of P/CAF by USF-1 (Fig. 5K). HDAC9 binding was not different between WT and SCID mice probably because cytoplasmic export of HDAC9 was not affected in SCID mice. Overall, these results show *in vivo* the requirement of DNA-PK for S262 phosphorylation of USF-1 and for P/CAF mediated K237 acetylation leading to transactivation of the FAS promoter.

Feeding-dependent activation of the FAS gene and *de novo* lipogenesis are diminished in DNA-PK-deficient SCID mice

Since phosphorylation/acetylation of USF-1 for FAS promoter activation is through the PP1/DNA-PK mediated signaling pathway, we assessed the transcriptional activation of the FAS gene in DNA-PK deficient SCID mice during fasting/feeding. We first measured the nascent FAS RNA levels in liver nuclei from WT or SCID mice that were either fasted or fed (Fig. 6A) by RT-PCR. In WT mice, the FAS nascent RNA was not detectable in fasting but increased drastically upon feeding. On the other hand, the nascent FAS RNA was barely detectable in either fasted or fed SCID mice. RT-qPCR analysis indicated a 50-fold increase in FAS nascent transcript in WT mice upon feeding, while in SCID mice the increase was 20-fold, representing approximately a 50-60% decrease (Fig. 6B). We next performed nuclear run-on assays using nuclei from WT and SCID mice upon feeding at various time points. The rate of transcription measured by RT-qPCR of the newly extended nascent transcripts increased up to 10-fold in WT mice 6 hrs after feeding, a result consistent with our previously published study. However, FAS transcription in SCID mice increased only by 6-fold, a 40% reduction compared to WT mice (Fig. 6C).

Since we observed transient DNA breaks in the FAS promoter region that preceded transcriptional activation upon feeding (Fig. 1I), we next examined whether the DNA break occurs in the FAS promoter region in SCID mice, but could not detect transient DNA breaks, which we clearly detected in WT mice after 3 hrs of feeding (Fig. 6D). Furthermore, in contrast to WT mice, ChIP analysis did not show binding of DNA-PK or TopoIIβ to the FAS promoter region in SCID mice. Since TopoIIβ catalyzes DNA breaks, the absence of DNA breaks in the FAS promoter region in SCID mice can be attributed to the impaired TopoIIβ recruitment that is dependent on the DNA-PK catalyzed phosphorylation of USF-1. Thus, not only the diminished acetylation of USF-1, but also the impaired recruitment of the DNA break/repair components, which is dependent on USF-1 phosphorylation, probably contributed to the attenuated feeding-dependent transcriptional activation of the FAS gene in SCID mice. Overall, these results clearly show *in vivo* the critical role of DNA-PK in activation of FAS transcription by feeding.

We examined *in vivo* hepatic *de novo* lipogenesis in WT and SCID mice using a stable isotope method. Fractional *de novo* lipogenesis was hardly detected in fasting but was increased drastically during a 24-hr period of feeding in WT mice (Fig. 6E). However, feeding induced fractional *de novo* lipogenesis was 60% lower in SCID mice after 24 hrs of feeding compared to WT mice. To confirm that the decrease in *de novo* lipogenesis in SCID mice was due to a decrease in FAS induction, we examined the FAS protein levels in livers of WT and SCID mice after 24 hrs of feeding. Indeed, FAS protein levels in SCID mice were significantly lower compared to WT mice (Fig. 6F). The hepatic triglyceride levels after 24 hrs feeding were

approximately 30% lower in SCID mice compared to WT mice; and serum triglyceride levels were also significantly lower in SCID mice (Fig. 6G). Thus, impairment of feeding-dependent activation of FAS transcription in SCID mice leads to blunted induction of *de novo* lipogenesis resulting in lower hepatic as well as, probably reflecting decreased VLDL secretion, serum triglyceride levels. In this regard, SCID mice also had a lower adipose tissue mass, indicative of a long-term defect in feeding induced lipogenesis (S. Table 1).

DISCUSSION

FAS levels in the liver change drastically during varying nutritional states, correlating with circulating insulin/glucagon levels. During fasting, fatty acid synthesis is virtually absent. However, upon feeding, accompanying insulin secretion, fatty acid synthesis is induced drastically. While many metabolic effects of insulin are mediated through protein phosphorylation by the activation of the well characterized PI3K cascade, insulin can also exert metabolic effects through dephosphorylation catalyzed mainly by PP1. A central issue in metabolic regulation is to define coordinated molecular strategies that underlie the transition from fasting to feeding, such as the transcriptional activation of lipogenesis along specific transduction pathways. Here, we report a novel pathway that underlies the feeding/insulin response, which is based on post-translational modifications of a key transcription factor, USF-1, by an atypical kinase, DNA-PK.

Differential binding of USF-1 interacting proteins to lipogenic gene promoters in fasted and fed states.

Our study shows that USF recruits three different coregulator classes to lipogenic gene promoters. They are a) the DNA break/repair machinery, b) kinase/phosphatase, and c) HAT/HDAC family. The distinct binding pattern of USF interacting proteins on the FAS promoter in response to feeding/fasting is correlated with lipogenic gene activation/repression which involve molecular events that require the presence of specific coactivators/corepressors, respectively.

FAS and other lipogenic enzymes such as mGPAT are coordinately regulated by feeding/insulin, involving USF and SREBP-1c binding to the closely spaced E-box and SRE, respectively. We show here that the USF-1 bound to the -65 E-box recruits various USF-1 interacting proteins as well as SREBP-1c to bind SRE. Herein, we address the molecular function of various USF-1 interacting proteins and USF-1 modifications required for FAS promoter activation. Furthermore, FAS and mGPAT have the same differential recruitment of distinct USF interacting proteins indicating a common key mechanism in the induction of lipogenic gene transcription in response to fasting/feeding.

Phosphorylation-dependent acetylation of USF-1 functions as a sensor for nutritional status

Since USF-1 levels and its binding to the E-box are unaltered between fasting/feeding, it can be predicted that USF-1 is regulated posttranslationally. Even though the changes in phosphorylation states of metabolic enzymes during the transition between fasting/feeding are common and well understood, the posttranslational modifications of transcription factors in these metabolic states are not well studied. We show here for the first time that S262 and the nearby K237 of USF-1 are modified in response to fasting/feeding. The S262 of USF-1 as well as nearby residues are conserved among mammalian species but is not found in USF-2 even though there is a 44% overall homology between USF-1 and USF-2 (Corre and Galibert, 2005).

Activation of the FAS gene by feeding has been shown to be impaired by 80% in either USF-1 or USF-2 knockout mice (Casado et al., 1999). Thus, USF functions as a heterodimer and both USF-1 and USF-2 were found to bind the FAS promoter (Wang and Sul, 1995; Wang and Sul, 1997). However, the unique S262 of USF-1 points towards its pivotal role as a sensor for lipogenic gene transcription.

There is increasing evidence for acetylation of some transcription factors in addition to the well-recognized histone acetylation (Gu and Roeder, 1997) and reversible acetylation may be critical in regulation of transcription factor activity in response to different stimuli. However, USF acetylation has never been reported. Here, we have addressed USF-1 as a primary substrate for HAT/HDAC. The functional significance of acetylation of transcription factors appears to be varied. In the case of p53, acetylation results in stimulation of DNA binding, whereas acetylation of E2F may change protein stability (Martinez-Balbas et al., 2000). The fact that USF levels do not change during fasting/feeding and that USF acetylation does not affect DNA binding but affects FAS promoter activation suggests transactivation results from USF acetylation, and our study demonstrates that acetylation of USF-1 at K237 increases FAS promoter activity. Further studies are needed to clarify the exact functional consequence of USF acetylation. Deacetylation is mainly mediated by HDACs which generally function as transcriptional repressors. HDAC9 is recruited to the FAS promoter in the fasted state to deacetylate USF-1. Although HDAC9 has been shown to associate with transcription factors to repress transcription (Mejat et al., 2005), to our knowledge, HDAC9 deacetylation of USF-1 that we report here, is the first non-histone substrate of HDAC9.

Cross talk between acetylation and phosphorylation is well recognized. In our present study, K237 acetylation is dependent on S262 phosphorylation in response to feeding/insulin by preferential interaction with P/CAF rather than HDAC9. Thus, the phosphorylation dependent acetylation of USF-1 functions as a dynamic molecular switch in sensing the nutritional transition from fasting to feeding. Such a multi-step switch provides a way to fine tune transcription of lipogenic genes in response to different nutritional states.

PP1 mediated dephosphorylation of DNA-PK is critical for feeding-dependent lipogenic gene transcription

It has been well established that PI3K pathway mainly mediates insulin signaling for metabolic regulation (Engelman et al., 2006). Our *in vitro* phosphorylation studies and the fact that S262 phosphorylation is abolished in DNA-PK deficient mice point to the notion that DNA-PK is the kinase for the S262 phosphorylation occurring in the fed condition. However, DNA-PK is not known to be a component in the PI3K pathway nor in the insulin signaling pathway. Although DNA-PK was previously implicated in phosphorylation of S473 of PKB/Akt (Feng et al., 2004), recent research indicates that mTORC2, another member of PIKK, is the authentic kinase that phosphorylates this critical site of PKB/Akt (Sarbassov et al., 2005). However, our present study shows a link between DNA-PK and insulin signaling pathway.

Although the molecular mechanism is complex, the stimulation of PP1 by insulin has been well documented. For example, insulin inhibits breakdown and promotes synthesis of glycogen by activating primarily PP1. PP1 is compartmentalized in cells by discrete targeting subunits and several proteins called PTG (protein targeting to glycogen) can target PP1 to the glycogen particle where PP1 dephosphorylates enzymes in glycogen metabolism (Printen, Brady, and Saltiel, 1997). Recent studies indicate that PP1 can rapidly move between subcellular

compartments with the aid of targeting units. PNUT, a PP1 associated cofactor, may act as a nuclear targeting subunit of PP1 (Allen et al., 1998). We postulate that feeding/insulin might regulate PNUT-mediated nuclear translocation of PP1 into the nucleus to activate DNA-PK. Thus, PP1 mediated dephosphorylation of DNA-PK is critical in transmitting the feeding/insulin signal to regulate lipogenic genes.

Among USF interacting proteins, DNA-PK along with Ku70/80, PARP-1 and TopoIIß are identified. These proteins are known to function in double strand DNA break/repair and it has recently been shown that a transient double strand DNA-break is required for estrogen receptor dependent transcription. Although Ku70, Ku80 and DNA-PK are in the same complex with PARP-1 and TopoIIß, their function in DNA-break for transcriptional activation has not been reported. Here, we identified all components of DNA break/repair machinery for transcriptional activation of the FAS promoter by fasting/feeding and we observed transient DNA breaks that preceded transcriptional activation.

We show here a unique function of DNA-PK as a signaling molecule in response to feeding/insulin. DNA-PK is required for USF-1 complex assembly and recruitment of its interacting proteins. Therefore, DNA-PK mediated USF-1 phosphorylation governs interaction between USF-1 and its partners. SREBP-1 interacts more efficiently with the phosphorylated USF-1, which in turn enhances the interaction between USF-1 and DNA-PK, leading to USF-1 phosphorylation, an indication of positive feed-forward regulation. Thus, impaired transcriptional activation of lipogenic genes in DNA-PK deficient SCID mice is probably due to the dual effects of DNA-PK on USF-1 phosphorylation for feeding/insulin signaling and the transient DNA breaks required for transcriptional activation. In SCID mice, the absence of the feeding-induced transient DNA breaks in the FAS promoter could be attributed to the impairment of feeding/insulin induced USF phosphorylation by DNA-PK, which results in a failure to recruit various USF-1 interacting proteins including those for transient DNA breaks such as TopoIIβ.

Taken together, we propose the following model for the mechanism underlying USF function in the transcriptional regulation of lipogenic genes during fasting/feeding (Fig. 6H). In the fasted state, USF-1 recruits HDAC9 which deacetylates USF-1 to repress transcription despite its binding to the E-box (left panel). Upon feeding, DNA-PK, which is dephosphorylated/activated by PP1, phosphorylates USF-1 which then recruits SREBP-1 and other USF-1 interacting proteins. Thus, DNA-PK catalyzed phosphorylation of USF-1 allows P/CAF recruitment and subsequent acetylation of USF-1 (right panel). As a result, FAS transcription is activated by USF-1 in a reversible manner in response to nutritional status.

Experimental Procedures

Additional experimental procedures are available in the supplemental data.

Purification of USF-1 interacting proteins and preparation of nuclear extracts

TAP was performed as described previously (Griffin et al., 2007). Purified protein mixture was subjected to mass spectrometry. Liver nuclear extracts were prepared by centrifugation through sucrose cushion in the presence of NaF.

Chromatin Immunoprecipitation
Livers from fasted or fed mice were fixed with DSG at 2 mM for 45 min at RT before formaldehyde cross-linking. ChIP was performed as described previously (Latasa et al., 2003).

***In vitro* phosphorylation, acetylation, and DNA-PK kinase assay**
In vitro phosphorylation and acetylation were performed using recombinant/purified enzymes. DNA-PK kinase assay was performed with nuclear extracts pretreated with or without wortmannin using SignaTect DNA-PK assay system (Promega) and γ^{32}P-ATP (Roche).

Nuclear run-on assay and preparation of nascent RNA
Nuclei were isolated as described previously (Paulauskis and Sul, 1989) for nascent RNA and nuclear run-on assay (See the Supplemental Experimental Procedures for further details).

Immunoprecipitation, GST-pull down, luciferase reporter assays
Immunoprecipitation from nuclear extracts was performed under standard procedures. GST pull-down was performed as described previously (Griffin et al., 2007). Luciferase assays were performed in 293FT cells using Dual-Luc reagent (Promega).

RT-PCR analysis
RNA was isolated and reverse transcribed for PCR or qPCR.

Measurement for metabolite and hormone levels
Insulin, glucose, NEFA, triglycerides were measured by ELISA (Crystal), glucometer (Roche), NEFA C kit (Wako), and Infinity kit (Thermo), respectively.

De novo lipogenesis (DNL)
Fatty acids formed during a 4 hrs ^2H_2O body water labeling (See the Supplemental Experimental Procedures for further details).

Statistical analysis
The data are expressed as the means ± standard errors of the means, Student's *t* test was used (*$\boldsymbol{P}$ < 0.05, **$\boldsymbol{P}$ < 0.01, ***$\boldsymbol{P}$ < 0.005 and ****$\boldsymbol{P}$ < 0.0001).

REFERENCES

Allen, P.B., Kwon, Y.G., Nairn, A.C., and Greengard, P. (1998). Isolation and characterization of PNUTS, a putative protein phosphatase 1 nuclear targeting subunit. J. Biol. Chem. *273,* 4089-4095.

Brady, M.J., and Saltiel, A.R. (2001). The role of protein phosphatase-1 in insulin action. Recent Prog. Horm. Res. *56,* 157-173.

Casado, M., Vallet, V.S., Kahn, A., and Vaulont, S. (1999). Essential role in vivo of upstream stimulatory factors for a normal dietary response of the fatty acid synthase gene in the liver. J. Biol. Chem. *274,* 2009-2013.

Collis, S.J., DeWeese, T.L., Jeggo, P.A., and Parker, A.R. (2005). The life and death of DNA-PK. Oncogene *24,* 949-961.

Corre, S., and Galibert, M.D. (2005). Upstream stimulating factors: highly versatile stress-responsive transcription factors. Pigment Cell Res. *18,* 337-348.

Danska, J.S., Holland, D.P., Mariathasan, S., Williams, K.M., and Guidos, C.J. (1996). Biochemical and genetic defects in the DNA-dependent protein kinase in murine scid lymphocytes. Mol. Cell. Biol. *16,* 5507-5517.

Dircks, L.K., and Sul, H.S. (1997). Mammalian mitochondrial glycerol-3-phosphate acyltransferase. Biochim. Biophys. Acta *1348,* 17-26.

Douglas, P., Cui, X., Block, W.D., Yu, Y., Gupta, S., Ding, Q., Ye, R., Morrice, N., Lees-Miller, S.P., and Meek, K. (2007). The DNA-dependent protein kinase catalytic subunit is phosphorylated in vivo on threonine 3950, a highly conserved amino acid in the protein kinase domain. Mol. Cell. Biol. *27,* 1581-1591.

Douglas, P., Moorhead, G.B., Ye, R., and Lees-Miller, S.P. (2001). Protein phosphatases regulate DNA-dependent protein kinase activity. J. Biol. Chem. *276,* 18992-18998.

Engelman, J.A., Luo, J., and Cantley, L.C. (2006). The evolution of phosphatidylinositol 3-kinases as regulators of growth and metabolism. Nat. Rev. Genet. *7,* 606-619.

Feng, J., Park, J., Cron, P., Hess, D., and Hemmings, B.A. (2004). Identification of a PKB/Akt hydrophobic motif Ser-473 kinase as DNA-dependent protein kinase. J. Biol. Chem. *279,* 41189-41196.

Griffin, M.J., Wong, R.H., Pandya, N., and Sul, H.S. (2007). Direct interaction between USF and SREBP-1c mediates synergistic activation of the fatty-acid synthase promoter. J. Biol. Chem. *282,* 5453-5467.

Gu, W., and Roeder, R.G. (1997). Activation of p53 sequence-specific DNA binding by acetylation of the p53 C-terminal domain. Cell *90,* 595-606.

Hashimoto, M., Rao, S., Tokuno, O., Yamamoto, K., Takata, M., Takeda, S., and Utsumi, H. (2003). DNA-PK: the major target for wortmannin-mediated radiosensitization by the inhibition of DSB repair via NHEJ pathway. J. Radiat. Res. (Tokyo) *44,* 151-159.

Jerkins, A.A., Liu, W.R., Lee, S., and Sul, H.S. (1995). Characterization of the murine mitochondrial glycerol-3-phosphate acyltransferase promoter. J. Biol. Chem. *270,* 1416-1421.

Ju, B.G., Lunyak, V.V., Perissi, V., Garcia-Bassets, I., Rose, D.W., Glass, C.K., and Rosenfeld, M.G. (2006). A topoisomerase IIbeta-mediated dsDNA break required for regulated transcription. Science *312,* 1798-1802.

Latasa, M.J., Griffin, M.J., Moon, Y.S., Kang, C., and Sul, H.S. (2003). Occupancy and function of the -150 sterol regulatory element and -65 E-box in nutritional regulation of the fatty acid synthase gene in living animals. Mol. Cell. Biol. *23,* 5896-5907.

Latasa, M.J., Moon, Y.S., Kim, K.H., and Sul, H.S. (2000). Nutritional regulation of the fatty acid synthase promoter in vivo: sterol regulatory element binding protein functions through an upstream region containing a sterol regulatory element. Proc. Natl. Acad. Sci. U. S. A. *97,* 10619-10624.
Lee, K., Villena, J.A., Moon, Y.S., Kim, K.H., Lee, S., Kang, C., and Sul, H.S. (2003). Inhibition of adipogenesis and development of glucose intolerance by soluble preadipocyte factor-1 (Pref-1). J. Clin. Invest. *111,* 453-461.
Martinez-Balbas, M.A., Bauer, U.M., Nielsen, S.J., Brehm, A., and Kouzarides, T. (2000). Regulation of E2F1 activity by acetylation. EMBO J. *19,* 662-671.
Mejat, A., Ramond, F., Bassel-Duby, R., Khochbin, S., Olson, E.N., and Schaeffer, L. (2005). Histone deacetylase 9 couples neuronal activity to muscle chromatin acetylation and gene expression. Nat. Neurosci. *8,* 313-321.
Moon, Y.S., Latasa, M.J., Kim, K.H., Wang, D., and Sul, H.S. (2000). Two 5'-regions are required for nutritional and insulin regulation of the fatty-acid synthase promoter in transgenic mice. J. Biol. Chem. *275,* 10121-10127.
Moustaid, N., Beyer, R.S., and Sul, H.S. (1994). Identification of an insulin response element in the fatty acid synthase promoter. J. Biol. Chem. *269,* 5629-5634.
Moustaid, N., Sakamoto, K., Clarke, S., Beyer, R.S., and Sul, H.S. (1993). Regulation of fatty acid synthase gene transcription. Sequences that confer a positive insulin effect and differentiation-dependent expression in 3T3-L1 preadipocytes are present in the 332 bp promoter. Biochem. J. *292 (Pt 3),* 767-772.
Moustaid, N., and Sul, H.S. (1991). Regulation of expression of the fatty acid synthase gene in 3T3-L1 cells by differentiation and triiodothyronine. J. Biol. Chem. *266,* 18550-18554.
Pajukanta, P., Lilja, H.E., Sinsheimer, J.S., Cantor, R.M., Lusis, A.J., Gentile, M., Duan, X.J., Soro-Paavonen, A., Naukkarinen, J., Saarela, J. *et al*. (2004). Familial combined hyperlipidemia is associated with upstream transcription factor 1 (USF1). Nat. Genet. *36,* 371-376.
Paulauskis, J.D., and Sul, H.S. (1989). Hormonal regulation of mouse fatty acid synthase gene transcription in liver. J. Biol. Chem. *264,* 574-577.
Paulauskis, J.D., and Sul, H.S. (1988). Cloning and expression of mouse fatty acid synthase and other specific mRNAs. Developmental and hormonal regulation in 3T3-L1 cells. J. Biol. Chem. *263,* 7049-7054.
Printen, J.A., Brady, M.J., and Saltiel, A.R. (1997). PTG, a protein phosphatase 1-binding protein with a role in glycogen metabolism. Science *275,* 1475-1478.
Sarbassov, D.D., Guertin, D.A., Ali, S.M., and Sabatini, D.M. (2005). Phosphorylation and regulation of Akt/PKB by the rictor-mTOR complex. Science *307,* 1098-1101.
Sawadogo, M., and Roeder, R.G. (1985). Interaction of a gene-specific transcription factor with the adenovirus major late promoter upstream of the TATA box region. Cell *43,* 165-175.
Shimomura, I., Bashmakov, Y., Ikemoto, S., Horton, J.D., Brown, M.S., and Goldstein, J.L. (1999). Insulin selectively increases SREBP-1c mRNA in the livers of rats with streptozotocin-induced diabetes. Proc. Natl. Acad. Sci. U. S. A. *96,* 13656-13661.
Shin, D.H., Paulauskis, J.D., Moustaid, N., and Sul, H.S. (1991). Transcriptional regulation of p90 with sequence homology to Escherichia coli glycerol-3-phosphate acyltransferase. J. Biol. Chem. *266,* 23834-23839.

Soncini, M., Yet, S.F., Moon, Y., Chun, J.Y., and Sul, H.S. (1995). Hormonal and nutritional control of the fatty acid synthase promoter in transgenic mice. J. Biol. Chem. *270,* 30339-30343.
Sul, H.S., Latasa, M.J., Moon, Y., and Kim, K.H. (2000). Regulation of the fatty acid synthase promoter by insulin. J. Nutr. *130,* 315S-320S.
Sul, H.S., and Wang, D. (1998). Nutritional and hormonal regulation of enzymes in fat synthesis: studies of fatty acid synthase and mitochondrial glycerol-3-phosphate acyltransferase gene transcription. Annu. Rev. Nutr. *18,* 331-351.
Taniguchi, C.M., Emanuelli, B., and Kahn, C.R. (2006). Critical nodes in signalling pathways: insights into insulin action. Nat. Rev. Mol. Cell Biol. *7,* 85-96.
Wang, D., and Sul, H.S. (1998). Insulin stimulation of the fatty acid synthase promoter is mediated by the phosphatidylinositol 3-kinase pathway. Involvement of protein kinase B/Akt. J. Biol. Chem. *273,* 25420-25426.
Wang, D., and Sul, H.S. (1997). Upstream stimulatory factor binding to the E-box at -65 is required for insulin regulation of the fatty acid synthase promoter. J. Biol. Chem. *272,* 26367-26374.
Wang, D., and Sul, H.S. (1995). Upstream stimulatory factors bind to insulin response sequence of the fatty acid synthase promoter. USF1 is regulated. J. Biol. Chem. *270,* 28716-28722. Correction: J. Biol. Chem. (1996) 271, 7873-7873
West, A.G., Huang, S., Gaszner, M., Litt, M.D., and Felsenfeld, G. (2004). Recruitment of histone modifications by USF proteins at a vertebrate barrier element. Mol. Cell *16,* 453-463.
Yet, S.F., Lee, S., Hahm, Y.T., and Sul, H.S. (1993). Expression and identification of p90 as the murine mitochondrial glycerol-3-phosphate acyltransferase. Biochemistry *32,* 9486-9491.
Yet, S.F., Moon, Y.K., and Sul, H.S. (1995). Purification and reconstitution of murine mitochondrial glycerol-3-phosphate acyltransferase. Functional expression in baculovirus-infected insect cells. Biochemistry *34,* 7303-7310.

SUPPLEMENTARY

Supplemental experimental procedures

Antibodies, animals, cell culture and transfection

Rabbit polyclonal antibodies were raised against peptides corresponding to aa 252-265 (QELRQSNHRL(S)EEL) and 231-244 (CSMEST(K)SGQSKGG) of USF-1. SCID in C57BL/6J background and wild type The following commercially available antibodies were used: Monoclonal Anti-USF-1 (M01,M02) (Abnova), M2 anti-FLAG (Sigma), anti-DNA-PK (4F10C5) (Upstate), anti-AcK (4G12) (Upstate), anti-phosphoserine (Calbiochem) , anti-S/TQ ATM/ATR substrate (Cell Signaling), anti-PAR (Alexis Biochemical), anti-HA (Covance) and polyclonal anti-USF-1 (C-20), anti-Actin, anti-Biotin, anti-p300, normal IgG, anti-HDAC9, anti-GAPDH, anti-PARP-1, anti-Ku70, anti-Ku80, anti-TopoIIβ anti-PP1, anti-P/CAF, anti-FAS (Santa Cruz) and anti-p53 (Santa Cruz).

HC57BL/6JH male mice (Jackson laboratory) were used at 7 wks of age unless specified. For fasting/feeding experiments, mice were fasted for 40 hrs and then fed a high carbohydrate, fat-free diet for indicated time periods. HepG2 cells were grown in DMEM supplemented with 10% fetal bovine serum and 100 units/ml penicillin/streptomycin. M059J and M059K were from ATCC and grown in the same medium containing 4mg/ml glutamine. HepG2 cells were maintained in serum free media overnight prior to insulin treatment. For insulin treatment, HepG2 cells were treated with 100 nM insulin or DMSO for 30 min. 293FT cells in DMEM supplemented with 10% fetal bovine serum and 100 units/ml penicillin/streptomycin/neomycin or 293F cells in 293 Freestyle medium were transfected with expression constructs or siRNA (Santa Cruz) using lipofectamine 2000 (Invitrogen) or 293 Fectin (Invitrogen), respectively. 293 cells were treated with either control DMSO or OA at 1uM and Taut at indicated concentrations for 2 hrs. Expression vectors for DNA-PK and mutants, HAT, HDAC9, PP1, Kus and -0.7 p53-Luc were from laboratories of Drs. Meek, Kouzarides, Zelent, Lamond, Shay and Oren respectively.

Purification of USF-1 interacting proteins and preparation of nuclear extracts

The 293F cells were transfected with USF-1-FLAG-TAP or empty TAP vector. Briefly, nuclear extracts were subjected to two-step affinity purification using calmodulin and streptavidin resins (stratagene) (Griffin et al., 2007). Purified proteins were concentrated by Centricon YM-3 (Amicon) and analyzed by SDS-PAGE, followed by silver staining (Invitrogen). Purified protein mixture was subjected to 2D “MudPIT” Run (cation exchange/RP LC-MS/MS) using a Finnigan LCQ Deca XP mass spectrometer in NanoLC/ESI mode. Sequest program was used for interpretation of the mass spectra.

For USF-1 interaction experiments, nuclear extracts were added to immobilized GST-USF-1-FLAG fusion protein and incubated overnight. After extensive washing, bound proteins were eluted with glutathione and then subjected to a second round of purification on anti-FLAG resins (Sigma). Eluted complexes were neutralized with glycine and subjected to MS analysis.

For liver nuclear extracts, mice were fasted for 40 hrs and then fed a high carbohydrate, fat-free diet for 16 hrs or indicated time periods. Nuclear extracts were prepared by centrifugation through sucrose cushion in the presence of NaF. (Griffin et al., 2007). For 293 cells, nuclear extracts were prepared by high salt extraction (Andrews and Faller 1991)

Chromatin Immunoprecipitation
Livers from fasted or fed mice were fixed with DSG at 2 mM for 45 min at RT before formaldehyde cross-linking. Soluble chromatin was quantified by absorbance at 260nm, and equivalent amounts of input DNA were immunoprecipitated. ChIP was performed as described previously (Latasa et al., 2003). For detection of DNA-break**,** DNA-breaks were labeled with Biotin-16-dUTP (Roche), and chromatin was subjected to ChIP using anti-biotin antibodies (Ju et al., 2006). For real time PCR of ChIP samples, the fold enrichment values were normalized to the control IgG.

***In vitro* phosphorylation, acetylation, and DNA-PK kinase assay**
In vitro phosphorylation reactions were performed using DNA-PK (Promega), PKA (Upstate), PKC (Upstate) and ATP (Promega). Wortmannin was used at 2uM for *in vitro* phosphorylation. For *in vitro* acetylation, proteins were incubated with P/CAF (Upstate) using acetyl CoA (Sigma) as the donor of the acetyl group. DNA-PK kinase assay was performed using mouse nuclear extracts pretreated with or without wortmannin (2uM) using SignaTect DNA-PK assay system (Promega) and γ^{32}P-ATP (Roche).

Nuclear run-on assay and preparation of nascent RNA
Nuclei from livers of 3-5 mice were isolated by centrifugation through sucrose cushion as described previously (Paulauskis and Sul, 1989). For nascent RNA measurement, nuclei were treated with DNase (Roche) and purified using RNeasy kit (Qiagen). For nuclear run-on assay, nuclei were either incubated with biotin UTP (Roche) or UTP (Sigma) in *in vitro* transcription buffer. Labeled RNA purified using RNeasy kit (Qiagen) were pulled down using avidin beads (Sigma) before RT-qPCR(Patrone et al., 2000).

Immunoprecipitation, GST-pull down, luciferase reporter assays
For immunoprecipitation, nuclear extracts were incubated with the specific antibodies overnight at 4°C followed by incubation with protein G agarose beads (Santa Cruz), washed and separated by SDS-PAGE. Proteins were transferred onto nitrocellulose membranes (Bio-Rad) and Western blotting was performed. For GST pull-down, bacterially expressed GST proteins were first incubated with glutathione-agarose (Santa Cruz) followed by incubation with ^{35}S labeled proteins, and autoradiography was performed (Griffin et al., 2007). Plasmids containing full length cDNA of PP1, PARP-1 and TopoIIβ (Open Biosystem) were used for *in vitro* translation. Purified recombinant PARP-1 (Alexis) and PP1 (New England Biolabs) were used in the GST-pull down assay. The 293FT cells were transfected with-444-FAS-Luc along with various expression constructs and siRNA (Santa Cruz) using Lipofectamine 2000 reagent (Invitrogen), and luciferase assays were performed using Dual-Luc reagent (Promega).

RT-PCR analysis
Four mg of total RNA isolated using Trizol reagent (Gibco BRL) were reverse transcribed and the resultant cDNAs were amplified by semi-quantitative PCR or real time qPCR. For Real-time RT-qPCR, the relative mRNA levels of gene markers were quantified with β-actin as the internal control using EVA dye (Biochain) as the probe. Statistical analysis of the qPCR was obtained using the ($2^{-\Delta\Delta Ct}$) method.

Measurements for metabolite and hormone levels
Insulin levels were measured by an insulin ELISA kit (Crystal). Whole blood glucose concentration was measured with ACCU-CHEK (Roche) glucometer. Serum NEFAs levels

were measured by NEFA C kit (Wako). Serum triglyceride levels and liver triglyceride levels after extraction by Folch method were measured by Infinity Triglyceride Kit (Thermo).

Measurement of de novo lipogenesis (DNL)
Fatty acids synthesized during a 4 hrs ^2H_2O body water labeling were measured as described previously (Turner et al., 2003). Mass isotopomer distribution analysis (MIDA) was used. Fractional DNL contribution was calculated as previously described by $f_{DNL} = M1_{FA} / A_{1\infty FA}$.

Blue Native -PAGE for Detection of USF-1 complex
For detection of USF-1 complex, TAP eluates were incubated with the BN-PAGE loading dye at 4°C for 30 min, the samples were loaded onto a 6% BN gel and subjected to PAGE. After electrophoresis, nitrocellulose membrane was destained with methanol before Western blotting with anti-FLAG antibodies. USF-1-TAP eluates were incubated at 4°C for 30 min with 2 µg of antibodies (anti-GAPDH or anti-USF-1) for supershifting (Schagger et al., 1994).

Primer sequences
Gene specific target sequences were as follows: The primer pairs used in semi-quantitative RT-PCR were GAPDH (sense-CATCACCATCTTCCAGGAGCG; antisense-TGACCTTGCCCACAGCCTTG); DNA-PK (sense- GCC AAA GCG CAT TGT TAT TCG; antisense- GGG GTC ACT GTT ATT AGC CAC); Ku70 (sense- TCC TGC AGC AGC ACT TCC GCA; antisense- CAG TGT AGG TAC AGT GAG CTT) Ku80 (sense- GCT TTC CGG GAG GAG GCC ATT; antisense- CTC TTG GAT TCC CCA CAC ATC); PARP-1 (sense- CTG CAC CAG ACA CCA CAA AAC; antisense- TTC CCT GGG GAA GCC AGT AAG); P/CAF (sense- AGA GGT AGT GTG CTT GAA GGA; antisense CTC TTT AAG GAT GTC TAC CCA); PP1α (sense- TGG ATG AGA CCC TCA TGT GTT; antisense- TGG GAG ATT AGA TGC TGC TAT); PP1γ (sense- GCA CGC CCT GGG GAT GAG GTG; antisense- CGC AGA ATA AAG AAT GTA GCC); Topoisomerase IIβ (sense- GTA AAG GCC GAG GGG CAA AGA; antisense-AAT GTT CGT GCT CTT TGG GCA).

The primer pairs used in quantitative RT-PCR were FAS (sense-TGCTCCCAGCTGCAGGC; antisense-GCCCGGTAGCTCTGGGTGTA), mGPAT (sense- CTG CTA GAA GCC TAC AGC TCT; antisense- CAG CAC CAC AAA ACT CAG AAT), p53(sense- AAA GGA TGC CCA TGC TAC AGA GGA; antisense- AGT AGA CTG GCC CTT CTT GGT CTT), β-actin (sense-GACCGAGCGTGGCTACAGCTTCA; antisense- CCGTCAGGCAGCTCATAGCTCT).

Primer sequences for amplification of the proximal region of the mouse mitochondrial GPAT promoter were 5'-ACAGCCACACTCACAGAGAATGGGGC-3' and 5'-GAAGAGGCAGACTCGGCGTTCCGGAG-3'. Primer sequences for amplification of the proximal region of the mouse p53 promoter were 5’- GTT ATG GCG ACT ATC CAG CTT-3’ and 5’- CCC CTA ACT GTA GTC GCT ACC-3’. Primer sequences for amplification of the proximal region of the human FAS promoter were 5'-GCA CAC GTG GCC CCG GCG GAC-3' and 5'-CAC GCC ACA TGG GCT GAC AGC-3'. Primer sequences for amplification of the proximal region of the FAS-Luc promoter were 5'-CAG CCC CGA CGC TCA TTG G-3' and 5'-CTT CAT AGC CTT ATG CAG TTG-3'. Primer sequences for amplification of the proximal region of the p53-Luc promoter were 5'-GAC TTT TCA CAA AGC GTT CCT-3' and 5'-AGC CAG GGT GAG CAC GTG GGA-3'. Primers used for real time PCR were identical to those used in determination of nascent RNA from mouse liver and they were β-actin (Sense:

GTGGCATCCATGAAACTACAT; antisense: GAGCCAGAGCAGTAATCTCCT); FAS (sense: ACGTGACACTGCTGCGTGCCA; antisense: ATACTCAGGTGTCATTCTGTG).

SUPPLEMENTAL REFERENCES

1. Andrews, N.C., and Faller, D.V. (1991). A rapid micropreparation technique for extraction of DNA-binding proteins from limiting numbers of mammalian cells. Nucleic Acids Res. *19,* 2499.

2. Bertos, N.R., Wang, A.H., and Yang, X.J. (2001). Class II histone deacetylases: structure, function, and regulation. Biochem. Cell Biol. *79,* 243-252.
3. Blunt, T., Gell, D., Fox, M., Taccioli, G.E., Lehmann, A.R., Jackson, S.P., and Jeggo, P.A. (1996). Identification of a nonsense mutation in the carboxyl-terminal region of DNA-dependent protein kinase catalytic subunit in the scid mouse. Proc. Natl. Acad. Sci. U. S. A. *93,* 10285-10290.
4. Cohen, P.T. (2002). Protein phosphatase 1--targeted in many directions. J. Cell. Sci. *115,* 241-256.
5. Coon, H., Xin, Y., Hopkins, P.N., Cawthon, R.M., Hasstedt, S.J., and Hunt, S.C. (2005). Upstream stimulatory factor 1 associated with familial combined hyperlipidemia, LDL cholesterol, and triglycerides. Hum. Genet. *117,* 444-451.
6. Galibert, M.D., Carreira, S., and Goding, C.R. (2001). The Usf-1 transcription factor is a novel target for the stress-responsive p38 kinase and mediates UV-induced Tyrosinase expression. EMBO J. *20,* 5022-5031.
7. Hosoi, Y., Miyachi, H., Matsumoto, Y., Ikehata, H., Komura, J., Ishii, K., Zhao, H.J., Yoshida, M., Takai, Y., Yamada, S., Suzuki, N., and Ono, T. (1998). A phosphatidylinositol 3-kinase inhibitor wortmannin induces radioresistant DNA synthesis and sensitizes cells to bleomycin and ionizing radiation. Int. J. Cancer *78,* 642-647.
8. Ju, B.G., Solum, D., Song, E.J., Lee, K.J., Rose, D.W., Glass, C.K., and Rosenfeld, M.G. (2004). Activating the PARP-1 sensor component of the groucho/ TLE1 corepressor complex mediates a CaMKinase IIdelta-dependent neurogenic gene activation pathway. Cell *119,* 815-829.
9. Kim, Y.M., Watanabe, T., Allen, P.B., Kim, Y.M., Lee, S.J., Greengard, P., Nairn, A.C., and Kwon, Y.G. (2003). PNUTS, a protein phosphatase 1 (PP1) nuclear targeting subunit. Characterization of its PP1- and RNA-binding domains and regulation by phosphorylation. J. Biol. Chem. *278,* 13819-13828.
10. Lesage, B., Beullens, M., Nuytten, M., Van Eynde, A., Keppens, S., Himpens, B., and Bollen, M. (2004). Interactor-mediated nuclear translocation and retention of protein phosphatase-1. J. Biol. Chem. *279,* 55978-55984.
11. Li, B., Samanta, A., Song, X., Iacono, K.T., Bembas, K., Tao, R., Basu, S., Riley, J.L., Hancock, W.W., Shen, Y., Saouaf, S.J., and Greene, M.I. (2007). FOXP3 interactions with histone acetyltransferase and class II histone deacetylases are required for repression. Proc. Natl. Acad. Sci. U. S. A. *104,* 4571-4576.
12. Lo, W.S., Trievel, R.C., Rojas, J.R., Duggan, L., Hsu, J.Y., Allis, C.D., Marmorstein, R., and Berger, S.L. (2000). Phosphorylation of serine 10 in histone H3 is functionally linked in vitro and in vivo to Gcn5-mediated acetylation at lysine 14. Mol. Cell *5,* 917-926.
13. Patrone, G., Puppo, F., Cusano, R., Scaranari, M., Ceccherini, I., Puliti, A., and Ravazzolo, R. (2000). Nuclear run-on assay using biotin labeling, magnetic bead capture and analysis by fluorescence-based RT-PCR. BioTechniques *29,* 1012-4, 1016-7.
14. Pavan Kumar, P., Purbey, P.K., Sinha, C.K., Notani, D., Limaye, A., Jayani, R.S., and Galande, S. (2006). Phosphorylation of SATB1, a global gene regulator, acts as a molecular switch regulating its transcriptional activity in vivo. Mol. Cell *22,* 231-243.

15. Pavri, R., Lewis, B., Kim, T.K., Dilworth, F.J., Erdjument-Bromage, H., Tempst, P., de Murcia, G., Evans, R., Chambon, P., and Reinberg, D. (2005). PARP-1 determines specificity in a retinoid signaling pathway via direct modulation of mediator. Mol. Cell *18,* 83-96.
16. Reisman, D., and Rotter, V. (1993). The helix-loop-helix containing transcription factor USF binds to and transactivates the promoter of the p53 tumor suppressor gene. Nucleic Acids Res. *21,* 345-350.
17. Schagger, H., Cramer, W.A., and von Jagow, G. (1994). Analysis of molecular masses and oligomeric states of protein complexes by blue native electrophoresis and isolation of membrane protein complexes by two-dimensional native electrophoresis. Anal. Biochem. *217,* 220-230.
18. Sirito, M., Lin, Q., Maity, T., and Sawadogo, M. (1994). Ubiquitous expression of the 43- and 44-kDa forms of transcription factor USF in mammalian cells. Nucleic Acids Res. *22,* 427-433.
19. Turner, S. M., Murphy, E. J., Neese, R. A., Antelo, F., Thomas, T., Agarwal, A., Go, C., and Hellerstein, M. K. (2003). Measurement of TG synthesis and turnover in vivo by 2H2O incorporation into the glycerol moiety and application of MIDA. Am J Physiol Endocrinol Metab 285(4), E790-803
20. Wang, A.H., Gregoire, S., Zika, E., Xiao, L., Li, C.S., Li, H., Wright, K.L., Ting, J.P., and Yang, X.J. (2005). Identification of the ankyrin repeat proteins ANKRA and RFXANK as novel partners of class IIa histone deacetylases. J. Biol. Chem. *280,* 29117-29127.
21. Zhou, X., Marks, P.A., Rifkind, R.A., and Richon, V.M. (2001). Cloning and characterization of a histone deacetylase, HDAC9. Proc. Natl. Acad. Sci. U. S. A. *98,* 10572-10577.

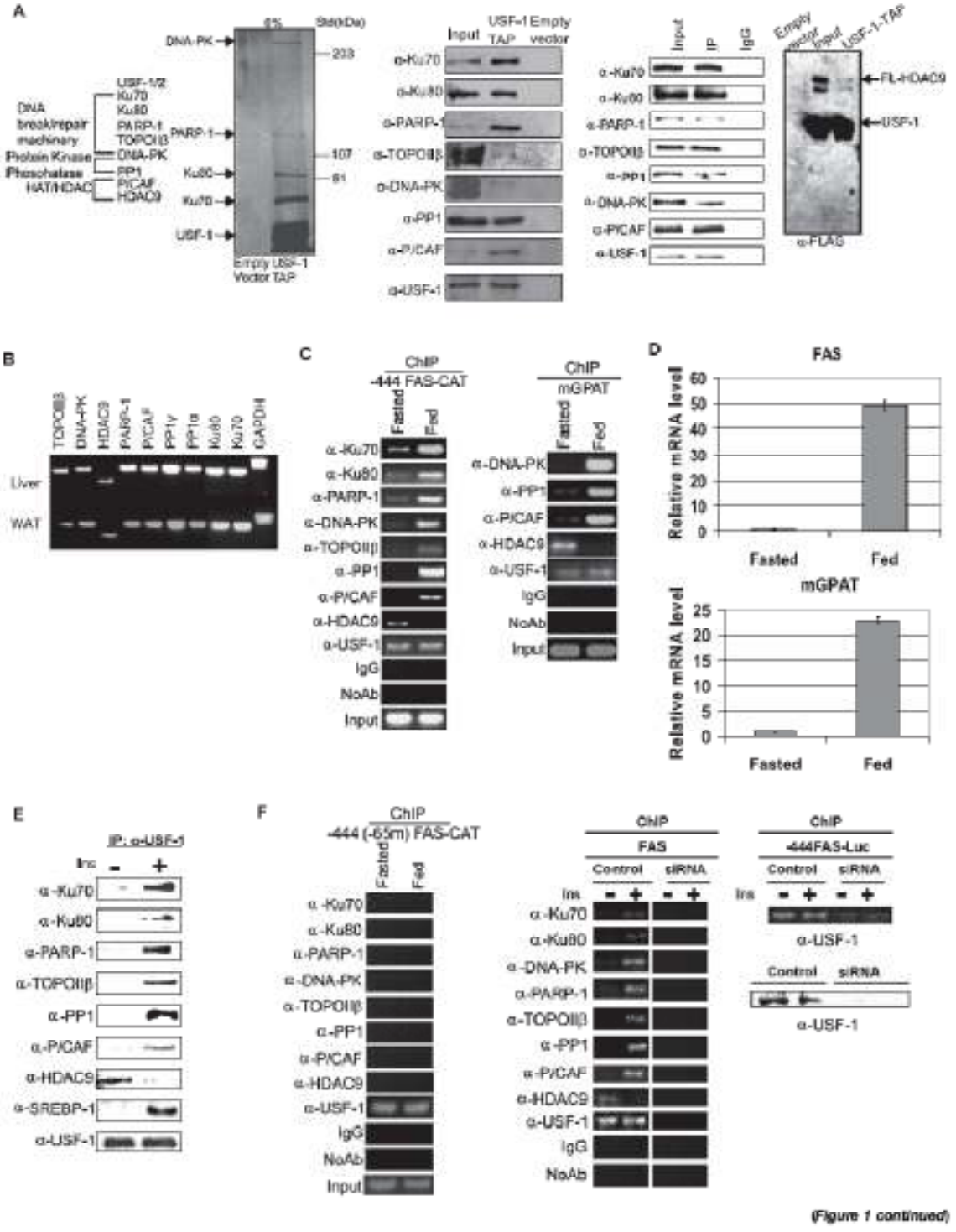

(Figure 1 continued)

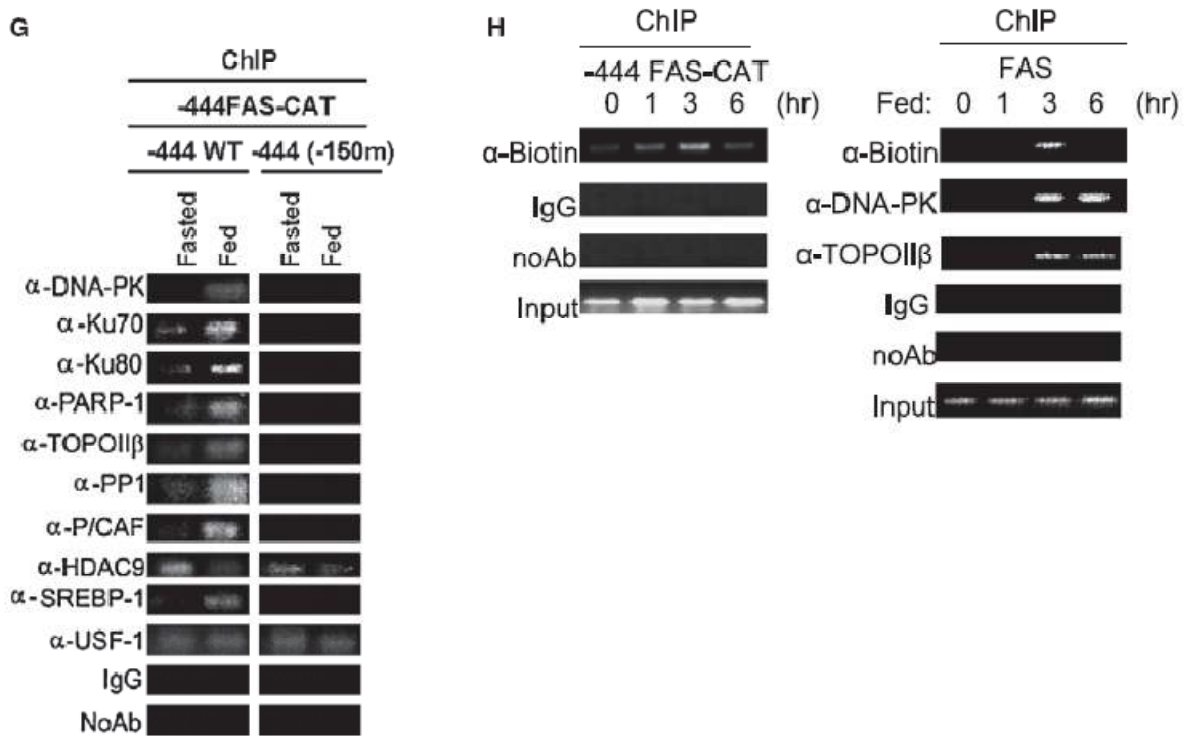

Figure III-1. Purification of USF-1 interacting proteins (A) The identities (left) of USF-1-associated polypeptides. Purified USF-1 eluates on SDS-PAGE by silver staining (2nd left). Immunoblotting of TAP eluates (middle). IP of USF-1 (2nd left) from 293F cells with monoclonal anti-USF-1 antibodies. TAP eluates from 293F cells were immunoblotted (right). (B) RNA from tissues were used for RT-PCR. (C) ChIP for association of USF-1 interacting proteins to the -444 FAS-CAT promoter (left) in FAS-CAT transgenic mice or the mGPAT promoter (right) in WT mice. (D) Expression in liver determined by RT-qPCR. (E) IP of FLAG-tagged USF-1 from HepG2 cells. (F) ChIP for association of USF-1 interacting proteins to the -444(-65m) FAS-CAT (left) promoter or the FAS promoter in HepG2 cells (right). USF-1 protein levels by immunoblotting (bottom right). (G) ChIP for binding of USF-1 interacting proteins to the -444 FAS-CAT (left) and -444(-150m) FAS-CAT (right) promoter. (H) ChIP analysis for DNA breaks and DNA-PK and TopoIIβ binding to the FAS-CAT (left) or the endogenous FAS promoter (right) in FAS-CAT transgenic or wild type mice.

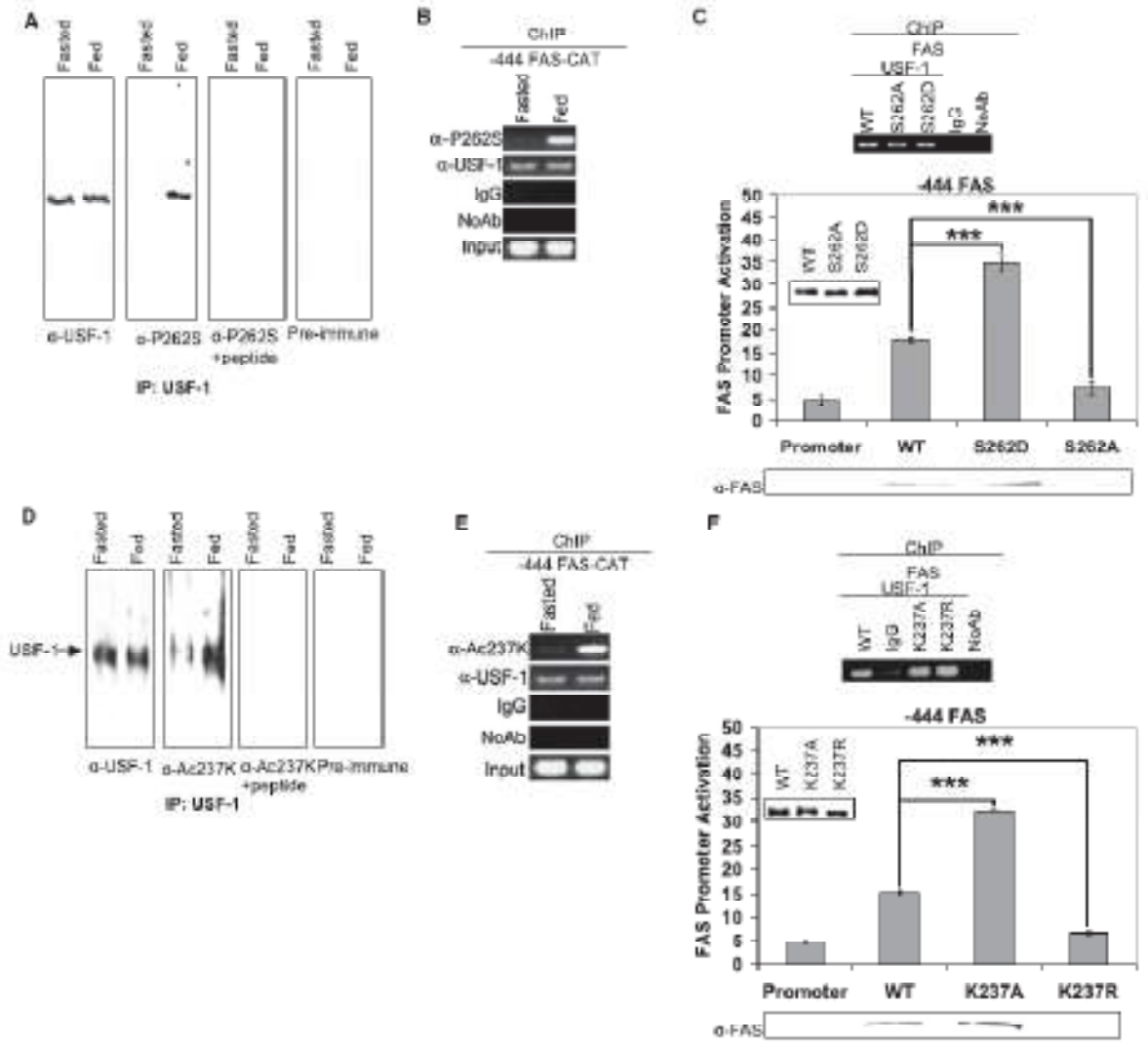

Figure III-2. Feeding-induced S262 phosphorylation and K237 acetylation of USF-1. (A) USF-1 immunoprecipitates using monoclonal anti-USF-1 was Western blotted with polyclonal anti-USF-1 or anti-P-USF-1. Immunoblotting with anti-P-USF-1 in the presence of peptide or with pre-immune serum are shown as controls. (B) ChIP for indicated proteins binding to the -444 FAS-CAT promoter. (C) ChIP (top) for WT USF-1 and S262 USF-1 mutant association to the FAS promoter in 293FT cells. The FAS promoter activity (bottom) was monitored. Immunoblotting for protein levels of WT, S262 USF-1 mutants (insert) and FAS are shown. (D) IP of USF-1. (E) ChIP for binding of indicated proteins to the -444 FAS-CAT promoter. (F) ChIP (top) for association of WT USF-1 and K237 USF-1 mutant to the FAS promoter. The promoter activity was measured.

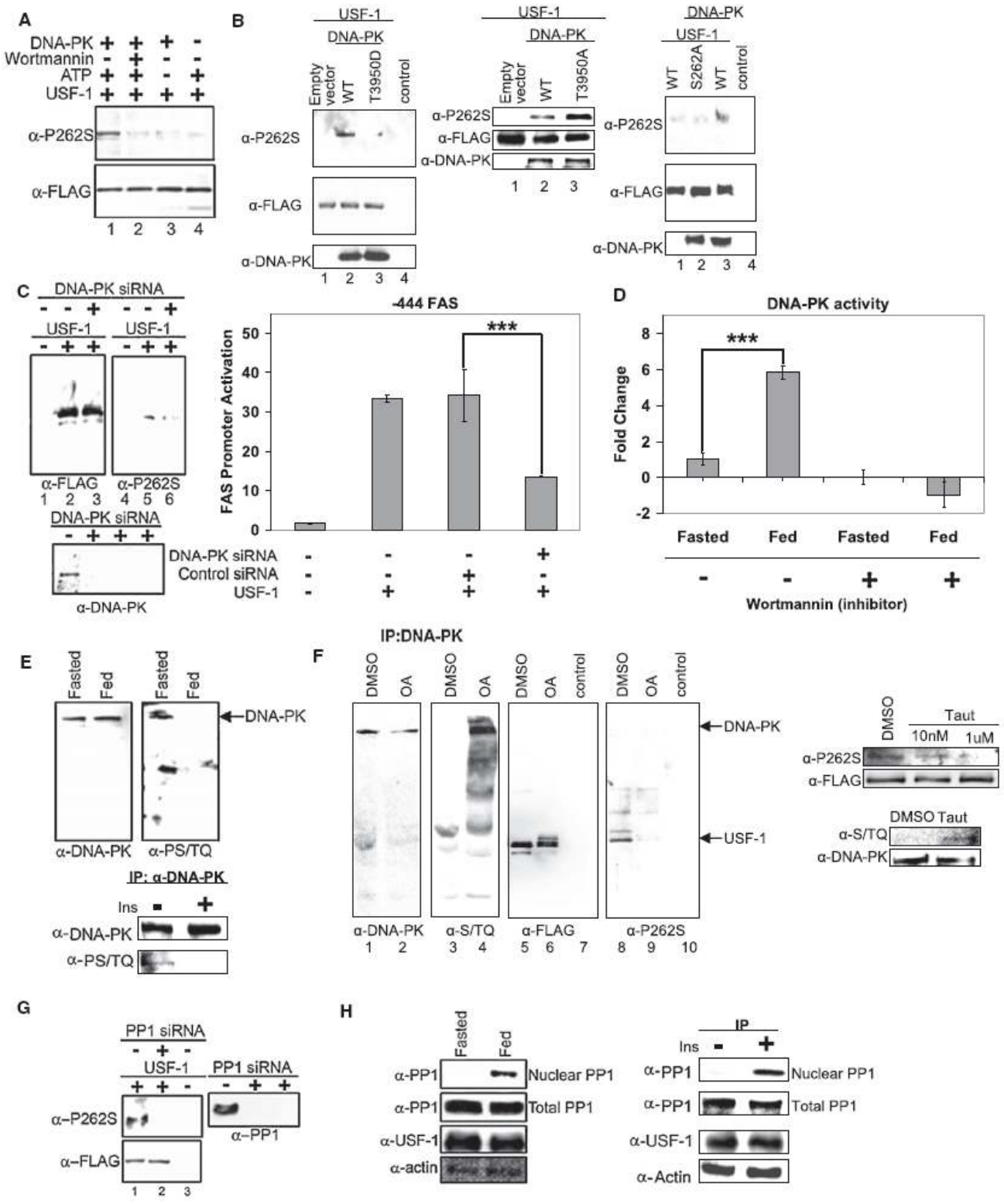

Figure III-3. Feeding dependent S262 phosphorylation of USF-1 is mediated by DNA-PK that is dephosphorylated/activated in feeding

(A) USF-1 was incubated with DNA-PK. (B) IP of USF-1. Immnoblotting for DNA-PK. (C) IP (left) of USF-1. The promoter activity of was measured (right). (D) DNA-PK activity was assayed. (E) IP of DNA-PK. (F) IP of USF-1-FLAG. Total and phosphorylated DNA-PK by westernblotting. (G) IP of USF-1. PP1 protein levels by Western blotting. (H) IP of PP1 from nuclear extracts or total lysates. USF-1 and □-actin protein levels by Western blotting.

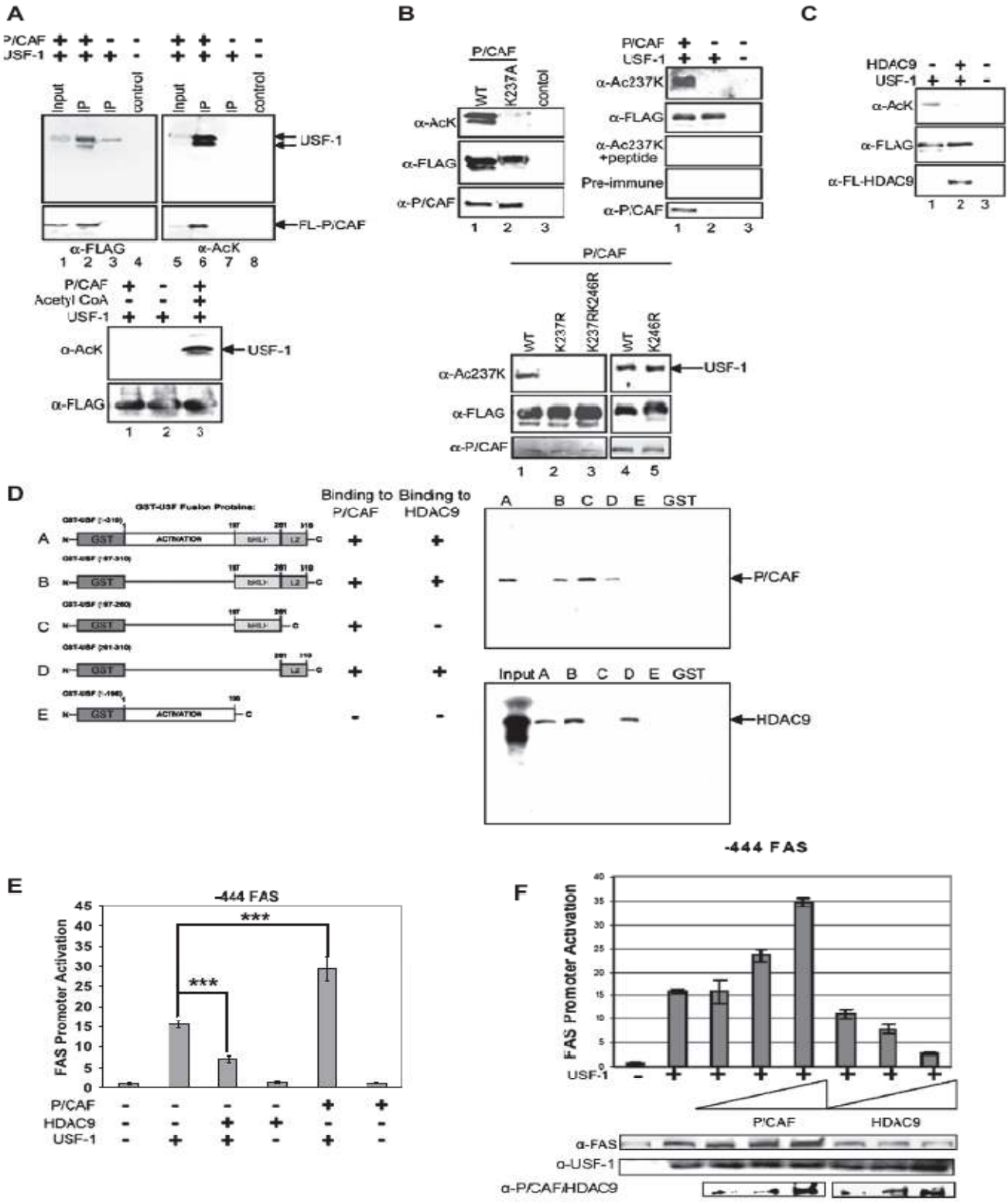

Figure III-4. Acetylation of K237 of USF-1 by P/CAF and deacetylation by HDAC9. (A) IP of USF-1 (top). USF-1 was *in vitro* acetylated with P/CAF (bottom). (B) IP of USF-1. P/CAF protein levels by immunoblotting. (C) IP of USF-1. (D) USF-1 was incubated with ***in vitro*** translated ^{35}S-labeled proteins before subjecting to GST-pull down. GST was used as a control. (E) The -444 FAS-Luc promoter activity was measured. (F) The -444 FAS-Luc promoter activity was measured. Total cell lysates were immunoblotted.

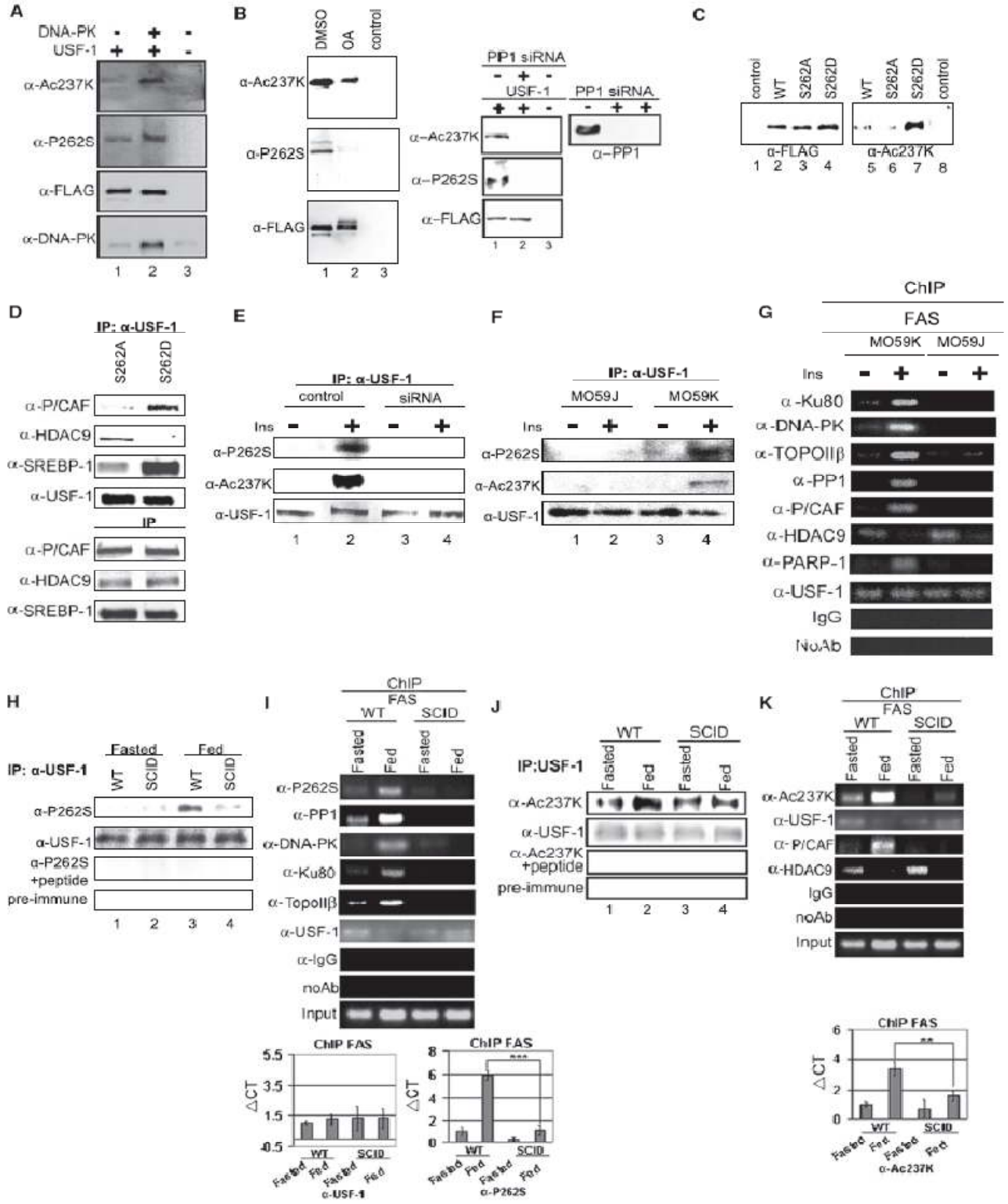

Figure III-5. Feeding/insulin induced phosphorylation and acetylation of USF-1 are greatly reduced in DNA-PK deficiency (A-C) IP of FLAG-tagged USF-1. Nuclear extracts from non-transfected cells were used as a control. (D) IP of USF-1-FLAG from HepG2 cells (top). Total protein levels by immnoblotting (bottom). IP of USF-1 from HepG2 cells (E) or from M059J or M059K cells (F). (G) ChIP for binding of indicated proteins to the FAS promoter. (H) IP of USF-1. (I) ChIP for indicated protein association to the FAS promoter. ChIP samples were analyzed by semi-quantitative PCR (top) or qPCR (bottom). (J) IP of USF-1. (K) ChIP for indicated protein association to the FAS promoter.

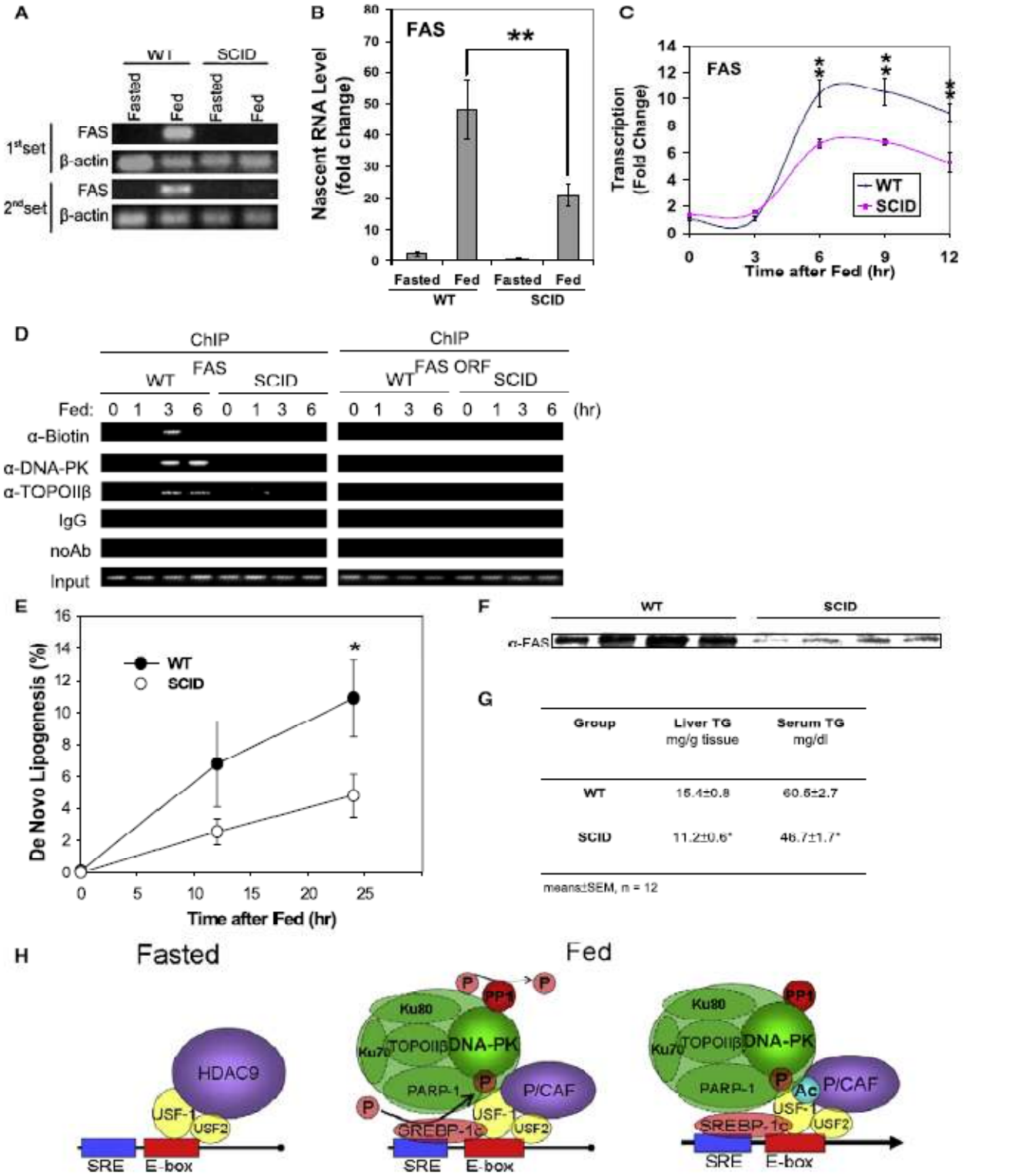

Figure III-6. Diminished FAS induction leading to blunted de novo lipogenesis and decreased triglyceride levels in liver and serum. Nascent RNA were used for (A) RT-PCR or (B) RT-qPCR. Fold induction normalized by β-actin. (C) Run-on of labeled nascent transcripts were analyzed by RT-qPCR. (D) ChIP for DNA breaks and indicated protein binding to the FAS promoter. (E) Newly synthesized labeled fatty acids in livers from 9-wk old mice were measured. Values are means±SEM, n = 12. (F) Immunoblotting of equal amounts of liver extracts from 9-wk old mice after 24 hrs of feeding. (G) Hepatic and serum triglyceride levels were measured in 9-wk old fed mice. (H) Schematic representation of USF-1 and its interacting partners and their effects on lipogenic gene transcription in fasting/feeding.

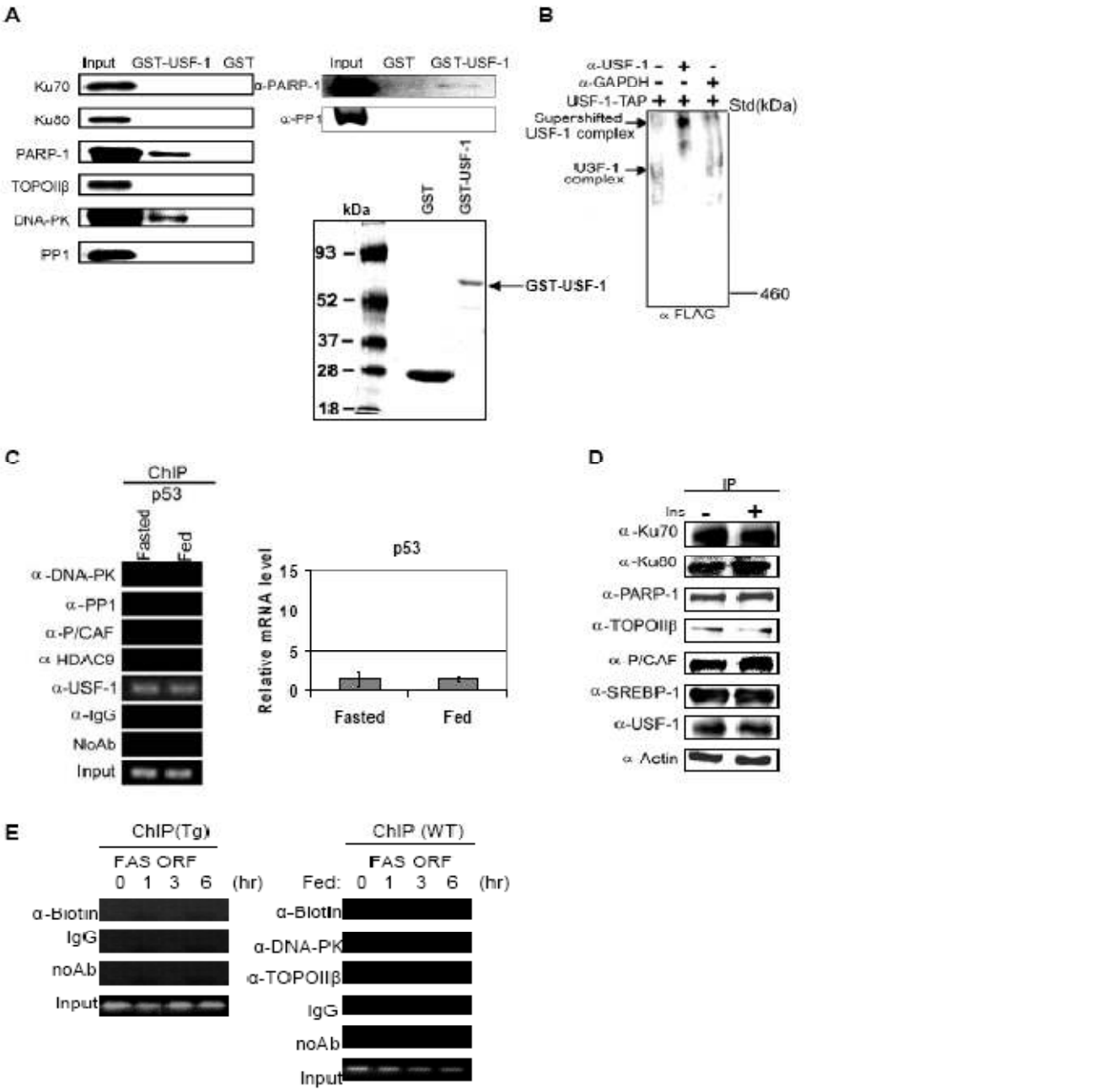

Figure III-S1

(A) Bacterially expressed USF-1-GST fusion protein was incubated with various ***in vitro*** translated ^{35}S-labeled interacting proteins individually before subjection to GST pull- down and autoradiography. Purified USF-1 complex was subjected to autoradiography (left) for labeled proteins. GST protein alone was used as a control. USF-1-GST fusion protein was incubated with purified recombinant PARP-1 or PP1 before subjection to GST pull- down and immunoblotting (top right) for indicated proteins. GST and GST-USF proteins after SDS-PAGE were stained with Coomassie blue (bottom right).

(B) Detection of USF-1 complex: TAP eluates were separated by BN-PAGE and then subjected to Western blotting with anti-FLAG for USF-1. In lanes 2 and 3, supershift assays were carried out with 2 µg polyclonal anti-USF-1 (lanes 2) or 2 µg control polyclonal anti-GAPDH (lane 3). A minor faster migrating complex observed was probably due to partial dissociation of USF-1 interacting proteins from the complex during the sample preparation.

(C) A representative ChIP for USF-1 interacting protein association to the p53 promoter in liver (left). p53 gene expression in livers from fasted or fed mice determined by RT-qPCR (right).

(D) IP of USF-1 interacting proteins from HepG2 cells treated with or without insulin at 100 nM for 30 min. Immunoprecipitates were Western blotted for each of the USF-1 interacting proteins.

(E) ChIP analysis for biotin incorporation into 3'-ends of DNA breaks and DNA-PK and TopoIIβ binding to the control FAS coding region in livers from fasted or fed FAS-CAT transgenic or wild type mice.

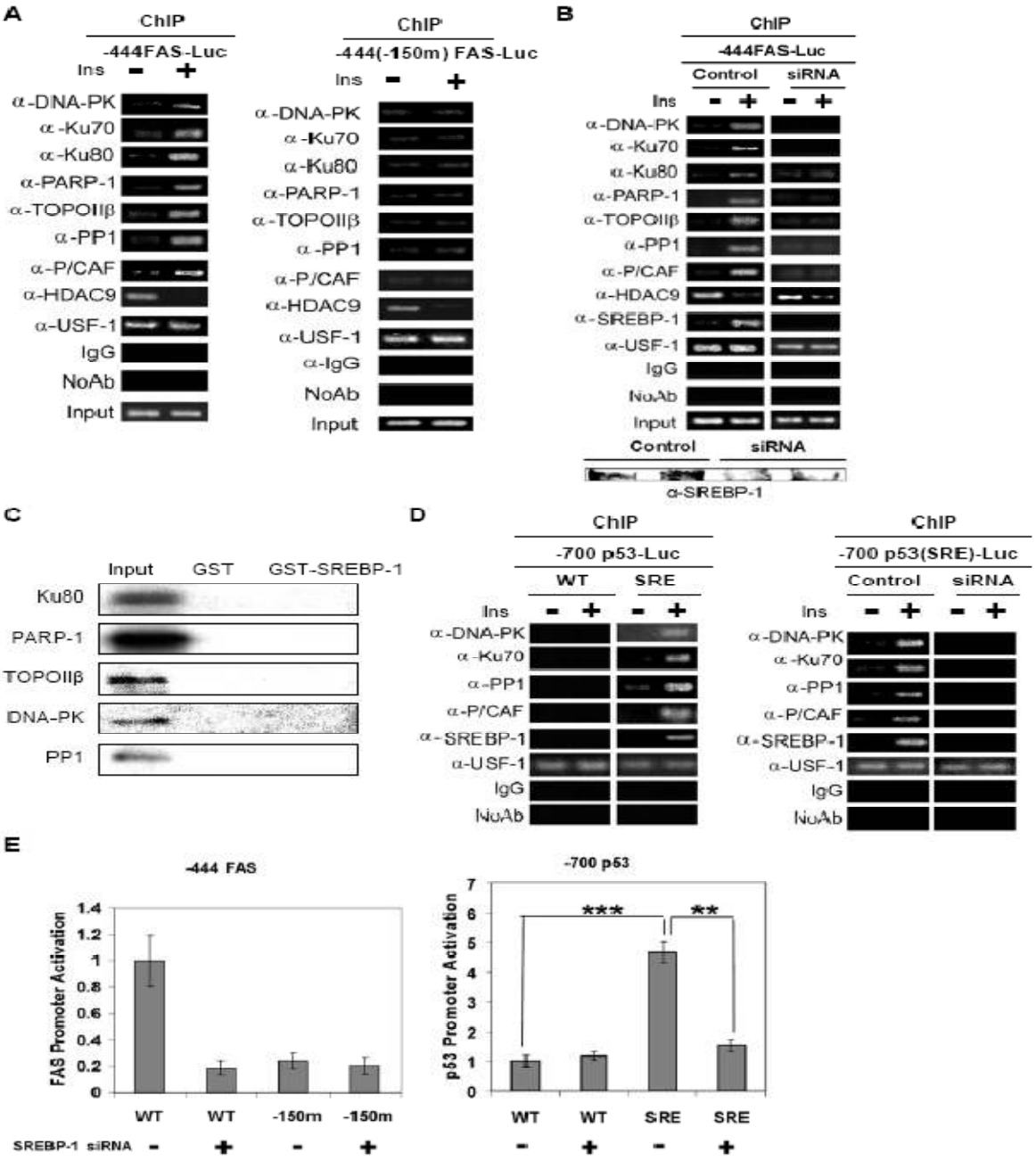

Figure III-S2

(A) ChIP for binding of various USF-1 interacting proteins to the -444 FAS-CAT (left) and -444(-150m) FAS-CAT (right) promoter regions in livers from fasted or fed FAS-CAT transgenic mice.

(B) ChIP for binding of USF-1 interacting proteins to the -444 FAS-Luc in HepG2 cells transfected with control or SREBP-1 siRNA. Cells were treated with or without 100 nM insulin for 30 min. SREBP-1 protein levels analyzed by Western blotting are shown (bottom).

(C) Bacterially expressed SREBP-1-GST fusion protein was incubated with various ***in vitro*** translated ^{35}S-labeled interacting proteins individually before subjection to GST pull- down and autoradiography. Purified SREBP-1 complex was subjected to autoradiography for labeled proteins. GST protein alone was used as a control.

(D) ChIP for binding of various USF-1 interacting proteins to the -700 p53-Luc and -700 (SRE) p53-Luc promoter regions (SRE was inserted 89 bases upstream of the proximal E-box of the p53 promoter, by substitution of CCTCAACCCAC to CATCACCCCAC) in HepG2 cells treated with or without 100 nM insulin for 30 min (left). ChIP (right) for binding of USF-1 interacting proteins to the -700 (SRE) p53-Luc in HepG2 cells transfected with control or SREBP-1 siRNA.

(E) The FAS promoter activity in cells transfected with the -444 FAS-Luc or -444 (-150m) FAS-Luc along with SREBP-1 siRNA was measured by luciferase reporter assay (left). The p53 promoter activity in cells transfected with the -700 p53-Luc or -700 (SRE) p53-Luc along with SREBP-1 siRNA was measured by luciferase reporter assay (right).

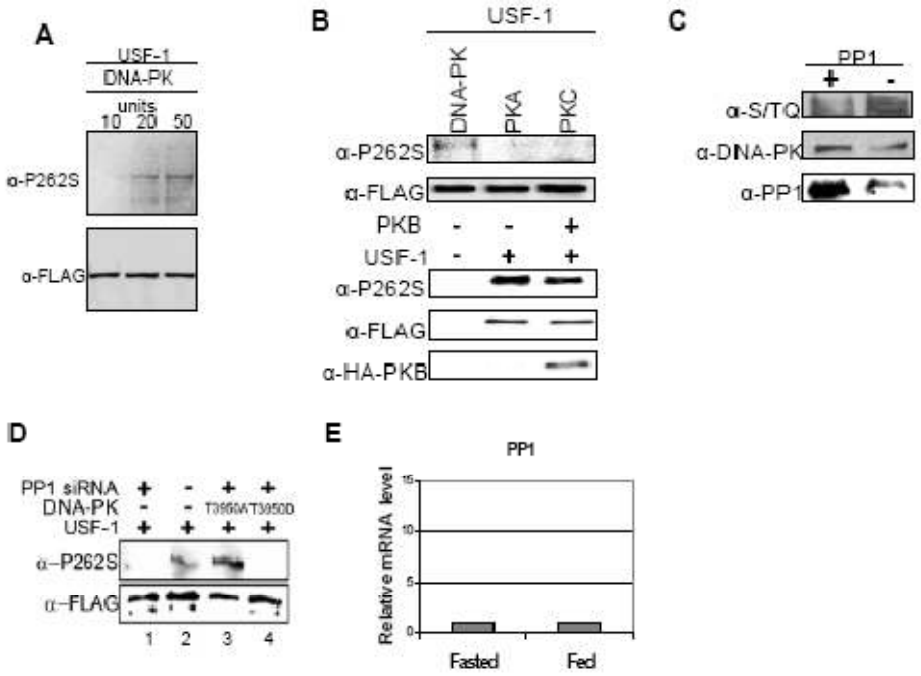

Figure III-S3
(A) Bacterially expressed USF-1incubated with varying concentrations of DNA-PK was immunoblotted for total USF-1 and P262S USF-1.
(B) Bacterially expressed USF-1 was incubated with DNA-PK, PKA, or PKC. Reaction mixtures were subjected to Western blotting for total USF-1 and P262S USF-1 (top). IP of 293F cells overexpressing USF-1 and PKB-HA with anti-FLAG antibodies. USF-1 immunoprecipitated with FLAG antibodies was Western blotted for total USF-1 and P262S USF-1 (bottom). PKB levels were analyzed by western blotting with anti-HA antibodies as shown.
(C) Levels of total DNA-PK and phosphorylated DNA-PK in cells overexpressing DNA-PK with empty vector or PP1 expression vector were analyzed by immunoblotting.
(D) IP of cells cotransfected with USF-1, control or PP1 siRNA, and DNA-PK mutants. Immunoprecipitated USF-1 was Western blotted for total USF-1 and P262S USF-1.
(E) PP1 gene expression in livers from fasted or fed mice was determined by RT-qPCR.

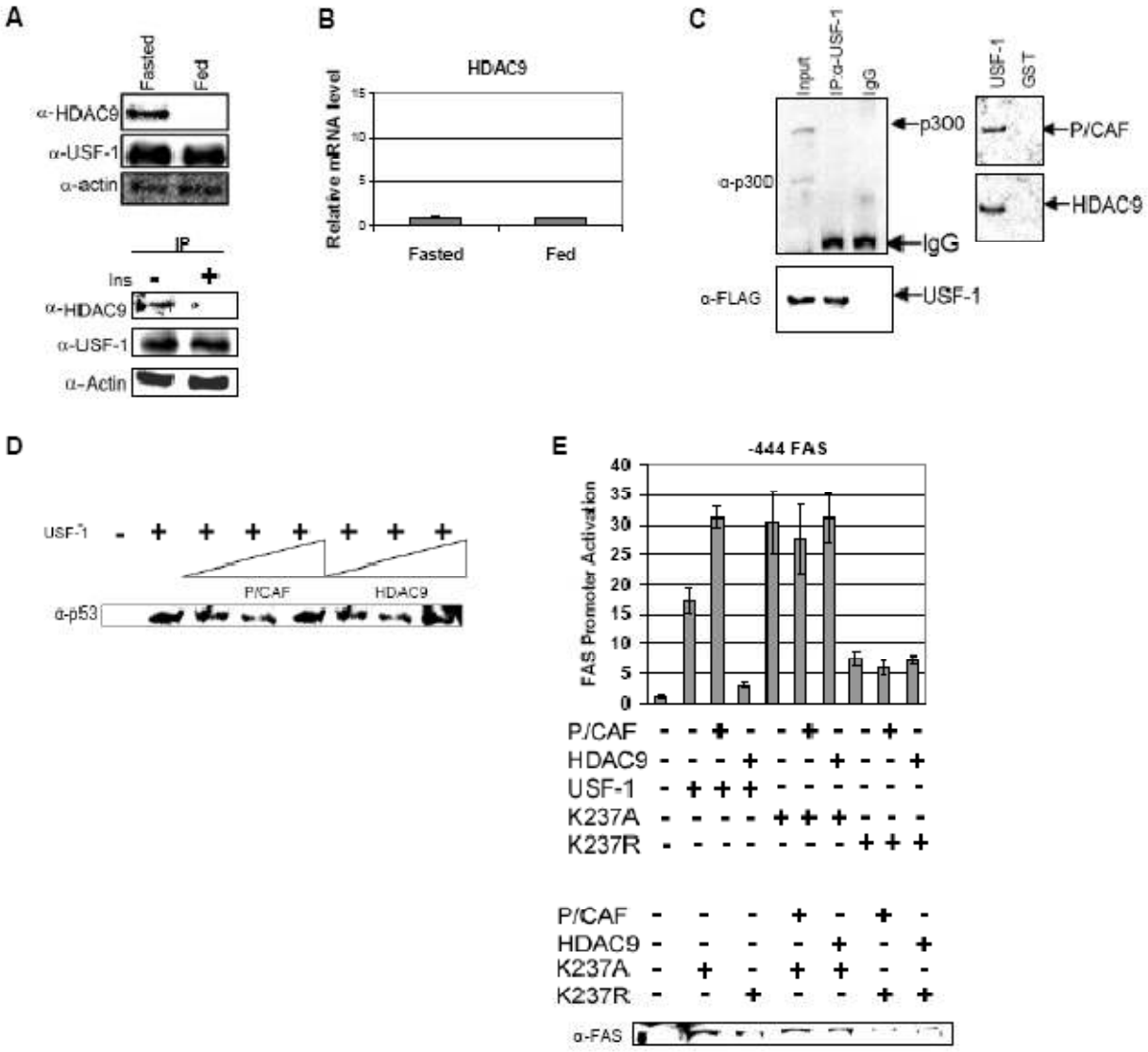

Figure III-S4

(A) IP of liver nuclear extracts with anti-HDAC9 antibodies. Immunoprecipitates were Western blotted for HDAC9. Immunoprecipitated HDAC9 from nuclear extracts of HepG2 cells treated with or without insulin at 100 nM for 30 min was Western blotted for HDAC9. USF-1 and □-actin protein levels were analyzed by Western blotting.

(B) HDAC9 gene expression in livers from fasted or fed mice was determined by RT-qPCR.

(C) IP of cells transfected with USF-1 using polyclonal anti-USF-1 antibodies. Immunoprecipitated USF-1 was Western blotted (left) for USF-1 and p300. Normal IgG was used as a control. Bacterially expressed USF-1 GST fusion protein was incubated with ***in vitro*** translated ^{35}S-labeled P/CAF or HDAC9 before subjecting to GST-pull down. Purified USF-1 was subjected to autoradiography (right) for labeled proteins. GST alone was used as a control.

(D) Total cell lysates in cells transfected with the -444 FAS-Luc, USF-1, and increasing amount of P/CAF or HDAC9 were Western Blotted for p53 protein levels

(E) FAS promoter activity in cells transfected with the -444 FAS-Luc and WT, K237A or K237R USF-1, along with P/CAF or HDAC9 was measured (top). Western blotting of total cell lysates for FAS protein levels (bottom).

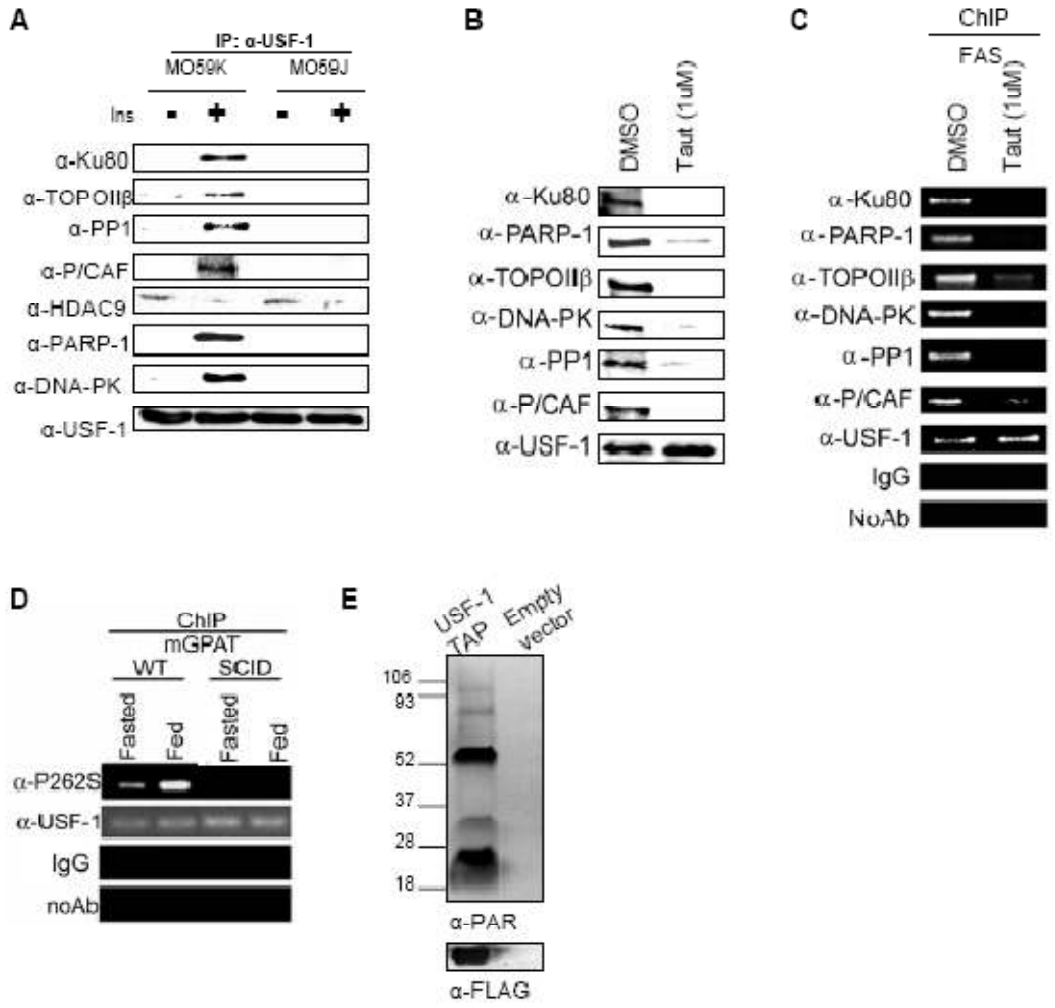

Figure III-S5
(A) IP of nuclear extracts from M059J or M059K cells with anti-USF-1 antibodies and subsequent Western blotting for total USF-1, and various USF-1 interacting proteins. Cells were treated with, or without, 100 nM insulin for 30 min.
(B) IP of USF-1-FLAG from 293 cells overexpressing USF-1 treated with either control DMSO and Taut at indicated concentrations for 2 hrs. USF-1 immunoprecipitated with FLAG antibodies was Western blotted for total USF-1 and various USF-1 interacting proteins.
(C) ChIP for binding of USF-1 and its interacting proteins to the FAS promoter in 293 cells that were treated with either control DMSO and Taut at indicated concentrations for 2 hrs.
(D) ChIP for P262S USF-1 and total USF-1 association to the mGPAT promoter in livers from WT and SCID mice.
(E) TAP-eluates from cells overexpressing USF-1-TAP was subjected to Western blotting using anti-poly(ADP-ribosyl)ated antibodies. Empty TAP vector was used as control.

Group	Glucose mg/dl	Insulin ng/ml	FFA mEq/l	TG mg/dl
WT	53.80±9.30	0.21±0.01	1.40±0.20	60.20±7.30
SCID	69.75±7.54	0.22±0.01	1.61±0.05	60.45±2.65

means±SEM, n = 20

Group	BW	Total Fat Pad	Epididymal Fat	Renal Fat	Inguinal Fat	Kidney	Heart	Liver	Spleen
	g	% Body Weight							
WT	17.5±0.5	0.60±0.03	0.43±0.03	0.07±0.01	0.04±0.01	1.31±0.02	0.81±0.04	6.60±0.25	0.21±0.03
SCID	15.0±0.4*	0.42±0.06*	0.28±0.06*	0.05±0.01*	0.05±0.02	1.35±0.04	0.86±0.05	6.26±0.10	0.16±0.02

means ± SEM, n = 10, No significant differences in food consumption between groups

Table III-1 Blood metabolite levels were measured from WT and SCID mice fasted for 40 hrs (top). No significant differences were found in blood glucose or serum insulin, NEFA and triglyceride levels between the two groups. Body weights and adipose and other organ weights of WT and SCID mice after 24 hrs feeding were measured (bottom). Body weights as well as weights of various fat depots expressed in percentage of body weight were lower in SCID mice compared to WT mice while no significant differences were detected in other organ weights. No significant differences were observed in food consumption between the two groups (3.8 g/day and 3.9 g/day for WT and SCID mice, respectively).

Protein	Peptide sequence	
USF-1	K.YVFRTENGGQVMYR.V2	K.ACDYIQELR.Q2
	R.QQVEDLKNKNLLLR.A2	K.YVFRTENGGQVMYR.V2
	K.YVFRTENGGQVM*YR.V2	R.TENGGQVMYR.V2
	R.THPYSPKSEAPR.T2	K.ACDYIQELR.Q1
	K.ACDYIQELR.Q2	R.LSEELQGLDQLQLDNDVLR.Q2
	R.LSEELQGLDQLQLDNDVLRQQVEDLKNK.N3	R.QQVEDLKNK.N2
	R.QQVEDLKNKNLLLR.A	
USF-2	R.RDKINNWIVQLSK.I2	R.DKINNWIVQLSK.I2
	R.DKINNWIVQLSK.I2	K.INNWIVQLSK.I
	K.INNWIVQLSK.I	
Ku70	R.ILELDQFKGQQGQKR.F2	R.IMLFTNEDNPHGNDSAK.A2
	K.AGDLRDTGIFLDLMHLK.K2	K.TRTFNTSTGGLLLPSDTKR.S3
	K.TRTFNTSTGGLLLPSDTKR.S2	R.TFNTSTGGLLLPSDTKR.S2
	K.GLEKEVAALCR.Y2	R.NLEALALDLMEPEQAVDLTLPK.V3
	R.NLEALALDLMEPEQAVDLTLPKVEAMNK.R3	R.LGSLVDEFKELVYPPDYNPEGK.V2
	R.NLEALALDLMEPEQAVDLTLPKVEAMNKR.L3	K.GTLGKFTVPMLK.E 2
	K.SGLKKQELLEALTK.H	
Ku80	R.HLMLPDFDLLEDIESK.I2	K.KYAPTEAQLNAVDALIDSMSLAK.K2
	K.YAPTEAQLNAVDALIDSMSLAK.K2	R.LFQCLLHR.A2
	K.IKTLFPLIEAK.K2	K.ASFEEASNQLINHIEQFLDTNETPYFMK.S
PARP-1	K.CSESIPKDSLR.M2	K.TAEAGGVTGKGQDGIGSKAEK.T2
	K.RKGDEVDGVDEVAK.K2	K.VCSTNDLKELIFNK.Q2
	R.VVSEDFLQDVSASTK.S2	K.SKLPKPVQDLIK.M2
	K.KPPLLNNADSVQAK.V	
TOPOIIIβ	K.GIIPVVEHKVEK.V2	R.RLHGLPEQFLYGTATK.H2
	R.LHGLPEQFLYGTATK.H2	
DNA-PK	R.CGAALAGHQLIR.G 2	R.ICSKPVVLPK.G2
	R.LYSLALHPNAFKR.L2	K.WLLAHCGRPQTECR.H2
	R.FNNVVDCMKK.F2	K.INQVFHGSGITEGNELTK.T2
	R.SSFDWLTGSSTDPLVDHTSPSSDSLLFAHK.R3	R.SSFDWLTGSSTDPLVDHTSPSSDSLLFAHKR.S3
	R.LGLPGDEVDNKVK.G2	R.LLQIIERYPEETLSLMTK.E2
	K.GANRTETVTSFR.K 2	K.KGGSWIQEINVAEKNWYPR.Q3
	K.KGGSWIQEINVAEKNWYPR.Q2	
PP1	K.NVQLQENEIR.G2	K.IKYPENFFLLR.G2
	K.IFCCHGGLSPDLQSMEQIRR.I2	K.IFCCHGGLSPDLQSMEQIRR.I3
	K.TFTDCFNCLPIAAIVDEK.I2	K.YGQFSGLNPGGRPITPPR.N2
	K.TFTDCFNCLPIAAIVDEK.I	K.YGQFSGLNPGGRQITQQR.N
P/CAF	K.MTDSHVLEEAKKPR.V2	K.MTDSHVLEEAK#KPR.V2
	K.HDILNFLTYADEYAIGYFK.K2	K.HDILNFLTYADEY.AIGYFKK.Q2
	K.YVGYIKDYEGATLMGCELNPR.I2	K.SK#EPRDPDQLYSTLK.S2
	K.SHQSAWPFMEPVKR.T2	K.SHQSAWPFMEPVKR.T3
	R.VFTNCKEYNPPESEYYK.C2	
HDAC9	K.QLQQELLLIQQQQQIQK.Q2	

Table III-2
Peptides of USF-1 interacting proteins identified by MS.

CHAPTER IV: Phosphorylation of BAF60c and acetylation of USF are required for the formation of lipoBAF to activate the lipogenic transcription program in response to insulin

Phosphorylation of BAF60c and acetylation of USF are required for the formation of lipoBAF to activate the lipogenic transcription program in response to insulin

Abstract

Dynamic chromatin structure plays an essential role in the control of gene expression. In mammals, the chromatin remodeling complex, BAF, alters the nucleosomes which is a required step for transcriptional activation. Within the BAF complex, BAF60 proteins function as the bridge between transcription factors and the BAF complex. However, the regulation of BAF60 proteins in response to cellular stimuli is not well understood. Here, we identified BAF60c as an USF interacting protein which is recruited to lipogenic gene promoters upon feeding. Our data show that, among the BAF60a, BAF60b and BAF60c, BAF60c is the only BAF60 specific to lipogenesis and recruits other BAF subunits including BAF155 and BAF190 for the formation of lipoBAF. We found BAF60c phosphorylated at S247 by aPKC upon feeding/insulin. We also show this nuclear translocation of BAF60c from the cytosol to the nucleus in response to feeding/insulin and is dependent on its S247 phosphorylation. Furthermore, this BAF60c phosphorylation together with USF acetylation are required for the interaction between two proteins. We also demonstrated the pivotal role of BAF60c in lipogenesis in vivo. Overexpression of BAF60c activates the lipogenic transcription program even in the fasted state in mice. Our data provides a novel mechanism to fine-tune lipogenic transcription in response to feeding/insulin.

Introduction

Dynamic chromatin structure plays an essential role in the control of gene expression and is tightly regulated. The inherent positioning of the nucleosomes hinders the regulated gene transcription, which can be alleviated by chromatin remodeling components of the BAF (Brg associated complex) complex[1, 2]. In mammals, the BAF complex is a multi-subunit complex that alters the nucleosomes, and is often considered the last step required for transcriptional activation. BAF190 (also called Brg1/Brm), the core unit of the BAF complex, is responsible for ATP hydrolysis. Within BAF complexes, there are BAF60s proteins which are thought to form a recruitment bridge between DNA binding factors and other BAF subunits including BAF190 physically regulating gene transcription[3-5]. Three distinct isoforms of BAF60 proteins BAF60a, BAF60b and BAF60c are known [6]and are able to form distinct complex with different subpopulations of BAFs based on promoter contexts to perform sophisticated cellular functions[7]. For example, specific BAF complexes are found in the heart to regulate differentiation as well as in ES cells to maintain pluripotency[3, 5, 8]. Despite the vital responsibility of BAF60s, overall regulation of BAF60 proteins is not clear.

Transmission of the signal from the plasma membrane to nucleus through cytoplasmic signaling kinases in response to an extracellular signal is a crucial step in the activation of protein kinase cascades. While it is clear that proper targeting of signaling components is essential, most signaling is mediated through phosphorylation or dephosphorylation. In some cases, transcription factors and coregulators are localized in cytosol but translocate into nucleus to transmit signals from protein kinases. In most cases, phosphorylation dependent interaction of specific transcription factors is required. However, protein-protein interaction is usually dependent on one of the partners but not both. Such multi-step regulation allows fine tuning of the interaction. Although a few BAF subunits have been reported to respond to

various signaling pathways[9-12], the regulation by phosphorylation of the anchoring subunit BAF60s has not been elucidated in a physiological manner.

Fatty acid and fat biosynthesis in liver and adipose tissue is under nutritional and hormonal control. Enzymes involved in these processes are tightly and coordinately regulated during fasting and feeding/insulin at the transcriptional level. This transcription of these enzymes is low in fasting, whereas a high carbohydrate meal that raises insulin levels activates the lipogenic transcription program[13-27]. Insulin-mediated activation of atypical PKCλ, PKCζ and AKT via the PI3K pathway is responsible for the protein phosphorylation aspect of insulin[28]. Insulin can also exert metabolic effects through dephosphorylation catalyzed mainly by PP1[29, 30]. Our last study showed that DNA-PK is activated by PP1 and functions as an insulin signaling molecule. Our previous study has identified transcription factors and coregulators required for the lipogenic gene transcription. However, the chromatin remodeling complex required for lipogenic gene transcription has yet to be identified. Also, in our last study, the consequence of acetylation of USF by coactivator P/CAF in response to feeding/insulin on lipogenic gene activation remains unresolved[29]. In this report, we identified BAF60c as USF interacting protein and found that BAF60c was phosphorylated at S247 by aPKC upon feeding/insulin. We also show that translocation of BAF60c from the cytosol to the nucleus in response to feeding/insulin and this nuclear translocation dependent on its S247 phosphorylation. Furthermore, this BAF60c phosphorylation together with USF acetylation are required for the interaction between two proteins. Our data provides a novel mechanism to fine-tune lipogenic transcription in response to feeding/insulin.

Results

Identification of USF interacting BAF complex subunits and their occupancy on lipogenic gene promoters during fasting/feeding

We have previously shown that USF is required for regulation of lipogenic gene promoter activity in fasting/feeding by recruiting distinct coregulators. USF is constitutively bound to the lipogenic gene promoters; however, bound USF is phosphorylated at S262 by DNA-PK and acetylated at K237 by P/CAF in response to feeing/insulin[27, 31, 32]. These results demonstrate the pivotal role of USF function as a molecular switch to recruit various factors to lipogenic gene promoters in a fasting/feeding dependent manner[29]. In an attempt to identify chromatin remodeling complex for lipogenic gene transcription, we performed tandem affinity purification (TAP) and mass spectrometry (MS) analysis using USF as described previously. We identified three BAF complex subunits BAF60c, BAF155 and BAF190. Immunoblotting of the TAP eluates using antibodies against each of the 3 polypepides further confirmed the presence of all 3 polypeptides that were co-purified with TAP-tagged USF-1 (Fig. 1A, left panel). These identified proteins were specific to USF-1, because none of them was found with the control TAP-tag. BAF60c functions as an anchor point between transcription factor and the rest of the BAF complex. Loss of BAF60c could result in failure recruiting BAF complex for chromatin remodeling required for transcriptional activation. BAF60c appears to serve as the anchor point bridging USF-1 and BAF complex for lipogenic gene transcription. The interaction between BAF60c and USF-1 was further confirmed by the detection of BAF60c co-purified with USF-1 by TAP in cells overexpressing BAF60c and USF-1 (Fig. 1A, right panel). Furthermore, GST-pull down assay showed BAF60c can directly interact with USF-1 (Fig. 1B). We therefore dissected the domains of USF-1 required for the interaction with BAF60c. As shown in Figure

1B, the bHLH domain of USF-1 was sufficient for the interaction with BAF60c. The bHLH domain containing K237 that is acetylated by P/CAF in response to feeding/insulin indicates a potential role of USF-1 K237 acetylation in its interaction with BAF60c.

We next investigated whether USF recruits the BAF complex including BAF60c, BAF155 and BAF190 to the lipogenic gene promoters in a fasting/feeding dependent manner. We performed ChIP in livers of fasted and fed transgenic mice expressing a CAT reporter gene driven by the -444 FAS promoter, a minimal FAS promoter sufficient for full response to fasting/feeding and diabetes/insulin treatments. As shown before, we detected binding of USF in both fasted and fed conditions (Fig 1C, left panel). Upon feeding, the FAS-CAT promoter was occupied by all identified USF-1 interacting BAF subunits including BAF60c, BAF155 and BAF190. Binding of BAF60c to the endogenous FAS promoter was observed only in the fed state and recruitments of other BAF60 subunits including BAF60a and BAF60b were not detected (Fig. 1C, 2nd left). This binding pattern indicates only specific BAF60 subunit BAF60c was bound to the FAS promoter upon feeding. We also performed ChIP analysis of the mGPAT promoter using antibodies against all BAF60 subunits. Similar to what we observed with the FAS promoter, USF-1 was bound to the mGPAT promoter in both fasted and fed conditions (Fig. 1C, 2nd right). As seen with the FAS promoter, only BAF60c subunit but not other BAF60s was bound to the mGPAT in the fed state. The similar binding pattern of BAF60c but not other BAF60s suggests a common mechanism for lipogenic induction involving USF and BAF60c in response to feeding. To investigate whether binding of BAF60c is specific to lipogenic gene promoters, we performed ChIP analysis of the Acaa 1b promoter, a fatty acid oxidative gene that is upregulated in fasting[33]. As previously shown, BAF60a was bound to this promoter in fasting while no recruitment of BAF60c was observed (Fig. 1C, right panel). By employing insulin responsive HepG2 cells, we also detected BAF60c binding to the FAS promoter in the presence of insulin while USF-1 was bound in both the presence and absence of insulin (Fig. 1D). Taken together, these data provide evidence that the recruitment of BAF60c is specific to lipogenic genes in response to feeding/insulin.

Feeding dependent recruitment of BAF60c by USF-1 activates the FAS promoter

The interaction between BAF60c and USF-1 brings transcriptional activation through the recruitment of the BAF complex. To test the functional significance of this interaction, we cotransfected cells with USF-1 and BAF60c. The expression of USF-1 with BAF60c resulted in a 3-fold increase in FAS promoter activity while BAF60c alone had no effect on FAS promoter activity (Fig. 1E). Moreover, cotransfection of BAF60c enhanced USF-1 activation of the FAS promoter in a dose-dependent manner (Figure not shown). To further verify the role of BAF60c in USF-1 activation of the FAS promoter, we transfected cells with BAF60c shRNA. FAS promoter activity in BAF60c shRNA plasmid transfected cells, that had more than an 80% decrease in BAF60c levels, was reduced by more than 70% when compared to the control plasmid transfected cells (Fig. 1F). Furthermore, to examine the functional role of BAF60c on lipogenic gene expression in cells, 293 cells were infected with adenovirus expressing BAF60c or shRNA of BAF60c. We also showed that both FAS mRNA and protein levels were unregulated in cells overexpressing BAF60c and downregulated in BAF60c silenced cells respectively (Data not shown). These data suggest that recruitment of BAF60c by USF-1 upon feeding/insulin is linked to lipogenic gene promoter activation.

BAF60c phosphorylation at S247 allows nuclear entry upon feeding/insulin

As shown in Figure 2A, left panel, we showed all identified USF-1 interacting BAF subunits were expressed in lipogenic tissues, liver and white adipose tissue (WAT). Since BAF60c was bound to lipogenic gene promoters in a fasting/feeding manner, we examined the expression of BAF60s in both fasted and fed conditions in mice. As predicted, FAS mRNA was upregulated upon feeding. While BAF60a expression was higher in fasted mice (Data not shown), BAF60c mRNA levels were unchanged between fasting and feeding. We also examined the BAF60c protein levels from total protein extracts prepared from livers of fasted and fed mice. Although FAS protein levels increased upon feeding, no change in protein abundance of BAF60c was observed. We also examined BAF60c protein levels in the nucleus and the cytosol. Surprisingly, as shown in Figure 2B and 2C, we detected significant BAF60c protein levels in liver nuclear extracts of the fed, but not fasted, mice (Fig. 2B) and in nuclear extracts of HepG2 cells cultured in the presence, but note in the absence, of insulin (fig. 2C). In contrast, we detected significant BAF60c protein levels in liver cytosolic extracts from fasted, but not fed, mice (Fig. 2B) and in nuclear extracts of HepG2 cells cultured in the absence, but not in the presence, of insulin (Fig. 2C). These experiments indicate that, in feeding/insulin, translocated into the nucleus and is then recruited to the lipogenic gene promoter by USF-1 to bridge the BAF complex for transcriptional activation.

Since BAF60c was translocated from cytosol to nucleus in response to feeding/insulin, we investigated whether BAF60c translocation can be regulated by phosphorylation in a fasting/feeding dependent manner. Phosphorylation of BAF proteins for regulation of metabolism was not reported. Although some subunits of the BAF complex have been shown to be phosphorylated, none of the BAF60 isoforms has ever been shown to be phosphorylated in a physiological context. We used NetPhos program to locate candidate sites for phosphorylation of BAF60 and found S247 to be most probable serine residue to be phosphorylated. Although S247 of BAF60c and its nearby amino acids are highly conserved among mammals (S1, left panel), this specific serine residue is not evolutionally conserved in lower organisms (S1, right panel). Interestingly, S247 is not found in other BAF60 isoforms in mammals, indicating S247 phosphorylation is unique to the function of BAF60c. To examine S247 phosphorylation in vivo, based on the nearby amino acid sequence, we tested a few site specific phosphoserine antibodies for the ability to recognize WT but not the phospho blocking mutant S247A BAF60c phosphorylation. We found that an antibody against Raf kinase inhibitor protein (RKIP) on S153 (referred as anti-P247S) indeed recognized BAF60c phosphorylated on S247 specifically (Fig. 2D). Using antibodies against pS153-RKIP, we then examined S247 phosphorylation in response to insulin. We detected higher S247 phosphorylation of BAF60c in HepG2 cells upon insulin treatment (Fig. 2E). Since BAF60c was localized in the nucleus upon feeding/insulin and is phosphorylated at S247 by feeding/insulin, the effect of S247 phosphorylation on BAF60c translocation into the nucleus was examined. We transfected 293 cells with either WT BAF60c or non-phosphorylatable S247A BAF60c and examined the exogenous BAF60c levels in both the nucleus and cytosol. The BAF S247A BAF60c was higher in abundance in the cytosol when compared to the WT while WT BAF60c was localized more in nucleus than S247A BAF60c (Fig. 2F). This data suggests that S247 phosphorylation of BAF60c governs its translocation in response to insulin. Because S247A BAF60c failed to be localized into the nucleus, we tested the functional significance of this S247 phosphorylation. As shown before, the WT BAF60c upregulated USF-dependent FAS promoter activation at a high level. In contrast, the phospho blocking S247A BAF60c mutant could no longer further activate the FAS promoter (Fig. 2G). Furthermore, by ChIP, we tested

whether the recruitment of BAF60c to FAS promoter by USF is dependent on S247 BAF60c phosphorylation, and found that WT BAF60c was found to be bound to the FAS promoter at a much higher level when compared to the S247A BAF60c mutant (Fig. 2H). These data suggest that S247 phosphorylation of BAF60c governs its nuclear entry in response to feeding/insulin.

aPKC mediates feeding-dependent phosphorylation of BAF60c

To further understand how the feeding/insulin dependent phosphorylation of BAF60c activates the FAS promoter, we attempted to identify the kinase that catalyzes this S247 phosphorylation. Search of phosphoprotein databases predicted that member of the PKC family of kinases probably phosphorylates the S247 site. Among the 10 PKC isoforms, atypical PKC isoforms λ and ζ that are activated by PI3K are known to be effectors of insulin action[28]. To examine whether S247 of BAF60c is a target of aPKC, we performed in vitro phosphorylation of in vitro translocated BAF60c by aPKC ζ and aPKC λ. Indeed, we could easily detect S247 phosphorylation of BAF60c by aPKC ζ (Fig. 3A, left panel) and aPKC λ (Fig 3A, right panel). Furthermore, S247 phosphorylation was abolished when cell-permeable myristoylated PKC-ζ/λ inhibitory peptide (Pep) was added at 100mM to inhibit aPKC activity (Fig. 3A)[34]. We also performed in vitro phosphorylation on the S247A BAF60c mutant. WT BAF60c but not S247A BAF60c was detected to have higher S247 phosphorylation upon incubation with both aPKC ζ and λ (Fig. 3B). Based on these results, we conclude that the S247 of BAF60c is a specific target of aPKC in vitro. We next tested S247 phosphorylation of BAF60c by aPKC in cultured cells. We could not detect S247 phosphorylation of BAF60c immuoprecipitated from cells overexpressing BAF60c upon treatment with Pep which inhibits aPKC activity (Fig 3C). As expected, phosphorylation of BAF60c was easily detected in control DMSO treated cells. Furthermore, we detected higher S247 phosphorylation of BAF60c from cells overexpressing BAF60c treated with AICAR at 2mM and Okadaic Acid (OA) at 1 uM, which could activate aPKC, compared to control treated cells (Fig. 3D)[35, 36]. We showed earlier that S247A BAF60c failed to be localized in the nucleus, which prompted us to ask whether inhibiting S247 phosphorylation would have an impact on BAF60c nuclear localization. BAF60c was higher in abundance in the cytosol in cells treated with Pep and RO31-8220 at 20mM (RO**,** a general PKC inhibitor) compared to control cells treated with DMSO while BAF60c was localized more in nucleus in control cells than cells treated with Pep and RO (Fig. 3E). These data along with the fact that aPKC is associated with insulin signaling demonstrate that aPKC mediated S247 phosphorylation of BAF60c governs its translocation in response to feeding/insulin.

We further tested S247 phosphorylation of BAF60c by overexpressing aPKC in cultured cells. Overexpression of aPKC λ enhanced S247 phosphorylation (Fig. 3F). To further verify the role of aPKC in S247 phosphorylation, we performed siRNA –mediated knockdown of both aPKC ζ and λ (Fig. 3G). We found that S247 phosphorylation was significantly reduced in the aPKC siRNA transfected cells that had more than an 80% decrease in aPKC levels. The BAF60c dependent FAS promoter activation in aPKC siRNA transfected cells was abolished when compared to the control siRNA transfected cells (Fig. 3H). These results demonstrate that S247 phosphorylation of BAF60c is mediated specifically by atypical PKC.

Interaction between BAF60c and USF-1 depends on their modifications: BAF60c phosphorylation and USF acetylation

We have previously shown that feeding/insulin mediated activation of DNA-PK results in phosphorylation and acetylation of USF-1 at K237. Although the USF acetylation is critical for transcriptional activation of lipogenic genes, the consequence of USF acetylation on transcriptional activation remains unclear[29]. Since BAF60c interacts with USF-1 in the domain containing K237, we tested whether acetylation of USF-1 could affect the interaction between USF-1 and BAF60c. Coimmunoprecipitation showed that the hyperacetylated K237A mutant of USF-1 preferentially interacted with BAF60c in comparison to the non-acetylatble K237R mutant (Fig. 4A). Since BAF60c is phosphorylated at S247, we next examined whether the S247 phosphorylation of BAf60c affects the interaction with USF-1. We found by GST-pull down that bacterially expressed USF-1 preferentially interacted with in vitro translated WT BAF60c but not with S247A BAF60c, indicating that USF interacts with phosphorylated BAF60c in higher affinity when compared to non-phosphorylated BAF60c. To verify the hypothesis that the interaction between USF-1 and BAF60c requires both USF acetylation and BAF60c phosphorylation, we performed an in vitro interaction between USF-1 and BAF60c with all possible modification combinations. We found that show that only hyperacetylated USF-1 was able to interact with WT BAF60c but not with the phospho blocking S247A BAF60c while nonacetylated USF-1 failed to interact with either WT or S247A BAF60c. Similar results were observed in ChIP analysis of FAS-Luc promoter in cells transfected with K237A or K237R USF-1 along with WT or S247A BAF60c. Hyperacetylated USF-1 displayed the highest recruitment of WT BAF60c to the FAS promoter (Fig. 4D).

To further confirm if the interaction between USF-1 and BAF60c is modification dependent, hyperphosphorylated or phosphorylated and non-phosphorylated S247 peptides were used to compete the interaction between in vitro translated BAF60c and GST USF-1fusion protein in vitro (Fig. 4E, top left and right panel). Bacterially expressed USF-1 was incubated with BAF60c in the presence or absence of pSer247 or Ser247A and the immunoblots were probed with BAF60c antibodies. In the presence of the pSer247 peptide, the pull-down BAF60c was significantly reduced, whereas the non-phosphorylated Ser247A peptide was unable to block the interaction between USF-1 and BAF60c (Fig. 4E, top left panel). Hyperphosphorylated S247D peptide also competed the interaction between BAF60c and USF-1 in vitro (Fig. 4E, top right panel). We also examined whether the pSer247 peptide could compete the endogenous interaction between USF-1 and BAF60c in cultured cells. Nuclear extract prepared from cells transfected with USF-1 and BAF60c was incubated in the presence or absence of pSer247 or Ser247A peptides. As expected, in the presence of the pSer247 peptide, the pull-down exogenous BAF60c was significantly reduced (Fig. 4E, bottom left panel). Furthermore, when cells were transfected with only USF-1, the endogenous interaction between USF-1 and endogenous BAF60c was disrupted in the presence of the pSer247 peptide but not S247A peptide (Fig. 4E, bottom right panel). These data show that phosphorylated S247 of BAF60c interacts with USF-1 with a much higher affinity compared to non-phosphorylatable BAF60c, and the peptide containing S247 and nearby residues is the site of interaction with USF-1.

BAF60c induces lipogenesis during fasting in mice

Since BAF60c is essential for lipogenic gene transcriptional activation upon feeding, we postulated BAF60c alone should activate lipogenic gene transcription program even in fasting. We assessed the transcriptional activation of the FAS gene and other lipogenic genes in mice

overexpressing BAF60c during fasting. We tail-vein-injected the animals with adenovirus expressing either BAF60c or GFP. We first measured BAF60c mRNA levels in the liver from control or BAF60c mice that were either fasted or fed (Fig. 4F) by RT-PCR. In control mice, BAF60c expression level was the same between fasting and feeding as predicted. RT-qPCR analysis indicated a 12-fold higher BAF60c in BAF60c adenovirus injected mice during fasting compared to the control mice. As predicted, FAS and mGPAT mRNA levels were very low in livers of fasted control mice, but upon feeding, they were induced drastically to approximately 20- fold. FAS and mGPAT mRNA levels in BAF60c overexpressed mice during fasting increased to a level similar to the levels of the control mice upon feeding. In addition, similar upregulation of lipogenic genes including SCD-1 and ACC in BAF60c overexpressed mice during fasting was observed (Fig. 4F). We then examined in vivo hepatic de novo lipogenesis in the control and BAF60c mice during fasting using a stable isotope method. Fractional de novo lipogenesis was increased by more than 2-folds in the BAF60c mice when compared to the control mice despite the lack of lipogenic substrates (Fig. 4G). Overall, these results clearly show in vivo the critical role of BAF60c in activation of lipogenic genes by feeding/insulin. Our in vivo data links BAF60c's function in chromatin remodeling to activation of the lipogenic transcription program upon feeding/insulin.

Discussion

A central issue in metabolic regulation is to define coordinated molecular strategies that underlie the transition from fasting to feeding, such as the transcription activation of lipogenesis along the specific transduction pathways. Although BAF60s is known to bridge transcription factors and BAF complex, is indispensable for regulated transcription. However, the regulation of BAF60s in response to cellular signaling is not well understood. Here, we define specific BAF60c recruits BAF subunits including BAF155 and BAF190 for the formation of lipoBAF complex for lipogenic gene transcription, which is based on phosphorylation-dependent translocation of BAF60c. Moreover, USF acetylation and BAF60c phosphorylation are required for the interaction between both in converging insulin signals.

BAF60c and its associated subunits define BAF complex specific for lipogenic gene transcription

BAF60s proteins are thought to form a recruitment bridge between DNA binding factors and BAF subunits in regulating gene transcription. Three distinct isoforms of BAF60 proteins BAF60a, BAF60b and BAF60c are identified and are able to form distinct complex based on promoter contexts to perform sophisticated cellular functions. BAF60a was reported to interact with PGC1 to coactivate fatty acid oxidative genes in liver[4]. Besides fatty acid oxidization, BAF60a is also required for ES cell maintenance and pluripotency[8]. Recently, BAF60a has been shown to be a target for miR122 which has implicated function in cholesterol and lipid metabolism[37]. A link between BAF60b and Rac signaling has also been demonstrated[38]. For BAF60c isoform, it has been reported to activate cardiac genes during heart development. However, none of the BAF60s isoforms has been shown to play a role in lipogenesis, despite chromatin remodeling is a required step for transcriptional activation. Our study shows that USF interacts with BAF60c, but not BAF60a or BAF60b, to recruit BAF subunits including BAF155 and BAF190 to lipogenic gene promoters. The distinct binding pattern of BAF60c, 155

and 190 on the lipogenic gene promoter in response to feeding/fasting is correlated with lipogenic gene activation/repression which involves chromatin remodeling events that require the presence of the BAF complex. Since BAF60c is the only BAF60 isoform specific for lipogenic gene activation, we hereby define the USF-1 interacting BAF subunits BAF60c recruits BAF subunits including BAF155 and BAF190 for the formation of the lipogenesis specific BAF complex (lipoBAF). This common binding pattern of the lipoBAF on lipogenic gene promoters indicates that a common key mechanism exists to induce lipogenic gene transcription in response to fasting/feeding.

Phosphorylation-dependent translocation of BAF60c in response to feeing functions as a novel regulation for BAF proteins

BAF60s isoforms have diverse and distinct cellular functions, however, the regulation or modifications such as phosphorylation of BAF60s have not been well understood. Few BAF subunits have been shown to be phosphorylated in general, however, none of the BAF60 isoforms have been reported to be a substrate for kinases in cultured cells or in vivo. Even though there are examples of changes in phosphorylation states of transcription factors between fasting/feeding, phosphorylation of the BAF complex including in these metabolic states have not been revealed. Since BAF60c levels are unaltered between fasting and feeding/insulin, it can be postulated that the differential binding pattern of BAF60c between fasting and feeding/insulin is because of the differential regulations of BAF60c.

As BAF complex governs the chromatin remodeling events for regulated transcription, BAF subunits are residents of nucleus. Here, first time for BAF proteins, we demonstrated the presence of BAF60c in the cytosol in a physiological condition[39]. We also showed that BAF60c can be translocated from the cytosol to the nucleus dynamically in response to a physiological signal – feeding/insulin. This translocation is regulated by aPKC mediated S247 phosphorylation, the first phosphorylated serine identified for BAF60s. The S247 of BAF60c as well as nearby residues are conserved among mammalian species but are not found in other BAF60 isoforms. While lower organisms have only one BAF60 isoform that does not contain S247, BAF60c in mammals appears to be a unique BAF subunit for complicated regulation of mammalian lipogenic metabolism.

Cross talk between phosphorylation and translocation is well recognized for transcription factors, however, a similar regulation have not been well understood for transcriptional coregulators including coactivators, corepressors, mediators and chromatin remodeling complexes. In our study, translocation of BAF60c to the nucleus in response to feeding/insulin is dependent on S247 phosphorylation. This regulation of BAF60c functions as a dynamic molecular switch in sensing the nutritional transition from fasting to feeding, providing an elegant way to fine tune lipogenic transcription.

Requirement of USF acetylation and BAF60c phosphorylation for the interaction between both converges insulin signals

It has been well established that the PI3K and PP1 pathways mediate insulin signaling for metabolic regulation by catalyzing opposing action, phosphorylation and dephosphorylation respectively. Our previous study showed that PP1activates DNA-PK by dephosphorylation. Activated DNA-PK then phosphorylates USF-1 at S262 which allows K237 acetylation by

P/CAF (Fig. 4H). Although K237 acetylation is critical for lipogenic gene activation, its function is unknown, here we show that K237 acetylation of USF-1 governs recruitment of BAF60c to the lipogenic gene promoters. The BAF complex will then be recruited by BAF60c to the lipogenic gene promoters to modify the chromatin, an essential step for transcriptional activation. On the other hand, the protein phosphorylation aspect of insulin signaling is mediated by PI3K which activates PKB and aPKC (Fig. 4H). While the role of PKB in GLUT4 translocation in response to insulin is well accepted, we showed here that BAF60c links aPKC to activation of lipogenic gene transcription[28, 40]. Our in vitro and in vivo phosphorylation studies and the fact that S247 phosphorylation is abolished in aPKC siRNA knockdown cells point to the notion that aPKC is the kinase for the S247 phosphorylation occurring during the feeing/insulin condition. Although the link between aPKC and transcription activation of lipogenesis is not well understood, our study provides direct evidence that BAF60c bridge the gap in between. Interestingly, besides translocation, BAF60c phosphorylation also regulates its interaction with USF-1, showing a dual role of S247 phosphorylation in BAF60c regulation. To our surprise, one sided modification of USF-1 or BAF60c, acetylation at K237 and phosphorylation at S247 respectively, is not sufficient for the interaction to occur at its full potential. This interaction requires modification of both USF acetylation and BAF60c phosphorylation. The regulation of the interaction represents a “dance” like concept that resembles a biological circuit. A high output (interaction in this case) results only if both the inputs (USF acetylation and BAF60c phosphorylation) to this biological circuit are high. This novel regulation provides a way to fine tune an interaction and might be identified in other protein-protein interactions across the field of biology. Taken together, we propose the following model for the mechanism underlying USF and BAF60c function in the transcriptional regulation of lipogenic genes during fasting/feeding (Fig. 4H). Upon feeding, opposing actions of insulin signaling activates aPKC and DNA-PK resulting in BAF60c phosphorylation and USF acetylation respectively. These modifications allow an interaction to occur and bring-in the chromatin remodeling machinery as the last step of transcriptional activation for lipogenic genes. This unique biological circuit converges two opposing signals of insulin into one unified and vital action.

Experimental Procedures

Additional experimental procedures are available in the supplemental data.

Purification of USF-1 interacting proteins and preparation of nuclear extracts

TAP was performed as described previously [29, 32]. Purified protein mixture was subjected to mass spectrometry. Liver nuclear extracts were prepared by centrifugation through sucrose cushion in the presence of NaF.

Chromatin Immunoprecipitation

Livers from fasted or fed mice were fixed with DSG at 2 mM for 45 min at RT before formaldehyde cross-linking. ChIP was performed as described previously[29].

In vitro phosphorylation

In vitro phosphorylation was performed using recombinant/purified enzymes.

Immunoprecipitation, GST-pull down, luciferase reporter assays

Immunoprecipitation from nuclear extracts was performed under standard procedures. GST pull-down was performed as described previously[29]. Luciferase assays were performed in 293FT cells using Dual-Luc reagent (Promega).

RT-PCR analysis

RNA was isolated and reverse transcribed for PCR or qPCR.

De novo lipogenesis (DNL)

Fatty acids formed during a 24 hrs $^{2}H_{2}O$ body water labeling (See the Supplemental Experimental Procedures for further details).

Statistical analysis

The data are expressed as the means ± standard errors of the means, Student's *t* test was used (**P* < 0.05, ***P* < 0.01, ****P* < 0.005 and *****P* < 0.0001).

Supplemental experimental procedures

Antibodies, animals, cell culture and transfection

Rabbit polyclonal antibodies were raised against peptides corresponding to aa 4-20 of mBAF60c (DEVAGGARKATKSKLFE). The following commercially available antibodies were used: Monoclonal Anti-USF-1 (M01,M02) (Abnova), M2 anti-FLAG (Sigma), anti-phosphoserine (Calbiochem), anti-HA (Covance) and polyclonal anti-USF-1 (C-20), normal IgG, anti-GAPDH, anti-155, anti-190, anti-BAF60a, anti-BAF60b, anti-pRKIP, anti-GFP, anti-aPKC, anti-lambinB1, anti-FAS (Santa Cruz).

C57BL/6J male mice (Jackson laboratory) were used at 8 wks of age unless specified. For fasting/feeding experiments, mice were fasted for 40 hrs and then fed a high carbohydrate, fat-free diet for indicated time periods. HepG2 cells were grown in DMEM supplemented with 10% fetal bovine serum and 100 units/ml penicillin/streptomycin. HepG2 cells were maintained in serum free media overnight prior to insulin treatment. For insulin treatment, HepG2 cells were treated with 100 nM insulin or DMSO for 30 min. 293FT cells in DMEM supplemented with 10% fetal bovine serum and 100 units/ml penicillin/streptomycin/neomycin or 293F cells in 293 Freestyle medium were transfected with expression constructs or siRNA (Santa Cruz) using lipofectamine 2000 (Invitrogen) or 293 Fectin (Invitrogen), respectively.

Purification of USF-1 interacting proteins and preparation of extracts

The 293F cells were transfected with USF-1-FLAG-TAP or empty TAP vector. Briefly, nuclear extracts were subjected to two-step affinity purification using calmodulin and streptavidin resins (stratagene) [32]. Purified proteins were concentrated by Centricon YM-3 (Amicon) and analyzed by SDS-PAGE, followed by silver staining (Invitrogen). Purified protein mixture was subjected to 2D “MudPIT” Run (cation exchange/RP LC-MS/MS) using a Finnigan LCQ Deca XP mass spectrometer in NanoLC/ESI mode. Sequest program was used for interpretation of the mass spectra.

For liver nuclear extracts, mice were fasted for 40 hrs and then fed a high carbohydrate, fat-free diet for 16 hrs or indicated time periods. Nuclear extracts were prepared by centrifugation through sucrose cushion in the presence of NaF. [32]. For 293 cells, nuclear extracts were prepared by high salt extraction [41]. Total protein extracts were prepared by homogenization of tissues/cells in RIPA buffer. Cystolic extracts were prepared by homogenization in L1 buffer (50 mM Tris pH8.0, 2 mM EDTA, 0.1% NP40, 10% glycerol) followed by ultracentrifugation.

Chromatin Immunoprecipitation

Livers from fasted or fed mice were fixed with DSG at 2 mM for 45 min at RT before formaldehyde cross-linking. Soluble chromatin was quantified by absorbance at 260nm, and equivalent amounts of input DNA were immunoprecipitated. ChIP was performed as described previously [42]. For real time PCR of ChIP samples, the fold enrichment values were normalized to the control IgG.

***In vitro* phosphorylation**

In vitro phosphorylation reactions were performed using aPKC (upstate) and ATP (Promega).

Immunoprecipitation, GST-pull down, luciferase reporter assays

For immunoprecipitation, nuclear extracts were incubated with the specific antibodies overnight at 4°C followed by incubation with protein G agarose beads (Santa Cruz), washed and separated by SDS-PAGE. Proteins were transferred onto nitrocellulose membranes (Bio-Rad) and Western blotting was performed. For GST pull-down, bacterially expressed GST proteins were first incubated with glutathione-agarose (Santa Cruz) followed by incubation with ^{35}S labeled proteins, and autoradiography was performed[29]. Plasmids containing full length cDNA of BAF60c (Open Biosystem) were used for *in vitro* translation. The 293FT cells were transfected with-444-FAS-Luc along with various expression constructs and siRNA (Santa Cruz) using Lipofectamine 2000 reagent (Invitrogen), and luciferase assays were performed using Dual-Luc reagent (Promega).

RT-PCR analysis

Four ug of total RNA isolated using Trizol reagent (Gibco BRL) were reverse transcribed and the resultant cDNAs were amplified by semi-quantitative PCR or real time qPCR. For Real-time RT-qPCR, the relative mRNA levels of gene markers were quantified with β-actin as the internal control using EVA dye (Biochain) as the probe. Statistical analysis of the qPCR was obtained using the ($2^{-\Delta\Delta Ct}$) method.

Production of recombinant adenoviruses

Adenoviruses were produced using the Ad-Easy adenovirus system according to the manufacturer's instructions (Stratagene). Briefly, pShuttle-CMV targeting vectors containing full-length BAF60c tagged with HA were linearized by digestion with *Pme*I and electroporated into BJ5183 electrocompetant cells. pShuttle-IRES-hrGFP-2 was used to generate control GFP adenovirus. Adenoviral vectors containing insert DNA were linearized with *Pac*I and transfected

into 293FT cells using Lipofectamine 2000. Following amplification in 293FT cells, infectious adenovirus was titred in 293FT cells. Adenoviruses were injected into animals via tail vein according to body weight.

Measurement of de novo lipogenesis (DNL)

Fatty acids synthesized during a 24 hrs $^{2}H_2O$ body water labeling were measured as described previously[43]. Mass isotopomer distribution analysis (MIDA) was used. Fractional DNL contribution was calculated as previously described by $f_{DNL} = M1_{FA} / A_{1\infty\ FA}$.

REFERENCES

1. Mohrmann, L. & Verrijzer, C. P. Composition and functional specificity of SWI2/SNF2 class chromatin remodeling complexes. *Biochim. Biophys. Acta* **1681**, 59-73 (2005).
2. Vicent, G. P. *et al*. Minireview: Role of Kinases and Chromatin Remodeling in Progesterone Signaling to Chromatin. *Mol. Endocrinol.* (2010).
3. Takeuchi, J. K. & Bruneau, B. G. Directed transdifferentiation of mouse mesoderm to heart tissue by defined factors. *Nature* **459**, 708-711 (2009).
4. Li, S. *et al*. Genome-wide coactivation analysis of PGC-1alpha identifies BAF60a as a regulator of hepatic lipid metabolism. *Cell. Metab.* **8**, 105-117 (2008).
5. Lickert, H. *et al*. Baf60c is essential for function of BAF chromatin remodelling complexes in heart development. *Nature* **432**, 107-112 (2004).
6. Wang, W. *et al*. Diversity and specialization of mammalian SWI/SNF complexes. *Genes Dev.* **10**, 2117-2130 (1996).
7. D'Alessio, J. A., Wright, K. J. & Tjian, R. Shifting players and paradigms in cell-specific transcription. *Mol. Cell* **36**, 924-931 (2009).
8. Ho, L. *et al*. An embryonic stem cell chromatin remodeling complex, esBAF, is essential for embryonic stem cell self-renewal and pluripotency. *Proc. Natl. Acad. Sci. U. S. A.* **106**, 5181-5186 (2009).
9. Bourachot, B., Yaniv, M. & Muchardt, C. Growth inhibition by the mammalian SWI-SNF subunit Brm is regulated by acetylation. *EMBO J.* **22**, 6505-6515 (2003).
10. Sif, S., Stukenberg, P. T., Kirschner, M. W. & Kingston, R. E. Mitotic inactivation of a human SWI/SNF chromatin remodeling complex. *Genes Dev.* **12**, 2842-2851 (1998).
11. Simone, C. *et al*. p38 pathway targets SWI-SNF chromatin-remodeling complex to muscle-specific loci. *Nat. Genet.* **36**, 738-743 (2004).
12. Foster, K. S., McCrary, W. J., Ross, J. S. & Wright, C. F. Members of the hSWI/SNF chromatin remodeling complex associate with and are phosphorylated by protein kinase B/Akt. *Oncogene* **25**, 4605-4612 (2006).
13. Paulauskis, J. D. & Sul, H. S. Cloning and expression of mouse fatty acid synthase and other specific mRNAs. Developmental and hormonal regulation in 3T3-L1 cells. *J. Biol. Chem.* **263**, 7049-7054 (1988).
14. Paulauskis, J. D. & Sul, H. S. Hormonal regulation of mouse fatty acid synthase gene transcription in liver. *J. Biol. Chem.* **264**, 574-577 (1989).
15. Moustaid, N. & Sul, H. S. Regulation of expression of the fatty acid synthase gene in 3T3-L1 cells by differentiation and triiodothyronine. *J. Biol. Chem.* **266**, 18550-18554 (1991).
16. Yet, S. F., Lee, S., Hahm, Y. T. & Sul, H. S. Expression and identification of p90 as the murine mitochondrial glycerol-3-phosphate acyltransferase. *Biochemistry* **32**, 9486-9491 (1993).
17. Moustaid, N., Sakamoto, K., Clarke, S., Beyer, R. S. & Sul, H. S. Regulation of fatty acid synthase gene transcription. Sequences that confer a positive insulin effect and differentiation-dependent expression in 3T3-L1 preadipocytes are present in the 332 bp promoter. *Biochem. J.* **292 (Pt 3)**, 767-772 (1993).
18. Moustaid, N., Beyer, R. S. & Sul, H. S. Identification of an insulin response element in the fatty acid synthase promoter. *J. Biol. Chem.* **269**, 5629-5634 (1994).
19. Yet, S. F., Moon, Y. K. & Sul, H. S. Purification and reconstitution of murine mitochondrial glycerol-3-phosphate acyltransferase. Functional expression in baculovirus-infected insect cells. *Biochemistry* **34**, 7303-7310 (1995).

20. Soncini, M., Yet, S. F., Moon, Y., Chun, J. Y. & Sul, H. S. Hormonal and nutritional control of the fatty acid synthase promoter in transgenic mice. *J. Biol. Chem.* **270**, 30339-30343 (1995).
21. Moon, Y. S., Latasa, M. J., Kim, K. H., Wang, D. & Sul, H. S. Two 5'-regions are required for nutritional and insulin regulation of the fatty-acid synthase promoter in transgenic mice. *J. Biol. Chem.* **275**, 10121-10127 (2000).
22. Sul, H. S., Latasa, M. J., Moon, Y. & Kim, K. H. Regulation of the fatty acid synthase promoter by insulin. *J. Nutr.* **130**, 315S-320S (2000).
23. Wang, D. & Sul, H. S. Insulin stimulation of the fatty acid synthase promoter is mediated by the phosphatidylinositol 3-kinase pathway. Involvement of protein kinase B/Akt. *J. Biol. Chem.* **273**, 25420-25426 (1998).
24. Sul, H. S. & Wang, D. Nutritional and hormonal regulation of enzymes in fat synthesis: studies of fatty acid synthase and mitochondrial glycerol-3-phosphate acyltransferase gene transcription. *Annu. Rev. Nutr.* **18**, 331-351 (1998).
25. Wang, D. & Sul, H. S. Upstream stimulatory factor binding to the E-box at -65 is required for insulin regulation of the fatty acid synthase promoter. *J. Biol. Chem.* **272**, 26367-26374 (1997).
26. Jerkins, A. A., Liu, W. R., Lee, S. & Sul, H. S. Characterization of the murine mitochondrial glycerol-3-phosphate acyltransferase promoter. *J. Biol. Chem.* **270**, 1416-1421 (1995).
27. Latasa, M. J., Moon, Y. S., Kim, K. H. & Sul, H. S. Nutritional regulation of the fatty acid synthase promoter in vivo: sterol regulatory element binding protein functions through an upstream region containing a sterol regulatory element. *Proc. Natl. Acad. Sci. U. S. A.* **97**, 10619-10624 (2000).
28. Taniguchi, C. M. *et al*. Divergent regulation of hepatic glucose and lipid metabolism by phosphoinositide 3-kinase via Akt and PKClambda/zeta. *Cell. Metab.* **3**, 343-353 (2006).
29. Wong, R. H. *et al*. A role of DNA-PK for the metabolic gene regulation in response to insulin. *Cell* **136**, 1056-1072 (2009).
30. Wong, R. H. & Sul, H. S. DNA-PK: relaying the insulin signal to USF in lipogenesis. *Cell. Cycle* **8**, 1977-1978 (2009).
31. Wong, R. H. *et al*. A role of DNA-PK for the metabolic gene regulation in response to insulin. *Cell* **136**, 1056-1072 (2009).
32. Griffin, M. J., Wong, R. H., Pandya, N. & Sul, H. S. Direct interaction between USF and SREBP-1c mediates synergistic activation of the fatty-acid synthase promoter. *J. Biol. Chem.* **282**, 5453-5467 (2007).
33. Li, S. *et al*. Genome-wide coactivation analysis of PGC-1alpha identifies BAF60a as a regulator of hepatic lipid metabolism. *Cell. Metab.* **8**, 105-117 (2008).
34. Farese, R. V. & Sajan, M. P. Metabolic functions of atypical protein kinase C: "good" and "bad" as defined by nutritional status. *Am. J. Physiol. Endocrinol. Metab.* **298**, E385-94 (2010).
35. Sajan, M. P. *et al*. AICAR and metformin, but not exercise, increase muscle glucose transport through AMPK- , ERK- and PDK1-dependent activation of atypical PKC. *Am. J. Physiol. Endocrinol. Metab.* (2009).
36. Standaert, M. L. *et al*. Okadaic acid activates atypical protein kinase C (zeta/lambda) in rat and 3T3/L1 adipocytes. An apparent requirement for activation of Glut4 translocation and glucose transport. *J. Biol. Chem.* **274**, 14074-14078 (1999).
37. Gatfield, D. *et al*. Integration of microRNA miR-122 in hepatic circadian gene expression. *Genes Dev.* **23**, 1313-1326 (2009).

38. Lores, P., Visvikis, O., Luna, R., Lemichez, E. & Gacon, G. The SWI/SNF protein BAF60b is ubiquitinated through a signalling process involving Rac GTPase and the RING finger protein Unkempt. *FEBS J.* **277**, 1453-1464 (2010).
39. Turelli, P. *et al*. Cytoplasmic recruitment of INI1 and PML on incoming HIV preintegration complexes: interference with early steps of viral replication. *Mol. Cell* **7**, 1245-1254 (2001).
40. Taniguchi, C. M., Emanuelli, B. & Kahn, C. R. Critical nodes in signalling pathways: insights into insulin action. *Nat. Rev. Mol. Cell Biol.* **7**, 85-96 (2006).
41. Andrews, N. C. & Faller, D. V. A rapid micropreparation technique for extraction of DNA-binding proteins from limiting numbers of mammalian cells. *Nucleic Acids Res.* **19**, 2499 (1991).
42. Latasa, M. J., Griffin, M. J., Moon, Y. S., Kang, C. & Sul, H. S. Occupancy and function of the -150 sterol regulatory element and -65 E-box in nutritional regulation of the fatty acid synthase gene in living animals. *Mol. Cell. Biol.* **23**, 5896-5907 (2003).
43. Turner, S. M. *et al*. Measurement of TG synthesis and turnover in vivo by 2H2O incorporation into the glycerol moiety and application of MIDA. *Am. J. Physiol. Endocrinol. Metab.* **285**, E790-803 (2003).

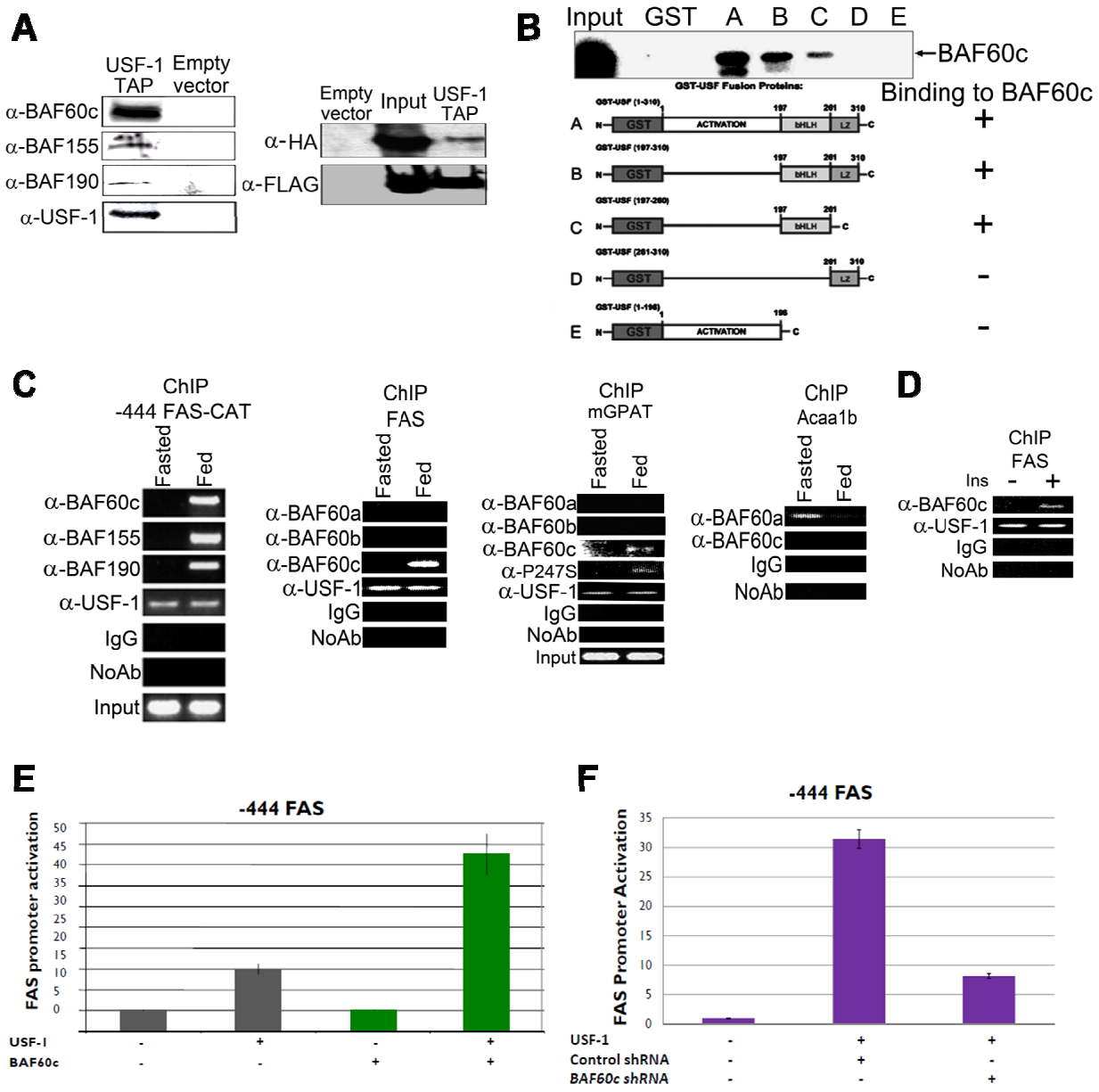

Figure IV-1. Purification of USF-1 interacting BAF complex

(A) The identities of USF-1-associated polypeptides. Purified USF-1 eluates on SDS-PAGE and immunoblotting of TAP eluates (left). TAP eluates from 293F cells overexpressing BAF60c-HA and USF-1-FLAG-TAP were immunoblotted (right).

(B) Interaction of BAF60c with USF-1 by GST-pull down assay. USF-1 was incubated with in vitro translated ^{35}S-labeled proteins before subjecting to GST pull-down. GST was used as a control.

(C) ChIP for association of USF-1-interacting proteins to the -444 FAS-CAT promoter (left) in FAS-CAT transgenic mice, or to the endogenous FAS promoter (2nd left), the mGPAT promoter (2nd right), and the Acca1b promoter (right) in WT mice.

(D) ChIP for association of USF-1-interacting proteins to the FAS promoter in HepG2 cells.

(E) FAS promoter activity was measured in cells transfected with -444 FAS-Luc and USF-1, along with BAF60c.

(F) FAS promoter activity was measured in cells transfected with -444 FAS-Luc and USF-1, along with BAF60c shRNA plasmid or control vector.

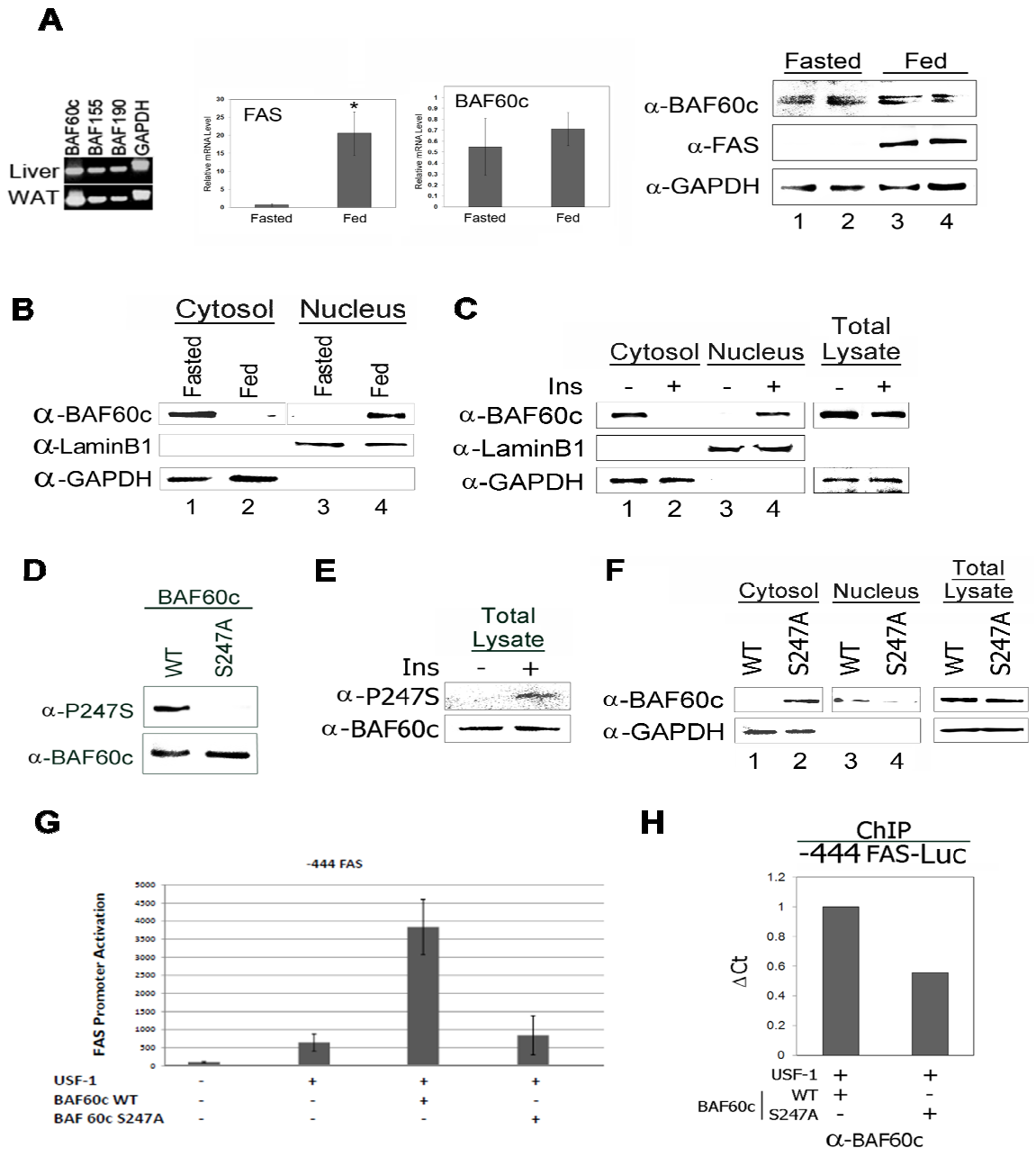

Figure IV-2. Feeding induced S247 phosphorylation of BAF60c

(A) RNA from tissues was used for RT-PCR (left). Expression in liver determined by RT-qPCR (middle). Immunoblotting of equal amounts of liver total lysates from 8-wk old mice (right).
(B) BAF60c protein levels in liver by Western blotting.
(C) BAF60c protein levels in HepG2 by Western blotting.
(D) Immunoblotting with anti-P247S in 293FT cells transfected with WT BAF60c-GFP or S247A BAF60c-GFP.
(E) BAF60c S247 phosphorylation levels in HepG2 by Western blotting.
(F) BAF60c protein levels in 293FT cells by transfected with WT BAF60c or S247A BAF60c by Western blotting.
(G) FAS promoter activity was measured in cells transfected with -444 FAS-Luc and USF-1, along with WT-BAF60c or S247A-BAF60c.
(H) ChIP for BAF60c association to the FAS promoter analyzed by qPCR in 293FT cells.

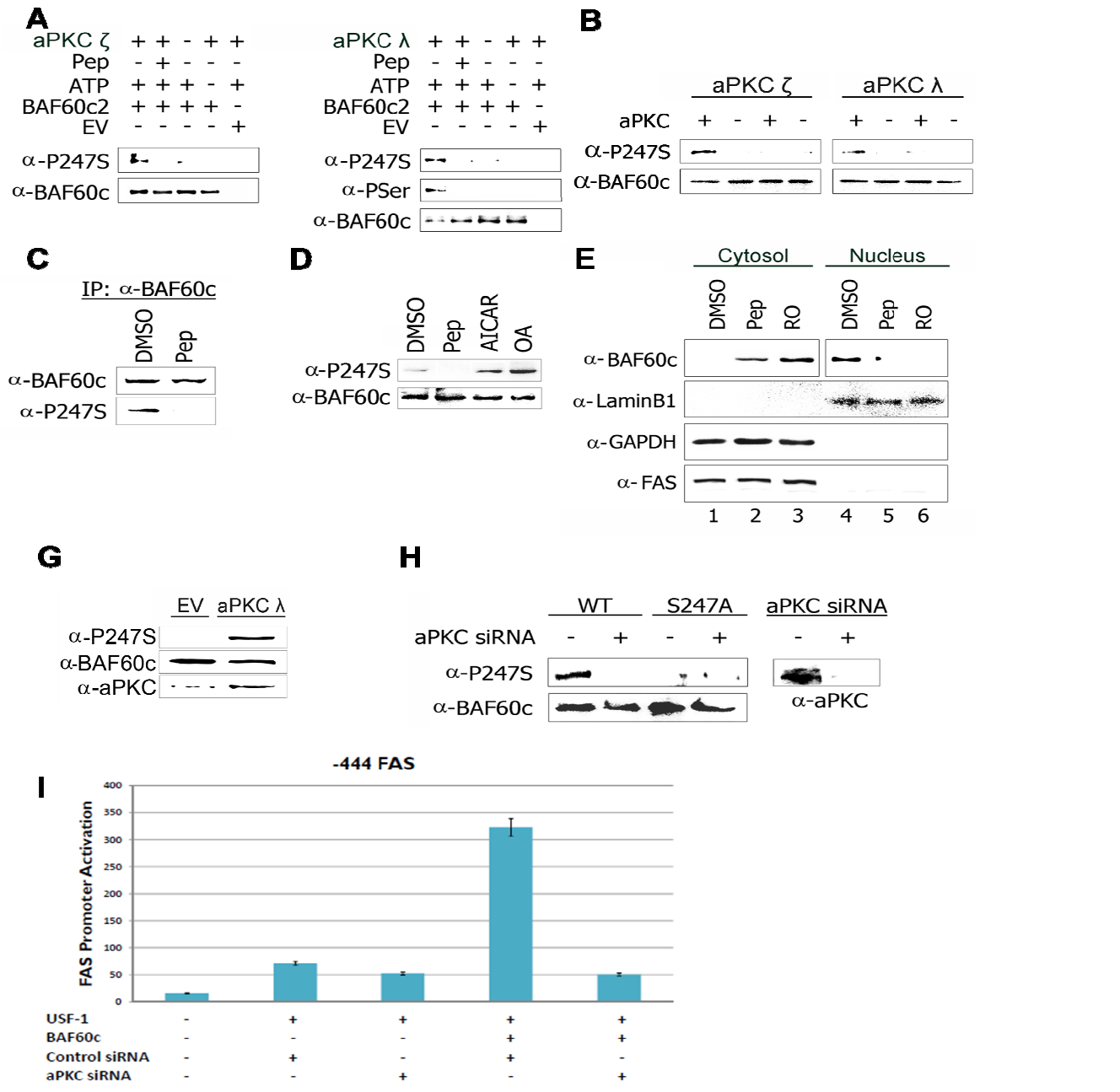

Figure IV-3. Feeding dependent S247 phosphorylation of BAF60c is mediated by aPKC.

(A) In vitro translated BAF60c-HA was incubated with aPKC ζ (left) and λ (right).
(B) In vitro translated WT-BAF60c-GFP or S247A-BAF60c-GFP were incubated with aPKC ζ (left) and λ (right).
(C) IP of BAF60c in total lysates prepared from 293FT cells transfected with BAF60c-HA.
(D) BAF60c protein levels in 293FT transfected with BAF60c-GFP by Western blotting.
(E) BAF60c protein levels in 293FT transfected with BAF60c-GFP by Western blotting.
(F) BAF60c protein levels in 293FT transfected with BAF60c-GFP along with aPKC λ or empty vector by Western blotting.
(G) BAF60c protein levels in 293FT transfected with BAF60c-GFP along with both aPKC ζ and λ siRNA or control siRNA by Western blotting.
(H) FAS promoter activity was measured in cells transfected with -444 FAS-Luc, USF-1, and BAF60c, along with control or aPKC siRNA.

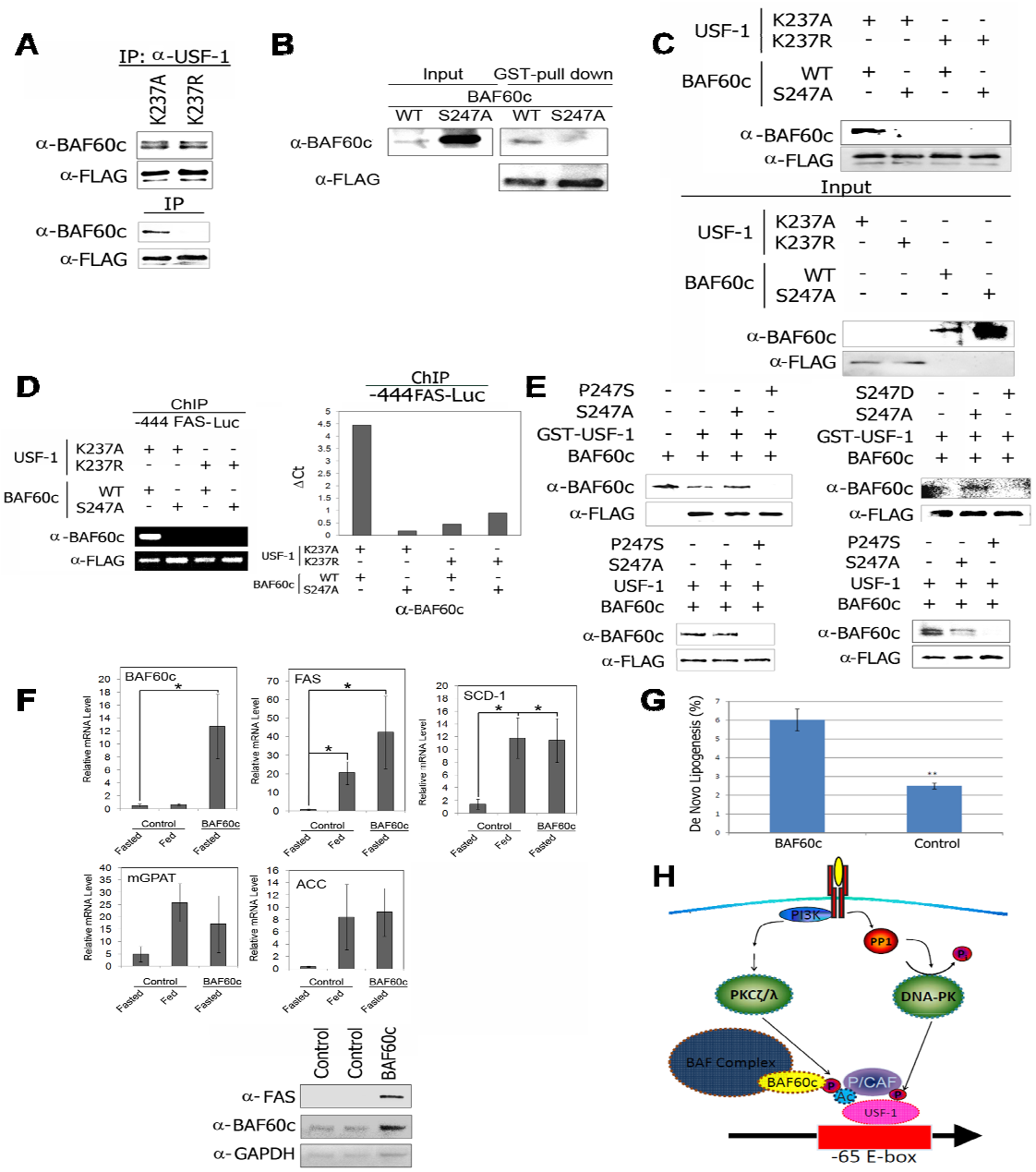

Figure IV-4. Requirement of USF and BAF60c modifications for their interaction

(A) IP of USF-1 acetylation mutants in 293FT cells. BAF60c protein levels by Immunoblotting.
(B) USF-1 was incubated with in vitro translated BAF60c proteins before subjecting to GST pull-down.
(C) In vitro translated USF-1 acetylation mutant was incubated with in vitro translated BAF60c proteins before subjecting to IP of USF-1.
(D) ChIP for association of BAF60c to the FAS-Luc promoter in cells transfected with USF-1 acetylation mutants along with WT BAF60c or S247A BAF60c analyzed by semi-quantitative PCR (left) and qPCR (right).
(E) USF-1 was incubated with in vitro translated WT BAF60c proteins before subjecting to GST pull-down in the presence or absence of indicated peptides (Top panels). IP of USF-1 from cells transfected with USF-1-FLAG and WT-BAF60c-GFP in the presence or absence of indicated peptides.
(F) Lipogenic gene expressions in liver determined by RT-qPCR (Top). Immunoblotting of equal amounts of liver total lysates from 8-wk old mice (bottom).
(G) Newly synthesized labeled fatty acids in livers from 8-week-old mice were measured. Values are means ± SEM. n=5
(H) Schematic representation of USF-1 and BAF-60c interaction and their associated insulin signaling.

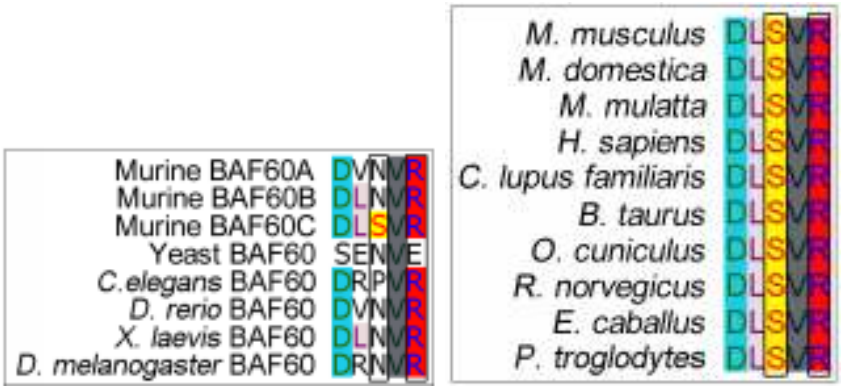

Figure IV -Supplemental Figure 1. Consensus map of the BAF60 isoforms amino acid sequence.